Journal of Physics G: Nuclear and Particle Physics

TOPICAL REVIEW

Signatures of quark-gluon plasma formation in high energy heavy-ion collisions: a critical review

To cite this article: S A Bass *et al* 1999 *J. Phys. G: Nucl. Part. Phys.* **25** R1

View the article online for updates and enhancements.

You may also like

- Lepton pair production from viscous QGP
A K Chaudhuri and Bikash Sinha
- The polarized charge distribution induced by a fast parton in the viscous quark–gluon plasma
Bing-feng Jiang and Jia-rong Li
- Updated analysis of jet quenching at RHIC and LHC within the light cone path integral approach
B G Zakharov

COMSOL

Track Charged Particles and Particles in Fluid Flow

Multiphysics simulation enhances the process of solving for trajectories of particles moving under the influence of various fields, such as ions or electrons in magnetic and electric fields or biological cells in drag force and gravity.

» Learn more about the COMSOL® software

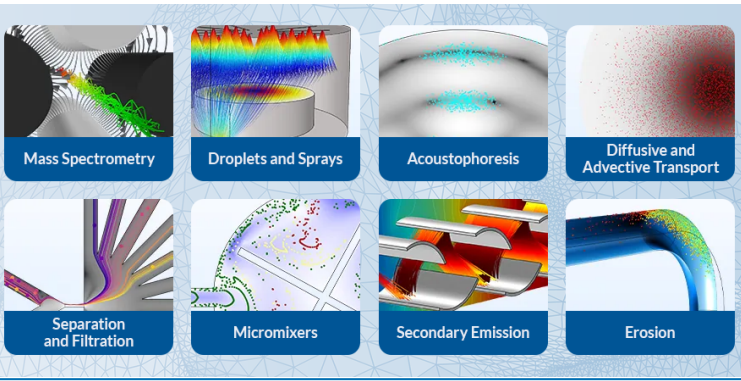

This content was downloaded from IP address 18.118.9.7 on 12/05/2024 at 22:52

J. Phys. G: Nucl. Part. Phys. **25** (1999) R1–R57. Printed in the UK PII: S0954-3899(99)36634-2

TOPICAL REVIEW

Signatures of quark-gluon plasma formation in high energy heavy-ion collisions: a critical review

S A Bass†‡¶, M Gyulassy‡§, H Stöcker‡‖ and W Greiner‖

† Department of Physics, Duke University, Durham, NC 27708-0305, USA
‡ Institute of Nuclear Theory, University of Washington, Seattle, WA 98195-1550, USA
§ Physics Department, Columbia University, 550 West 120th, New York, NY 10027, USA
‖ Institut für Theoretische Physik, Johann Wolfgang Goethe Universität, D-60054 Frankfurt am Main, Germany

Received 8 October 1998, in final form 8 December 1998

Abstract. A critical review on signatures of quark-gluon plasma (QGP) formation is given and the current (1998) experimental status is discussed. After giving an introduction to the properties of QCD matter in both, equilibrium and non-equilibrium theories, we focus on observables which may yield experimental evidence for QGP formation. For each individual observable the discussion is divided into three sections: first the connection between the respective observable and QGP formation in terms of the underlying theoretical concepts is given, then the relevant experimental results are reviewed and finally the current status concerning the interpretation of both, theory and experiment, is discussed. A comprehensive summary including an outlook towards RHIC is given in the final section.

1. Probing dense matter of elementary particles

Ultra-relativistic heavy-ion collisions offer the unique opportunity to probe highly excited dense nuclear matter under controlled laboratory conditions. The compelling driving force for such studies is the expectation that an entirely new form of matter may be created from such reactions. That form of matter, called the quark-gluon plasma (QGP), is the QCD analogue of the plasma phase of ordinary atomic matter. However, unlike such ordinary plasmas, the deconfined quanta of a QGP are not directly observable because of the fundamental confining property of the physical QCD vacuum. What is observable are hadronic and leptonic residues of the transient QGP state. There is a large variety of such individual probes. Leptonic probes, γ, e^+e^-, $\mu^+\mu^-$ carry information about the spectrum of electromagnetic current fluctuations in the QGP state; the abundance of quarkonia Ψ, Ψ', Υ, Υ' (also observed via l^+l^-) carry information about the chromoelectric field fluctuations in the QGP. The arsenal of hadronic probes, π, K, p, $\bar{p}$, Λ, Ξ, Ω, ϕ, ρ, ... provide information on the quark flavour chemistry and baryon number transport. Theory suggests that with decays such as $\rho \to e^+e^-$ the properties of the hadronization and chiral symmetry breaking can be indirectly studied. Quantum statistical interference patterns in $\pi\pi$, KK, pp, $\Lambda\Lambda$ correlations provide somewhat cloudy lenses with which the spacetime geometry of hadronic ashes of the QGP can be viewed. The detailed rapidity and transverse momentum spectra of hadrons provide barometric information of pressure gradients during the explosive expansion of the QGP drop.

¶ Feodor Lynen Fellow of the A v Humboldt Foundation.

0954-3899/99/030001+57$19.50 © 1999 IOP Publishing Ltd

The central problem with all the above probes is precisely that they are all indirect messengers. If we could see free quarks and gluons (as in ordinary plasmas) it would be trivial to verify the QCD prediction of the QGP state. However, nature choses to hide those constituents within the confines of colour-neutral composite many-body systems—hadrons.

The QGP state formed in nuclear collisions is a transient rearrangement of the correlations among quarks and gluons contained in the incident baryons into a larger but globally still colour-neutral system with, however, remarkable theoretical properties. The task with heavy-ion reactions is to provide experimental information on that fundamental prediction of the standard model.

This topical review covers current (1998) theoretical and experimental attempts to disentangle popular scenarios on QGP signatures from the complex, off-equilibrium physics. The start of the RHIC experiment programme is only a year away. This will be a dedicated machine to study the QGP. Nevertheless, a very large effort has been made at the AGS and SPS over the last 12 years resulting in an impressive amount of exciting new findings. The search for the QGP can be traced via the proceedings of the high energy heavy ion studies [1–10] and schools [11–13] and the 'quark matter', 'nucleus–nucleus' and 'strange quark matter' conferences [14–33]. Some textbooks [34–38], and a vast number of review papers have been published—reference samples of early [39–46] and of the latest [47–51] review papers are given here. The list of more than 500 references given in this topical review is by no means complete. Apologies are offered to those whose contributions could not be included in the references.

2. QCD matter and relativistic heavy-ion collisions

2.1. Infinite stationary systems in equilibrium

2.1.1. The deconfinement phase transition and chiral symmetry restoration. Phase transitions are among the most dramatic many-body effects in physics. Examples for restored symmetry via a phase transition at high temperatures, T_C, are ferro-magnetism, super-conductivity and the solid–liquid phase transition. In nuclear physics evidence for a liquid–gas phase transition of nuclear matter has been claimed for temperatures of $T \approx 5$ MeV [52]. Phase transitions to abnormal nuclear matter states at high densities have also been predicted early on [53, 54].

QCD is a non-abelian gauge theory, its basic constituents are quarks and antiquarks interacting through the exchange of colour-charged gluons. At short spacetime intervals—large momentum transfers—the effective coupling constant decreases logarithmically ('asymptotic freedom'—meaning weak coupling of quarks and gluons) whereas it becomes strong for large distances and small relative momenta. This results in the phenomena of chiral symmetry breaking and quark-gluon confinement.

At very high temperatures and densities, in the domain of weak coupling between quarks and gluons, long-range interactions are dynamically screened [55, 56]. Quarks and gluons are then no longer confined to bound hadronic states ('deconfinement'). Furthermore, chiral symmetry is restored—for baryon-free matter—apparently at the same temperature T_C. This novel phase of nuclear matter is called the *quark-gluon plasma* (QGP) [55].

A transition from the deconfined quark-gluon phase to confined colour singlet states has (probably) occured during the rapid expansion of the early universe. Temperatures were very high then, but the net baryon density was small. Therefore one often assumes zero baryon chemical potentials in calculating the thermodynamic properties of strongly interacting matter in the early universe. It is sought to re-establish these conditions and thus enable a study of quark deconfinement in the laboratory via heavy-ion collisions [57, 58]. At the highest in the

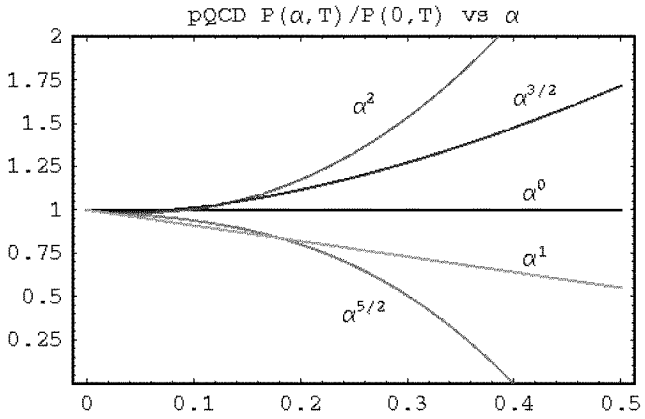

Figure 1. Perturbative contributions up to O(g^5) [67] to the pressure versus the coupling constant.

near future obtainable energies (LHC) the initial net baryon density may be around nuclear matter ground state density. The entropy per baryon ratio, however, is estimated to be in the order of 10^3 to 10^4 [59] (early universe: 10^9) and thus a vanishing baryon chemical potential is considered a viable approximation.

The energy densities currently achievable in ultra-relativistic heavy-ion collisions at the AGS and SPS are on the order of 0.5–10 GeV fm^{-3} [60] and temperatures are in the range of 100–200 MeV. At temperatures $T_C \sim$ 150–200 MeV, the effective coupling constant of QCD, however, is still of the order of one. Therefore, perturbative techniques of QCD [61–63] are not applicable. The situation may change at extremely high energies (LHC?) where QCD predicts a large cross section for minijet production. Then there may exist a possibility to reach a new regime of large parton densities at a small coupling constant. The QCD interaction in this regime would be highly nonlinear [64]. Recent calculations of the Debye screening mass using *lattice gauge simulations*, however, indicate that perturbative QCD techniques may not even be applicable at such energies [65].

2.1.2. Perturbation theory. The fundamental asymptotic property of QCD leads to the naive expectation that the properties of a QGP can be calculated via perturbation theory. However, due to infrared divergences, especially in the chromo-magnetic sector, perturbation theory may not even be applicable for temperatures far above T_C. QCD perturbation theory has been improved [62] by resummation to screen colour-electric divergences. These 'hard-thermal-loop' methods, originally developed for zero baryon density, have now been extended to finite densities [66]. Nevertheless, its applicability at temperatures and densities *accessible to experiment* is severely limited. At energy densities of the order of 20 GeV fm^{-3} the temperature is in the order of 600 MeV and the coupling constant g is still of the order of two, which invalidates the necessary assumption $gT \ll T$ for the hard-thermal-loop resummation scheme. Only at the Planck scale is QCD a weakly interacting theory as QED [65]. Recent calculations of the perturbative contributions up to O(g^5) [67] to the pressure are shown in figure 1. The oscillation of the results suggest a zero radius of convergence of thermal pQCD.

2.1.3. Lattice gauge theory. *Lattice gauge simulations of QCD* [68,69] provide, therefore, the only rigorous method to compute the *equation of state* (EoS) of strongly interacting elementary particle matter. In principle, both the non-perturbative hadronic matter and the non-perturbative

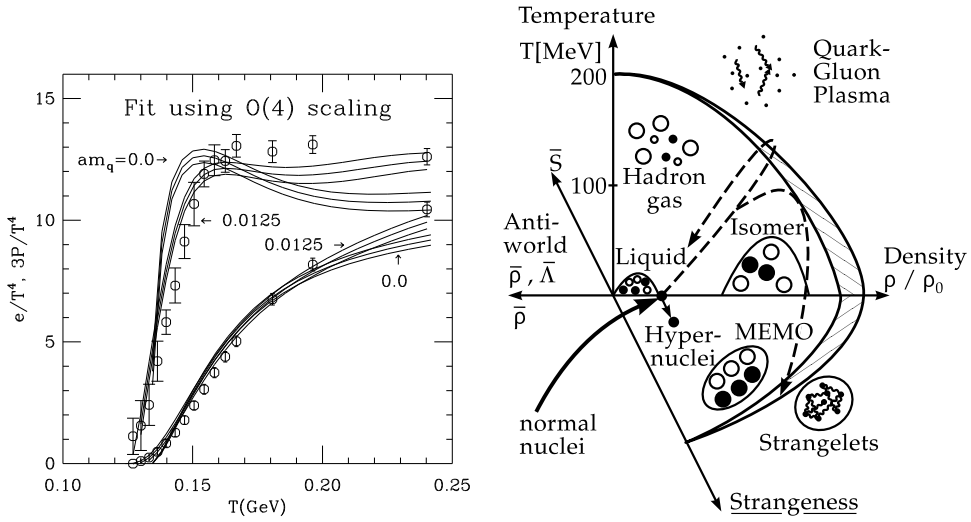

Figure 2. Left: lattice calculation (circles) of the EoS for two-flavour QCD [75]. The curves show fits using O(4) scaling and extrapolations to zero quark mass. The critical temperature is of the order of 140 MeV. Right: schematic overview of theoretical phases of QCD matter.

QGP phases of QCD can be investigated. The main disadvantage of lattice simulations is the practical restriction to finite, periodic, baryon-free systems in global equilibrium, a scenario far from the highly inhomogeneous off-equilibrium situation found in complex heavy-ion reactions. Technically, the strong dependence of the results on the lattice spacing and periodic box size is presently a problem. Nevertheless, lattice data provide the most compelling theoretical evidence of a rapid transition region from the confined to the QGP state.

Lattice calculations at least allow the computation of thermodynamic averages of different quantities related to hadron masses and to the phase transition (in the infinite volume and zero baryon number limit). There have been considerable improvements in algorithms [70] and in computing power in recent years. For finite temperature, full QCD simulation lattices with spatial sizes of 24^3 and 48 points in Euclidean time direction have been used [71, 72], while for pure gauge theory (without quarks) lattices of $32^3 \times 12$ [73, 74] are in use.

Lattice calculations yield a critical temperature of $T_C = 265^{+10}_{-5}$ MeV in the quenched approximation [70]—where neither dynamical quarks, nor a chiral phase transition exist. Simulations including dynamical quarks at $\mu_B = 0$ indicate a critical temperature of the order of $T_C = 140$ MeV (see figure 2). However, in this case finite-size effects of the lattice have not yet been fully overcome and the precision is not as high as in the quenched case [70]. The inclusion of the second most important thermodynamic variable, the chemical potential μ_B, into a fully fledged lQCD calculation is, presently, still out of reach. This raises a practical question: whether conclusions based on $\mu_B = 0$ estimates might misguide physical argumentation for observables in nuclear collisions. This warning is particularly appropriate for those QGP signals, where a 50% quantitative change of an observable is used to differentiate QGP production scenarios from ordinary hadronic transport ones.

The behaviour of order parameters as a function of temperature, such as the quark condensate, indicate that the transition between the confined and deconfined state of QCD may show a discontinuity of some thermodynamic derivative—i.e. a phase transition. The order of this phase transition is crucial for some proposed signatures of the QGP. Many striking signatures depend heavily on the assumption of a first-order phase transition and

the existence of a mixed phase of QCD matter. For *pure* $SU(3)$ gauge theory and for *full* QCD with four massless flavours of dynamical quarks, lattice QCD results and universality class arguments [76,77] indicate a first-order phase transition. For two (massless) flavours, however, these arguments predict [77,78] that *if* the phase transition is of second order, it should have the critical exponents of the O(4) Heisenberg anti-ferromagnetic spin model in three dimensions. Numerical evidence for this was recently obtained [79], suggesting that the transition in this case is indeed of second order. With three light flavours, the chiral phase transition corresponds to a change in a continuous symmetry (i.e. chiral symmetry) and is automatically of second order.

For the most realistic case of QCD with two flavours of light quarks with masses between 5 and 10 MeV and one flavour with a mass around 200 MeV, the situation remains unclear: the order of the phase transition seems to depend on the numerical values for the masses of the light and heavy quarks [80]. If the latter is too heavy, the transition might be smeared out to a mere rapid increase of the energy density over a small temperature interval. In this case the use of simple deconfinement scenarios may lead to wrong expectations for observables. The elementary excitations in such a phase transition region ought not be described by quarks and gluons but could physically resemble more hadronic excitations with strongly modified 'in-medium' properties [81].

In any case, the QCD phase transition observed on the lattice is—when dynamical quarks are included—only very weakly first order, if there is a discontinuity at all. The latent heat across the discontinuity is at most a small fraction of the total jump in the normalized entropy density s/T^3 between the hadronic phase and the asymptotic QGP. A real phase coexistence region between hadrons and (possibly strongly interacting, but deconfined) quarks and gluons, as often discussed in the past, therefore seems no longer a realistic possibility. However, nothing is known from first principles about the phase transition at finite baryon density and therefore a strong first-order transition (with a phase coexistence region) is still a possibility at large baryon densities [82,83]. An additional complication is that for systems of finite volume ($V \leqslant 100$ fm^3) the deconfinement cannot be complete. Fluctuations lead to a finite probability of the hadronic phase above T_C. The sharp discontinuity (e.g. ε/T^4) is thus smeared out [84].

Purely hadronic models, such as the σ–ω model or the linear σ-model exhibit a similar phase transition (from normal to abnormal nuclear matter), but are not constrained to $\mu_B = 0$. The EoS for nuclear matter does not only depend on temperature and density but will also depend on the net strangeness content, which may be nonzero in subsystems (e.g. individual phases) present in heavy-ion collisions. A schematic view of the resulting complex multidimensional phase diagram is illustrated on the right in figure 2.

2.2. Non-equilibrium models

In order to connect the theoretical thermodynamic properties of a QGP with experimental data on finite nuclear collisions, many non-equilibrium dynamical effects must also be estimated. Transport theory is the basic tool to address such problems. Non-equilibrium effects are certain to arise from the rapid time dependence of the system (even the use of the term 'state' seems questionable), finite-size effects, inhomogeneity, N-body phase space, particle/resonance production and freeze-out and collective dynamics. Such microscopic and macroscopic (hydrodynamical) models attempt to describe the full time evolution from an assumed initial state of the heavy-ion reaction (i.e. the two colliding nuclei) up to the freeze-out of all initial and produced particles after the reaction. Hydrodynamical models neglect most of these effects by making the assumption that the initial condition can be assumed to be in local thermal equilibrium and that local equilibrium is maintained during evolution. Fireball models simply

parametrize final spectra and abundances via freeze-out parameters, e.g. T, μ_B, $\vec{v}_f$. However, the initial condition in nuclear collisions is a coherent state $|AB\rangle$ of two quantal ($T = 0$) nuclear systems. A non-equilibrium quantum evolution of $|AB\rangle$ introduces complex high-order Fock-state components. A key dynamical assumption is that decoherence occurs rapidly during the early phase of the collision yielding a mixed state density matrix (with $S = \mathrm{Tr}\,\rho \ln \rho > 0$). There is no theorem to insure that ρ evolves to a local equilibrium form $\exp(-u_\mu p^\mu / T)$ at any time during the reaction. That can only be tested via a transport theory approximation to the evolution equations. The question of the form of the initial state $\rho(\tau_0)$ must still be addressed, but once that is specified, transport theory can reveal if local equilibrium is achieved and what observables are least sensitive to uncertainties in $\rho(\tau_0)$.

Depending on the most convenient basis for expanding $\rho(\tau_0)$, transport theory assumes different forms. At low energies the initial ensemble is most conveniently described in terms of mesons and baryons. Here hadronic transport theory is appropriate. At collider energies, pQCD minijet processes are expected to produce a high-density mostly gluonic gas. In that regime parton cascade models are more appropriate.

2.2.1. Parton cascades Parton cascade models [85–90] evolve partonic degrees of freedom. They are therefore mostly applied to study the initial compressional and the high-density phase of ultra-relativistic heavy-ion collisions (collider energies, $\sqrt{s} \geqslant 200$ GeV). These models all contain the general structure [86]:

(i) Initialization: the nucleons of the colliding nuclei are resolved into their parton substructure according to the measured nucleon structure functions and yield the initial parton distributions.

(ii) Interaction: parton interactions as described by perturbative QCD are used to model the evolution of the ensemble of partons during the course of the collision. This includes multiple scatterings together with associated space-like and time-like parton emission processes before and after each scattering. The sequence of scatterings is, however, incoherent and the neglect of quantum interference effects is questionable.

(iii) Hadronization: partons are recombined or converted via string fragmentation into final hadron states.

The propagation is performed on straight lines—soft non-perturbative collective field effects have so far been neglected. On the other hand, hadronization has to be modelled by brute force to mock up confinement in the final reaction stage.

One of the central issues addressed by parton cascades is the question of energy deposition processes in spacetime as well as momentum space. Partonic cascades predict that roughly 50% of the expected energy deposition at RHIC and a larger fraction at LHC takes place at the partonic level [91]. Rapid thermalization is caused by radiative energy degradation and spatial separation of partons with widely different rapidities due to free streaming; transverse momentum distributions of initially scattered partons are almost exponential if radiative corrections are taken into account [49]. For RHIC energies thermalization is predicted on a proper timescale of 0.3–0.5 fm/c [91]. A recent analysis of parton cascade evolution [92] shows that local equilibrium is not maintained due to rapid expansion. Very large dissipative corrections to hydrodynamics appear. The thermalized QGP is initially gluon rich and depleted of quarks due to the larger cross section and higher branching ratios for gluons [93]. Chemical equilibrium is achieved over a time of several fm/c [94,95]. This may be reduced if higher-order pQCD processes are taken into account [96].

2.2.2. Hadronic transport models. Hadronic transport models treat relativistic heavy-ion collisions as sequences of binary/N-body collisions of mesons, baryons, strings and their constituents, diquarks and quarks. The real part of the interaction can be obtained in principle from G-matrix calculations, with the in-medium self-energy and the imaginary part is modelled via hard scattering cross sections [97–110]. For high beam energies most models include particle production via string formation—either using the Lund [111–113] or a pomeron exchange scheme [114]. Partonic degrees of freedom are not treated explicitly and therefore these models do not include a phase transition. However, some models contain further speculative scenarios such as colour ropes [115, 116], breaking of multiple strings [117] or decay of multi-quark droplets [118] which clearly go beyond hadronic physics.

Hadronic transport models are critical for assessing the influence of ordinary or exotic hadronic phenomena on the observables proposed to search for a QGP. They therefore provide a background basis to evaluate whether an observable shows evidence for non-hadron physics.

2.2.3. Nuclear fluid dynamics. NFD is so far the only dynamical model in which a phase transition can explicitly be incorporated (see e.g. [44, 60, 119, 120] for details). This is possible since the EoS (including a phase transition) is a direct input for the calculations. However, NFD is an idealized continuum description based on local equilibrium and energy–momentum conservation. Therefore it is very well suited to study kinematic observables such as collective flow. Since NFD is a macroscopic kinetic theory it is not directly applicable to the study of hadron abundances and particle production. However, NFD calculations predict (local) temperatures and chemical potentials which can be used, e.g. by chemical equilibrium calculations of hadron abundances, to study particle production. Different observables predicted by nuclear fluid dynamics will be discussed in section 3.3.

In the ideal fluid approximation (i.e. neglecting off-equilibrium effects), the EoS is the *only* input to the equations of motion that relates directly to properties of the matter under consideration. The EoS influences the dynamical evolution of the system, and final results are uniquely determined. The initial condition can be chosen from two colliding nuclei (in a full 3D calculation with up to three fluids) or an equilibrated QGP or hadronic matter with prescribed temperature and chemical potential and velocity/flow profiles (for simpler, more schematic calculations). The time evolution is then studied until hadronic freeze-out for which a decoupling (freeze-out) hyper-surface needs to be specified.

However, the ideal fluid ansatz is only a rough approximation. In the parton cascade study [92] for example, large deviations from even the Navier–Stokes fluid approach were found.

3. Observables: prospects and limitations

As we have seen in the previous section it is obviously difficult to find a robust theoretical description of relativistic heavy-ion collisions involving the QCD phase transition to predict observables. Not only is even the order of the phase transition from $\mu = 0$ not known from the *ab initio* lQCD calculations, but also has the physical situation of present or near-future relativistic heavy-ion collisions, namely finite μ_B, not been addressed yet in this theory. However, even if this were to be the case, one would only know the behaviour for static infinite systems. The second major unknown is the influence of the non-equilibrium evolution on the (small) many-body system. The very nature of even the thermodynamic limit of a QGP is not completely understood. Real time response has only been studied via pQCD, which however may have zero radius of convergence in g in the thermodynamic limit. Theory in

this situation can thus serve mainly to motivate particular experimental studies and provide overall consistency checks in the interpretation of data. Data are needed to fix the uncertain phenomenological parameters of the transport models, while such model calculations with plausible parameters are essential to motivate the taking of the data in the first place. This symbiotic relation between theory and experiment in this field is very important as emphasized also, for example, by Van Hove [121] and Kajantie [122].

A strategy for the detection of quark matter—in our opinion—must collect at least circumstantial evidence from several 'signals' or anomalies. In the following we discuss each of the individual signals. The strategy does then consist in a systematic variation of an external parameter (system size, impact parameter and—in particular—bombarding energy); i.e. the measurement of excitation functions of several signals which in the case of a phase transition show *simultaneously* the predicted anomalous behaviour.

3.1. Creation of high baryon density matter: nuclear stopping power

3.1.1. Theoretical concepts. It was proposed more than two decades ago that head-on collision of two nuclei can be used to create highly excited nuclear matter [57, 58]. The longitudinal momentum is converted via multiple collisions into transverse momentum and secondary particles, causing the creation of a zone of high energy density. Nuclear shock waves have been suggested as a primary mechanism of creating high energy densities in collisions with $\sqrt{s} \leqslant 20$ GeV. [54, 57, 58]. This is analogous to the well known Rankine–Hugoniot analysis of ordinary dense matter up to $\sim$1 Mbar pressures. In the nuclear shock wave case, the Rankine-Hugoniot analysis predicts that pressures up to 10^{23} Mbar ($\sim$100 MeV fm^{-3}) may be reached.

The term *nuclear stopping power* [123] characterizes the degree of stopping which an incident nucleon suffers when it collides with another nucleus. For A + A collisions stopping manifests itself in a shift of the rapidity distributions of the incident nucleons towards mid-rapidity. The heaviest systems available, such as Pb + Pb or Au + Au, are best suited for the creation of high baryon density matter.

The shape of the baryon rapidity distribution can give clear indications on the onset of critical phenomena. Due to the strong dependence of the baryon rapidity distribution on the baryon–baryon cross section [124–126], a rapid change in the shape of the scaled $\mathrm{d}N/\mathrm{d}(y/y_p)$ distribution with varying incident beam energy is a clear signal for new degrees of freedom which show up during the reaction (i.e. deconfinement), e.g. due to phenomena such as critical scattering [127]. The width of the $\mathrm{d}N/\mathrm{d}(y/y_p)$ distribution for baryons is inversely proportional to their cross section.

Hadronic transport model calculations have predicted stopping for heavy collision systems at CERN/SPS energies [128, 129] (see figure 4). Even for RHIC energies the central rapidity zone is not expected to be net-baryon free. RQMD has predicted a net baryon number density of >10 at mid-rapidity [130] and HIJING/B yields similar estimates [131] (see figure 5).

The creation of a zone of high baryon and energy density around mid-rapidity results in massive excitation of the incident nucleons. A state of high-density resonance matter may be formed [58, 135, 136]. Transport model calculations indicate that this excited state of baryonic matter is dominated by the Δ_{1232} resonance. They predict a long apparent lifetime (>10 fm/c) and a rather large volume (several hundred fm^3) for this Δ-matter state in central Au + Au collisions at the AGS [137] (see figure 6).

The degree of stopping can furthermore be used to estimate the achieved energy density in the course of the collision within the Bjorken scenario of scaling hydrodynamics [60]. For such an estimate not the rapidity distribution of the incident, leading particles is required, but that

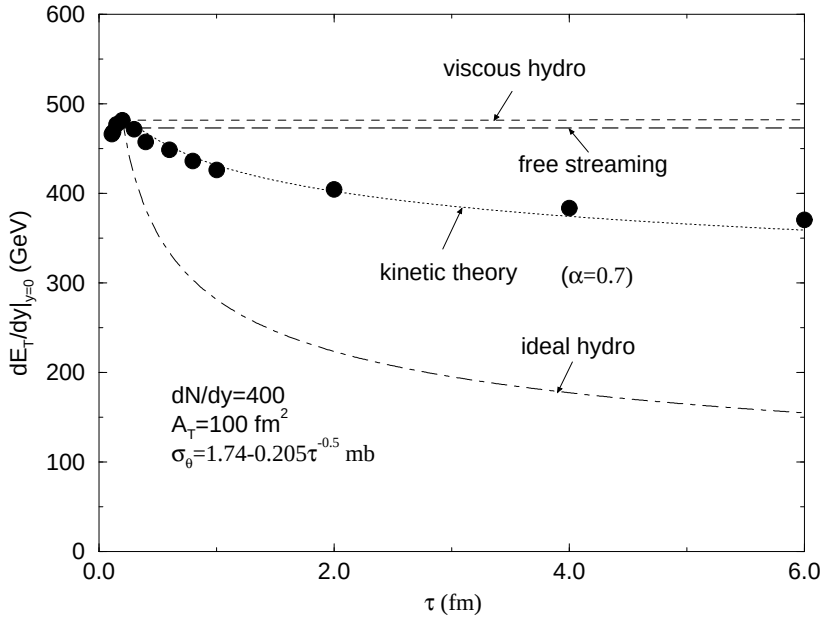

Figure 3. Comparison of time evolution of transverse energy per rapidity in analytic kinetic theory results with numerical parton cascade calculations [92]. Strong deviations from hydrodynamic behaviour are visible.

of secondary particles, those produced during the course of the reaction. One often assumes that particles produced at $y = y_{CM}$ originate from the central reaction zone at $z = 0$ and the initial proper time τ_0. The rapidity distribution of these produced particles could then be used to estimate the initial energy density in the central reaction zone:

$$\epsilon_0 = \frac{m_T}{\tau_0 A} \frac{\mathrm{d}N}{\mathrm{d}y}\bigg|_{y=y_{CM}}. \tag{1}$$

Here A is the transverse overlapping region area in the collision and m_T the transverse mass of the produced particles. The proper production time τ_0 is very uncertain and estimates are on the order of 0.5–1 fm/c. Estimates for the CERN/SPS energy density at proper time $\tau_0 \sim 1$ fm/c are on the order of $\epsilon \approx$ 1–5 GeV fm^{-3} [60], with baryon densities up to $\rho \leqslant 1$ fm^{-3}. In [131] extrapolations to RHIC suggest that energy densities up to 20 GeV fm^{-3} at $\rho \sim 2\rho_0$ may be reached (see figure 5).

3.1.2. Experimental status. At AGS and SPS an extensive investigation of the nuclear stopping power is near completion. Proton–proton [139] and peripheral nucleus–nucleus interactions at AGS [140, 141] and SPS [142] energies yield a forward–backward peaked $\mathrm{d}N/\mathrm{d}y$ distribution in the CM frame, and a low degree of baryon stopping.

A higher degree of stopping is observed for central collisions of intermediate mass nuclei (Si + Si at AGS, S + S at SPS): the rapidity distribution is flat at CM rapidities, two broad bumps are observed between projectile/target and CM rapidities respectively [140–142]. The heaviest collision systems (gold and lead respectively) exhibit the largest stopping power and thus correspond to the creation of the highest baryon densities: at AGS energies, the baryon rapidity distribution exhibits a pile-up at mid-rapidity [134, 143] (see figure 4). Whether the shape of the $\mathrm{d}N/\mathrm{d}y$ distribution at SPS energies is flat or shows two bumps is currently not fully

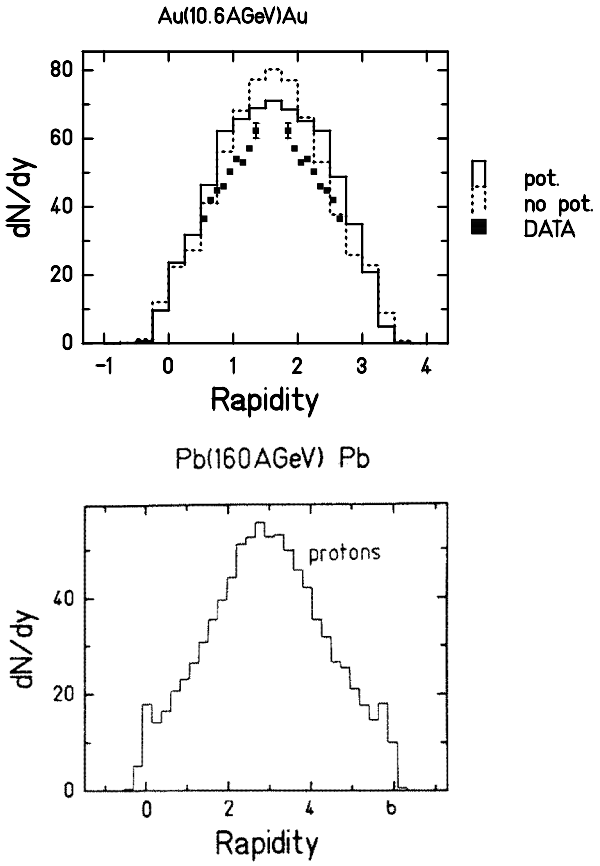

Figure 4. Top: RQMD prediction [132] of stopping in central Au + Au collisions at 10.6 GeV/nucleon. The preliminary data are from the E866 collaboration [133]. Note that the current status of data analysis indicates a flatter shape for the experimental distribution [134]. Bottom: RQMD prediction [129] of stopping in central Pb + Pb collisions at 160 GeV/nucleon.

resolved (the SPS data are preliminary). There are indications, however, that with rising beam energy the scaled $\mathrm{d}N/\mathrm{d}(y/y_p)$ distribution stretches over the increasing rapidity gap between projectile and target; this can be seen in figure 7. Recently the NA49 collaboration [144] reported a Λ rapidity distribution which may be peaked strongly at mid-rapidity for Pb + Pb at 160 GeV/nucleon. This finding, however, is preliminary and in disagreement with equally preliminary results by the WA97 collaboration [145], which indicate rapidity densities for Λ lower by a factor of 2–3.

Transverse energy measurements at the AGS [146] indicate that the transverse energy E_T increases by 50% faster than predicted by an independent nucleon–nucleon interaction model when going from a light system (Si + Al) to a heavy system (Au + Au). In terms of a microscopic hadronic model this can be understood as a strong increase in baryonic density in the initial reaction phase and a corresponding large increase in the volume of high density matter [99, 147].

The $\Delta(1232)$ abundance has been measured via π^+–p correlations at the AGS by the E814 and E877 collaborations [148, 149]. The pion spectra can be decomposed into a thermal contribution and a contribution due to Δ-resonance decays. The $\Delta(1232)$-to-nucleon ratio

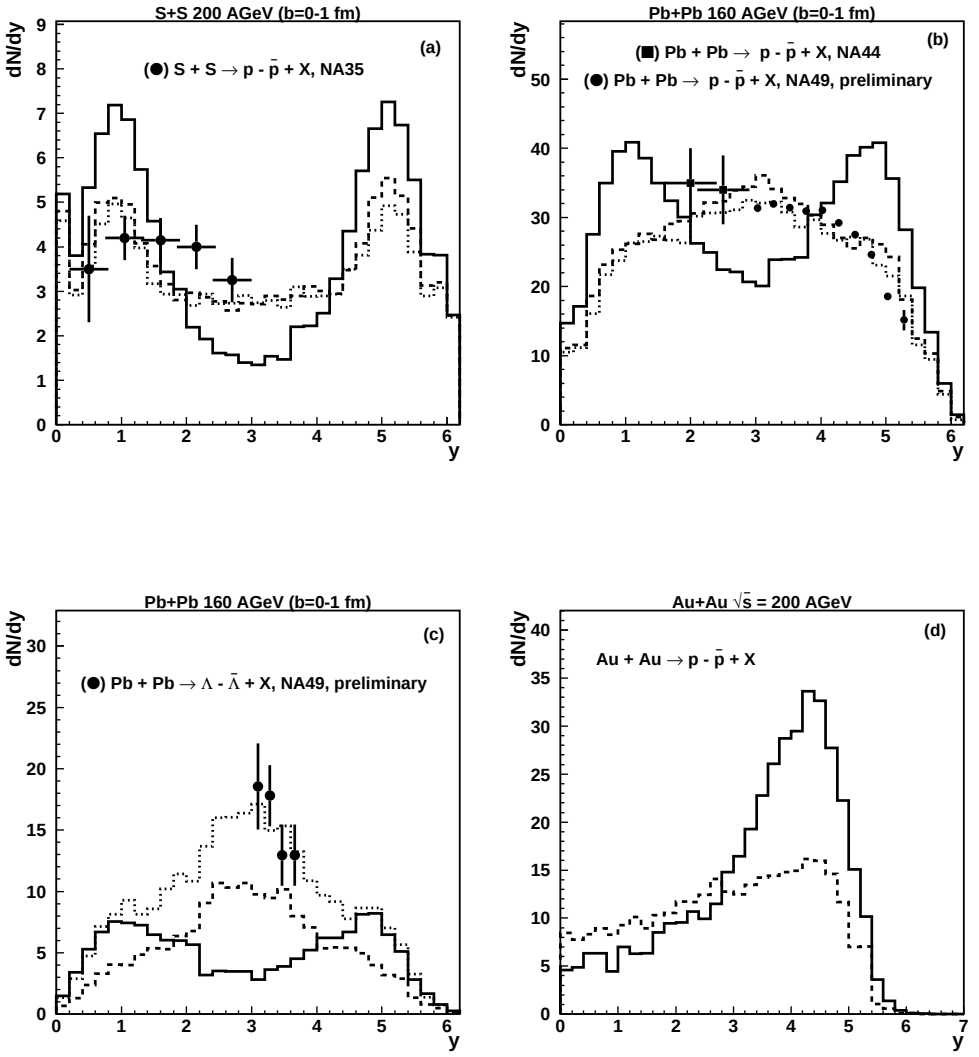

Figure 5. Comparison of baryon stopping in HIJING (solid), HIJING/B (dashed) and HIJING/B with 'ropes' with various data [131].

at freeze-out was determined to be ≈35% for central silicon nucleus collisions. Hence, one can conclude that a large fraction of the system resides in hadron resonances, which produce most of the observed hadrons by their decay ('feeding'), after the resonances have decoupled. The dense state before this decay can therefore be called 'resonance matter'. It exists due to the inertial confinement of energy and baryon number in the early phase of the reaction (see figure 6).

At CERN/SPS measurements of E_T have been used to estimate the created energy density: for 200 GeV/u S + Au central collisions [150] ϵ reaches ≈3 GeV fm^{-3}. For the Pb + Pb experiment at 160 GeV/u similar values were extracted [151], but over a much larger volume. The reader is reminded here of the sensitivity of these extracted values on the hadron production time τ_0, which is uncertain by at least a factor of two.

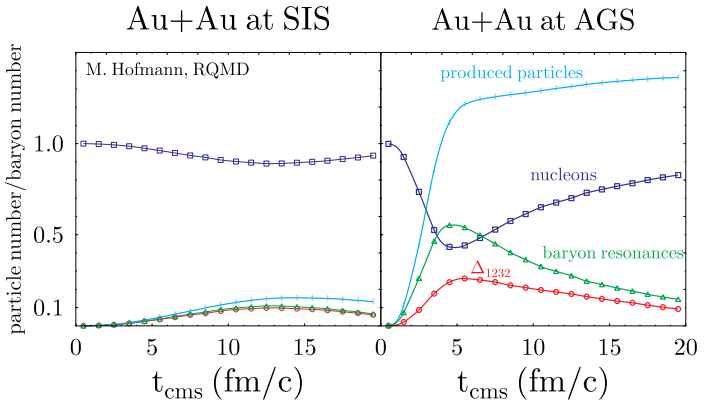

Figure 6. Time evolution of particle multiplicities (scaled with the number of incident nucleons) for central Au + Au collisions at 1 GeV/nucleon (SIS) and at 10.6 GeV/nucleon (AGS). At SIS energies, only about 10% of the nucleons are excited to resonances whereas at AGS energies the degree of excitation exceeds 50%. For a timespan of up to 10 fm/c the baryons are in a state of Δ-matter. The figure has been taken from [137].

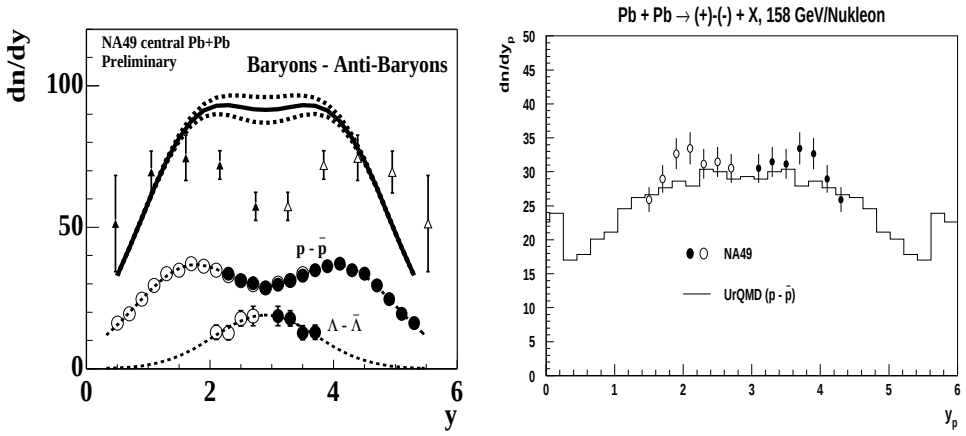

Figure 7. Baryon stopping in central Pb + Pb collisions at 160 GeV/nucleon. Left: data by the NA49 collaboration (preliminary, figure taken from [138]). The solid line shows the rapidity distribution for net baryons which can be decomposed into contributions from net protons and net Λ. For comparison the net baryon distribution for central S + S collisions is also plotted (triangles). Right: UrQMD prediction compared with the same data (figure taken from [110]).

The mass dependence of the rapidity distribution of produced particles, i.e. pions or kaons, can also be used to search for scaling violations which could signal the onset of new physics phenomena. A comparison of the negative hadron rapidity distributions for S + S [152] with those for the lead on lead run [153] shows that the preliminary lead data can be matched by scaling the sulfur data with a factor 6.6, close to the relative number of participant nucleons in central lead–lead collisions ($A_{Pb}/A_S = 208/32 \approx 6.5$) [153] (figure 8).

3.1.3. Discussion. The form of the measured baryon rapidity distributions shows experimentally that the central rapidity region up to $E_{lab} \sim 200$ GeV/nucleon is not net-baryon free, in contrast to what had been expected in most early papers. Rather strong

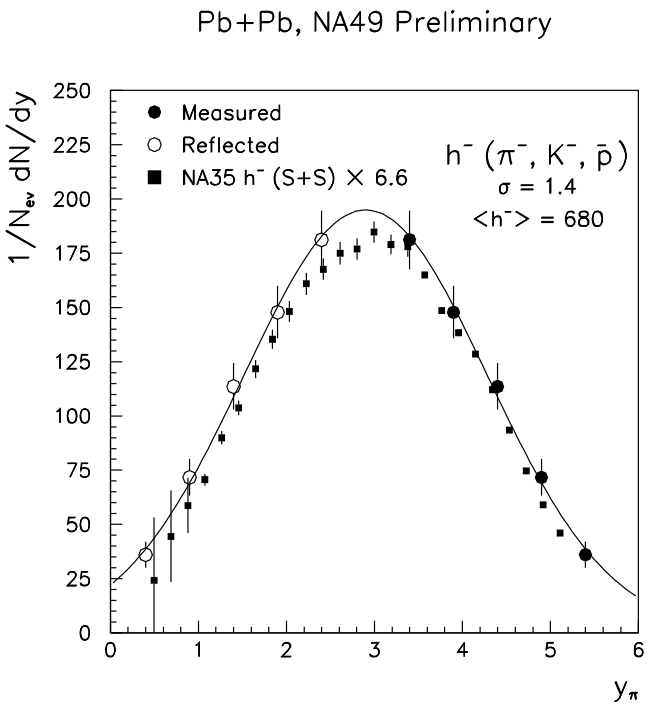

Figure 8. Rapidity density of negative hadrons for central collisions. The circles represent the preliminary Pb+Pb measurement by the NA49 collaboration [153], whereas the squares are from the NA35 S + S experiment [152]. The latter are scaled by a factor of 6.6, which corresponds to the relative number of participants. This scaled sulfur distribution agrees well with the lead distribution. The figure has been taken from [157].

stopping as assumed first in hydrodynamic model studies [43, 44] is observed. Therefore, results of theoretical analyses, which rely heavily on a net baryon-free mid-rapidity region with zero baryo-chemical potential have to be taken with care. The quantitative measurements of the A-dependent stopping of baryons is one of the most important results of the AGS and SPS measurements.

If the preliminary findings of a strongly peaked Λ rapidity distribution [144] and a rather broad Gaussian or flat baryon rapidity distribution [153] by the NA49 collaboration are both confirmed, then this would be a hard obstacle for models which rely on global thermal equilibrium (plus flow) for the description of the final state of the reaction [154–156].

Simple 'first collision models' without rescattering [111–114] do not suffice to reproduce the data, whereas transport theory has correctly predicted the observed degree of baryon stopping [99, 110, 126, 128, 129, 132]. An alternative mechanism of baryon stopping based on diquark breaking [158] is also able to describe the corresponding experimental data, in contrast to the simple first collision approach. These models extrapolated to RHIC energies imply that even at $\sqrt{s} = 200$ GeV/nucleon the dense matter is created with baryon density $\sim 2\rho_0$ at $\tau \sim 1$ fm/c. In [131] the beam energy dependence of the initial baryon density is estimated to vary as $1/s^{1/4}$.

The energy densities of $\epsilon \approx 3$ GeV fm^{-3} estimated (with a factor of $\approx$3 uncertainty) from rapidity distributions of produced particles indicate that part of the system may have entered the predicted state of deconfinement [49]. Hadronic transport models, however, predict or

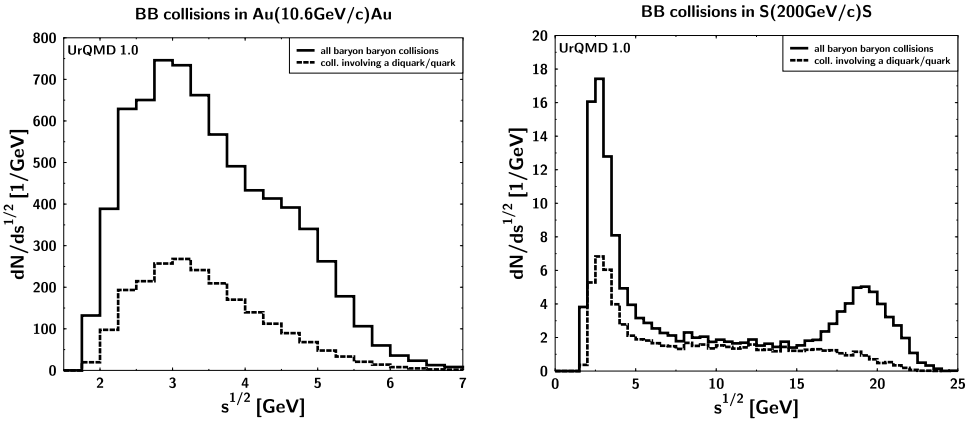

Figure 9. E_{CM}^{coll} distribution for baryon–baryon collisions in central Au + Au reactions at the AGS (left) and in central S + S reactions at the SPS, calculated with the UrQMD transport model [110].

reproduce the measured rapidity distributions, if baryon and meson rescattering and particle production via string decay [99,110,116,128,129] are included. Also, hadronic models which include multi-quark droplets [118] above $\epsilon_{\rm crit}$ seem to give similar results.

The inclusion of string excitations, collisions and decays are a first step towards modeling the parton/quark substructure of hadrons. In this sense these models go beyond what one would term a purely hadronic model. Figure 9 shows $\sqrt{s}$ distributions of baryon–baryon interactions for Au + Au collisions at AGS and S + S collisions at SPS energies [110]. At the AGS, the collision spectrum is dominated by collisions of fully formed baryons. It exhibits a maximum at low energies, $\sqrt{s} \approx 3$ GeV. Approximately 20% of the collisions involve a diquark, i.e. a leading baryon originating from a string decay. In contrast to the heavy system at AGS, the collision spectrum for S + S at SPS exhibits two pronounced peaks. They are dominated by full BB collisions, one peak at the energy of initial projectile–target collisions, and one peak in the low ('thermal') energy range. Approximately 50% of the BB collisions, most of them represented by the bump at intermediate $\sqrt{s}$ values, involve diquark or constituent quark collisions with baryons.

The linear scaling behaviour of the mass dependence of the negative hadron rapidity distributions precludes a strong pQCD minijet component at these energies. We note that the agreement of the VNI parton cascade model with the E_T systematics at SPS [159] may be due to adjusting a strongly model-dependent soft beam jet component to fit proton–proton data. This issue is important because in [160] it was claimed that at SPS already a partonic energy density $\geqslant$5 GeV fm^{-3} was created. The A^1 scaling of E_T therefore constrains very strongly against hard scattering models used, for example, in [161] to argue for a QGP interpretation of J/Ψ suppression. We return to this point later.

The experimental results demonstrate that highly excited dense matter is formed at mid-rapidity. They prove that a new state of elementary matter has been created. However, the inclusive central distributions do not give a clear and decisive answer to the question of whether this matter is predominantly of hadronic or quark nature.

3.2. Creation of high temperatures: particle spectra

3.2.1. Theoretical concepts. The hot, dense reaction zone consists of slowed down incident nucleons and produced particles. The *fireball* model considers these hadrons as a mixture of

ideal gases in thermodynamic equilibrium. For temperatures above 50 MeV and moderate densities, the Fermi and Bose–Einstein distribution functions for baryons and mesons (except for the pions) may be approximated by a Maxwell–Boltzmann distribution [162, 163] with the temperature T and the chemical potentials μ_i (connected to conserved quantum numbers i) as the only free parameters.

Kinetic equilibration is thought to be visible predominantly in the transverse degrees of freedom; therefore, transverse momentum or transverse mass distributions are used to extract temperatures from the spectral slopes.

It has been suggested that abnormal nuclear matter, e.g. a QGP, may be observed via a secondary, high-temperature component in the particle spectra or via a shoulder in the pion multiplicity distributions [164].

It has also been suggested that the EoS, that is the energy density ϵ versus temperature T, can be probed experimentally by plotting the mean transverse momentum $\langle p_t \rangle$ versus the rapidity density $\mathrm{d}N/\mathrm{d}y$ or the transverse energy density $\mathrm{d}N/\mathrm{d}E_T$. If a phase transition occurs (i.e. a rapid change in the number of degrees of freedom) one expects a monotonously rising curve interrupted by a plateau: this plateau is caused by the saturation of $\langle p_t \rangle$ during the mixed phase. After the phase transition from e.g. colour singlet states to coloured constituents has been completed [165] the mean transverse momentum rises again. However, detailed hydrodynamical studies [166, 167] showed that the plateau is washed out due to collective flow.

Collective (radial) flow [54, 164, 182] as well as feeding from resonances strongly influence the shape of the particle spectra [164, 168–173]. For light composite particles, such as deuterons, the influence of collective flow is visible in a shoulder-arm shape of the transverse momentum spectra [164]. This can be seen in figure 10. In order to account for flow effects, the spectra can be fitted with a thermal distribution including collective flow. The temperature T and the transverse flow velocity β_t are the fit parameters. The shapes of the velocity profile and density profile at freeze-out should enter as additional degrees of freedom in the analysis. Usually a box-shaped density profile and a linearly increasing transverse velocity profile are assumed [155, 164, 168, 174]. This results in severe distortions into the analysis, as discussed below [175].

When extracting temperatures and flow velocities from microscopic calculations, the system is divided into cells and the *local* transverse and longitudinal velocity distributions are analysed [125, 137, 173, 176]. The temperatures extracted via a global two-parameter fit are more than a factor of two higher than the temperatures gained from such a microscopic analysis at beam energies in the 100 MeV/nucleon to 10 GeV/nucleon regime [176]. The reason for this discrepancy lies mostly in the assumed shape of the freeze-out density profiles.

Whereas a linearly increasing transverse freeze-out velocity profile seems a tolerable assumption, the shape of the freeze-out density profile has—due to collective flow—a Gaussian shape (centred at $r_t = 0$), rather than the usually assumed box-shape distribution. When realistic density and velocity profiles are used, one finds that the high m_t components of the particle spectra reflect contributions of large collective flow effects (i.e. the high expansion velocity). This analysis yields substantially lower values for the temperatures T. Such microscopic analyses of the spectra of protons, mesons and light composite particles at AGS energies show also that β_t and T depend on the mass of the particle [173, 177].

3.2.2. Experimental status. Data taken at the AGS with Si beams [140] seem on first sight to be consistent with an expanding, hadro-chemically and thermally equilibrated system with a temperature of 130 ± 10 MeV and a transverse flow velocity of $\beta_t \approx 0.36$ [155, 174]. CERN SPS data with S beams have been fitted in the same fashion, with apparent temperatures

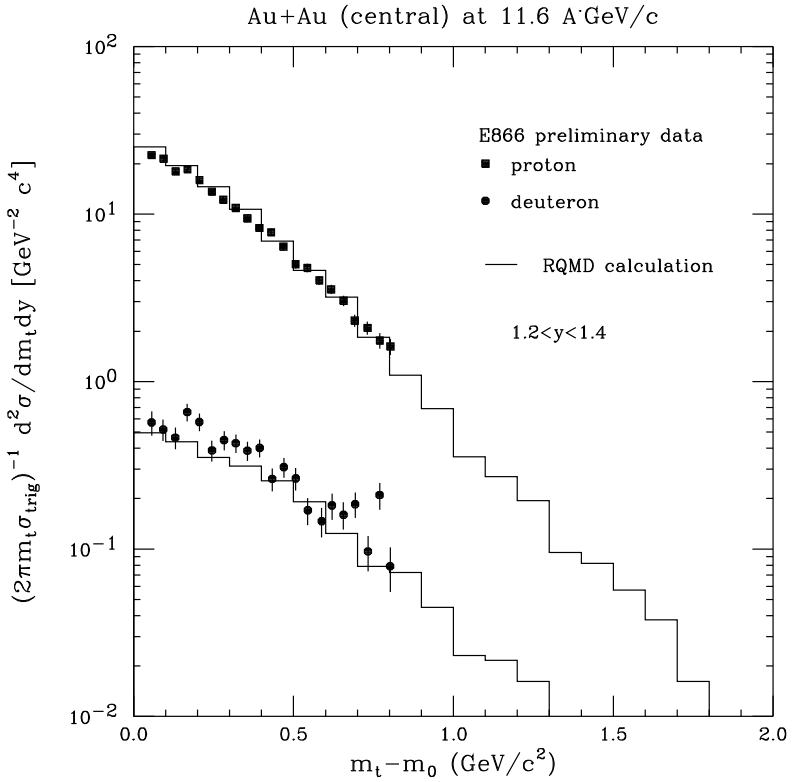

Figure 10. RQMD prediction of transverse mass spectra for protons and deuterons in central Au + Au collisions at the AGS compared with preliminary data by the E866 collaboration. For deuterons a shoulder is visible in the low m_t range of the spectrum. This structure is due to collective flow. The figure has been taken from [173].

around 150 MeV and flow velocities between 0.35 and 0.41 [156, 170]. Figure 11 shows the extracted excitation function for the temperature T and the average transverse expansion velocity β_t [178], including also SIS and BEVALAC data.

In order to disentangle collective flow contributions from thermal motion, the dependence of the slope parameter T_{sl} (which includes collective flow effects) on the collision system mass and the particle mass has been studied by the NA44 and NA49 collaborations [153, 179] at the SPS. Results can be seen in figure 12. In proton–proton collisions obviously no collective effects are visible and an inverse slope parameter of $T_{sl,pp} = 145$ MeV is extracted for all analysed particle species (π, K and p). When going to heavier collision systems, collective flow effects become obvious: the inverse slope parameter T_{sl} increases with the mass of the emitted particle (see figure 12). Empirically one finds $T_{sl} = T_{sl,pp} + m \cdot \langle\beta_t\rangle^2$. β_t is the mean expansion velocity which depends on the mass of the collision system and m is the mass of the particle analysed.

The constant $T_{sl,pp}$ in the empirical result therefore hints at the predicted *limiting temperature* [164, 181] of $140 \leqslant T \leqslant 200$ MeV. The observation of the increase of the flow effects for massive particles and heavy collision systems had been predicted with early hydrodynamical and microscopic calculations [43, 164, 180, 182, 183, 187].

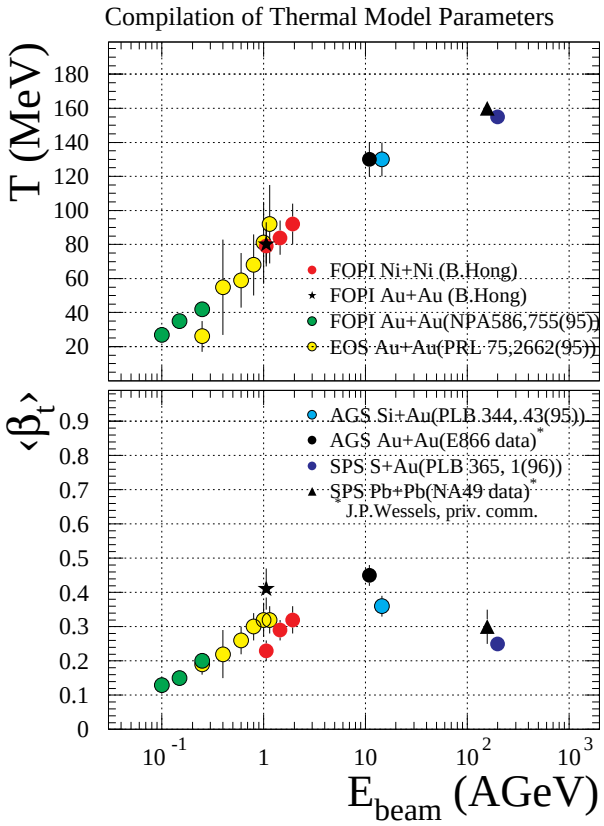

Figure 11. Excitation function of temperature T and average transverse expansion velocity β_t. The figure has been taken from [178].

3.2.3. Discussion. The data at AGS and CERN seem compatible with a hadro-chemically and thermally equilibrated system. However, this does not mean that the system necessarily evolved through thermal and chemical equilibrium states [176, 184, 185]. The fits to the spectra, with the temperature T and the transverse expansion velocity β_t as parameters, have to be performed with great care. There is a broad range of T and β_t values which are compatible with the same spectrum [164, 170, 171, 176], where the temperature T depends crucially on the freeze-out density and velocity profiles—at least in the case of composite particles such as deuterons and tritons [173, 175, 180, 186].

The finding of one global freeze-out temperature T and velocity β_t [155, 174] is to be contrasted with the independent analysis based on RQMD and UrQMD calculations of spectra of light composite particles [173, 175, 184] and on spectra of mesons [110, 184, 187]. These models are well able to reproduce the data and the analysis indicates different values (with a variation of $\sim$20%) for β_t and T, depending on the mass of the particle. The simplified thermal plus flow model [155, 164, 170, 174] should not be taken literally. In reality we expect a complicated spacetime-dependent non-equilibrium freeze-out, details depending on inelastic production and absorption cross sections. In particular, the antibaryon annihilation cross sections play an important role, as will be discussed below (section 3.3). Furthermore, flow of mesons versus baryons [188, 189] in opposite directions clearly indicate strong deviations from the single source fits as discussed in the following section.

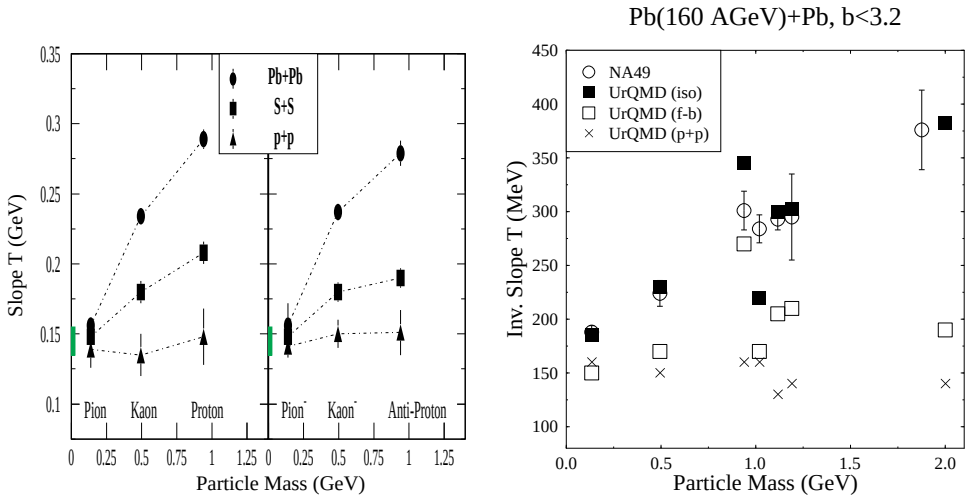

Figure 12. Mass and collision system dependence of the inverse slope parameter T measured by the NA44 collaboration [179] (left) and calculated by the UrQMD model (right) [180].

Recently, the WA98 collaboration reported π^0 spectra in Pb + Pb reactions for p_t up to 4 GeV/c [190]. The data could be fit well by hydrodynamical models [191]. However, it was found in [192] that the data were well reproduced by the QCD parton model. In this sense (the non-equilibrium) quark plasma is seen in the high p_t spectra. However, as emphasized in [193], at SPS the parton model is hypersensitive to models for soft multiple collisions. Hydrodynamics just happens to be one of the soft multiple collision models that can account for the data.

3.3. Transverse collective radial and directed flow

3.3.1. Theoretical concepts. The excitation function of transverse collective flow is the earliest predicted signature for probing compressed nuclear matter [54, 57]. It has been shown that the excitation function of flow is sensitive to the EoS and can be used to search for abnormal matter states and phase transitions [43, 194, 195].

In the fluid dynamical approach, the transverse collective flow is directly linked to the pressure of the matter in the reaction zone.

With the pressure $P(\rho, S)$ (depending on the density ρ and the entropy S), one can get a physical feeling for the generated collective transverse momentum $\vec{p}_x$ by writing it as an integral of the pressure acting on a surface and over time [196]:

$$\vec{p}_x = \int_t \int_A P(\rho, S)\, \mathrm{d}A\, \mathrm{d}t \tag{2}$$

where $\mathrm{d}A$ represents the surface element between the participant and spectator matters and the total pressure is the sum of the potential pressure and the kinetic pressure: the transverse collective flow depends directly on the EoS, $P(\rho, S)$.

Directed collective flow has been predicted by NFD [54, 57, 197–199]. Microscopic models such as VUU (Vlasov–Uehling–Uhlenbeck), and QMD (quantum molecular dynamics) have predicted smaller flow than ideal NFD, these models show good agreement with viscous NFD [126] and with the experimental findings [124, 200–202]. It has been discovered initially at the the BEVALAC [203–205] for charged particles by the Plastic Ball and Steamer Chamber

collaborations [206], at SATURNE by the DIOGENE collaboration [207] and has been studied extensively at GSI by the FOPI [178, 208], LAND [209], TAPS [210] and KaoS [211] collaborations.

One has to distinguish two different signatures of directed collective flow:

(a) The *bounce-off* [197] of compressed matter *in the reaction plane* and
(b) the *squeeze-out* [198] of the participant matter *out of the reaction plane*.

The most strongly stopped, compressed matter around mid-rapidity is seen directly in the *squeeze-out* [212]. A strong dependence of these collective effects on the nuclear EoS is predicted [202]. For higher beam energies, however, projectile and target spectator decouple quickly from the reaction zone, giving way to a preferential emission of matter in the reaction plane, even at mid-rapidity [213]. An excitation function of the *squeeze-out* at mid-rapidity, possibly showing the transition from out-of-plane enhancement to preferential in-plane emission has been predicted to enhance the sensitivity to the nuclear EoS [110, 214].

Apart from the above-discussed *directed* flow, the so-called 'radial', i.e. undirected, flow component can be used for simplicity (azimuthal symmetry) [164, 182]. It has to be taken into account for the interpretation of particle spectra used for temperature extraction which may drop by as much as a factor of two.

Due to its direct dependence on the EoS, $P(\rho, T)$, flow excitation functions can provide unique information about phase transitions: the formation of abnormal nuclear matter, e.g., yields a reduction of the collective flow [194]. A directed flow excitation function as signature of the phase transition into the QGP has been proposed by several authors [43, 119]. A microscopic analysis showed that the existence of a first-order phase transition can show up as a reduction in the directed transverse flow [212].

For first-order phase transitions, the pressure remains constant in the region of the phase coexistence. This results in a vanishing velocity of sound $c_s = \sqrt{\partial p/\partial \varepsilon}$.

The expansion of the system is driven by the pressure gradients, therefore expansion depends crucially on c_s^2. Matter in the mixed phase expands less rapidly than a hadron gas or a QGP at the same energy density and entropy. In case of rapid changes in the EoS without phase transition, the pressure gradients are finite, but still smaller than for an ideal gas EoS, and therefore the system expands more slowly [166, 167].

This reduction of c_s^2 in the transition region is commonly referred to as *softening* of the EoS. The respective region of energy densities has been called the *soft region* [183, 215–217]. Here the flow will temporarily slow down (or possibly even stall). Consequently a *time delay* is expected in the expansion of the system. This prevents the deflection of spectator matter (the *bounce-off*) and, therefore, causes a reduction of the directed transverse flow [218, 219] in semi-peripheral collisions. The softening of the EoS should be observable in the excitation function of the transverse directed flow of baryons (see figure 13).

The overall decrease of $\vec{p}_x$ seen in figure 13 for $E_{lab} > 10$ GeV both for the hadronic and the QGP EoS demonstrates that faster spectators are less easily deflected (because A and t in equation (2) are decreasing with E_{lab}) by the hot, expanding participant matter. For the QGP EoS, however, these one-fluid calculations show a *local minimum* in the excitation function, at about 6 GeV/nucleon. This can be related to the QGP phase transition, i.e. to the existence of the *soft region* in the EoS.

The limitation of one-fluid hydrodynamic calculations is that they assume instantaneous thermalization. This becomes unrealistic for increasing beam energies since due to the average rapidity loss of only one unit per proton–proton collision, nucleons require several collisions for thermalization. A more realistic three-fluid calculation, in which the third fluid represents the *fireball* of produced particles and only local thermal equilibrium is assumed, yields much lower

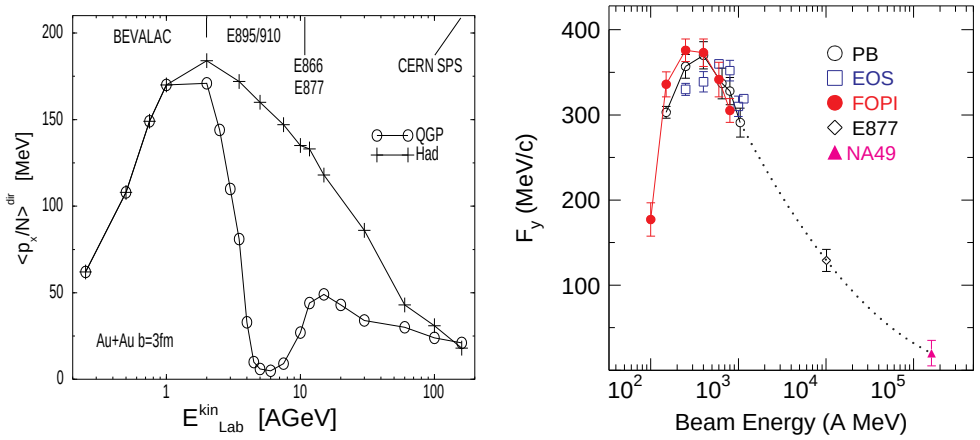

Figure 13. Excitation function of directed transverse flow. Left: prediction in the framework of nuclear hydrodynamics [216, 219], with and without deconfinement phase transition. In the case of a phase transition a minimum in the excitation function is clearly visible. Right: Data compilation taken from [443].

flow values—even without a first-order phase transition [120]. The position of the minimum (the magnitude of the overall effect) therefore strongly depends on the degree of stopping (i.e. which type of fluid-dynamical model is employed) and on the details of the chosen EoS and phase transition parameters.

Taking the finite volume of the reaction zone into account, one finds that fluctuations hinder a sharp separation between the QGP phase and the hadronic phase and lead to a *rounding* of the phase transition [84]. For realistic reaction volumes the softening of the EoS is reduced considerably and thus the minimum signal in the flow excitation function is washed out.

A second-order phase transition may not exhibit this minimum in the flow excitation function: The existence of a minimum in $p_{x,dir}(E_{lab})$ is rather a *qualitative* signal for a strong first-order transition. If such a drop of $p_{x,dir}(E_{lab})$ is observed, it remains to be seen which phase transition caused this behaviour: a hadron–quark-gluon phase transition or, e.g., a resonance matter to ground state matter phase transition in confined nuclear matter [135, 220].

3.3.2. Experimental status. Collective flow measurements have first been performed at the BEVALAC [203–205] for charged particles by the Plastic Ball and Streamer Chamber collaborations. A more detailed investigation of the excitation function between 0.1 and 1.2 GeV/nucleon for Au + Au has been performed by the FOPI, KaoS, LAND and TAPS collaborations at GSI [178, 209–211] and the EOS–TPC collaboration at LBNL [221] (see figure 15).

At 10.6 GeV collective flow has recently been discovered by the E877 collaboration [222, 223]. Figure 16 shows $\mathrm{d}v_1/\mathrm{d}\eta = \mathrm{d}(\langle E_x\rangle/\langle E_T\rangle)/\mathrm{d}\eta$ for different centrality bins. The E895 group has measured the flow excitation function for Au + Au at the AGS in the energy range 2.0–10.6 GeV/nucleon [224]. Their data show a smooth decrease in $\langle p_x\rangle$ from 2–8 GeV/nucleon and are corroborated by measurements of the E917 collaboration at 8 and 10.6 GeV/nucleon [225].

The E895 collaboration has also measured an elliptic flow excitation function indicating a transition from out-of-plane enhancement (i.e. *squeeze-out*) to in-plane enhancement around 5 GeV/nucleon [226].

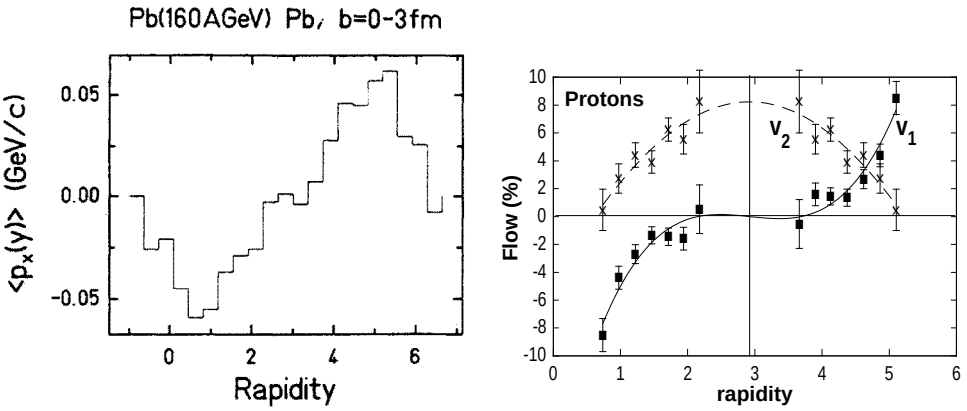

Figure 14. RQMD 1.05 prediction of collective sideward flow for the system Pb + Pb at 160 GeV (left, figure taken from [129]). The rhs shows data on directed and elliptic flow versus rapidity by the NA49 collaboration (figure taken from [231]).

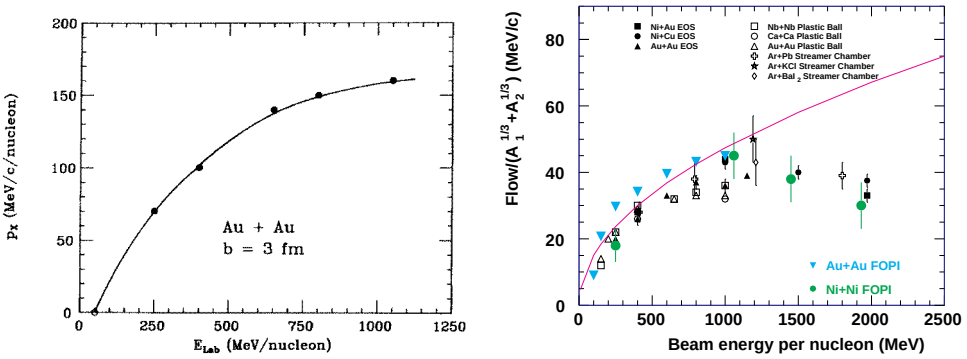

Figure 15. Excitation function of directed transverse flow for different collision systems from 100 MeV/nucleon up to 2 GeV/nucleon. Left: VUU prediction [43, 101] for the system Au + Au. Right: data from the Streamer Chamber, Plastic Ball and EOS experiments at the BEVALAC and from the FOPI experiment at SIS [178, 203–205, 221] (the figure has been taken from [178]). The data has been scaled by $(A_1^{\frac{1}{3}} + A_2^{\frac{1}{3}})$ to account for the different collision systems.

At CERN/SPS, the existence of undirected flow has been deduced from a combined analysis of particle spectra [156, 227] and HBT correlations [228] (see also sections 3.2 and 3.4).

First observations of a directed transverse flow component have been reported by the WA98 collaboration [229, 230] using the Plastic Ball detector located at target rapidity for event plane reconstruction. They show a strong directed flow signal for protons and 'antiflow' for pions, both enhanced for particles with high transverse momenta. The same findings have been reported from the NA49 collaboration which, due to its larger acceptance, allows for an even more detailed investigation. They report a quite strong elliptic flow signal near mid-rapidity at 160 GeV/nucleon [231] (see figure 14).

3.3.3. Discussion. An observation of the predicted local minimum in the excitation function of the directed transverse flow [216,219] would be an important discovery, and an unambiguous signal for a phase transition in dense matter. Its experimental measurement would serve as

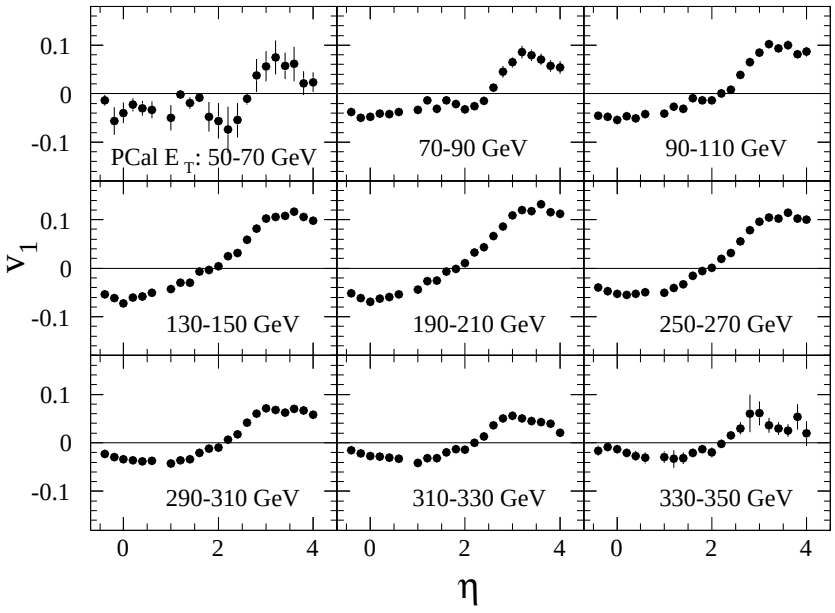

Figure 16. Transverse collective flow measured at the AGS by the E877 collaboration [223]. Plotted is $\mathrm{d}v_1/\mathrm{d}\eta = \mathrm{d}(\langle E_x\rangle/\langle E_T\rangle)/\mathrm{d}\eta$ which is a similar quantity as $\mathrm{d}(\langle p_x\rangle/\langle p_t\rangle)\mathrm{d}y$, used at lower beam energies.

strong evidence for a QGP and a strongly first-order deconfinement transition at nonzero baryon density.

A strong experimental effort at the AGS and SPS has led to the discovery of flow even at these ultra-relativistic energies. The search for the minimum signal in the excitation function is under way.

The absolute values for the ideal NFD prediction of directed flow shown in figure 13 overestimate the experimental values considerably [216, 217] due to lack of viscosity [126]. The position of the minimum in $p_{x,dir}(E_{lab})$ depends on the EoS—therefore it is by no means clear where (in E_{lab}) the deconfinement phase transition will occur. Furthermore, finite-volume corrections reduce the *softening* of the EoS and might reduce the minimum signal considerably [84].

The combined efforts of the FOPI and EOS/E895 collaborations will allow the mapping experimentally of the region from 0.1–10 GeV/nucleon. However, the current data show a smooth decrease in the flow from 2–10 GeV. This seems to favor a hadronic scenario without a phase transition. An experimental search for this outset of flow in the energy range 10–200 GeV/nucleon seems necessary.

The recent measurement of the *squeeze-out* excitation function between 2–8 GeV/nucleon may offer a new approach for studying the nuclear EoS [110, 214, 226].

The comparison of proton spectra with ϕ-meson spectra may help to disentangle 'early', QGP-related flow components from 'late', hadronic contributions. Transport model calculations have shown that the ϕ-meson decouples much earlier from the system ($\approx$12 fm/c) than the nucleons [232]. Since both particles have approximately the same mass, their 'thermal' motion and undirected flow components should be identical and any differences in the spectra should arise only through the additional interaction the nucleons suffer in the later reaction stages [232].

3.4. Spacetime pictures of the reaction: HBT source radii

3.4.1. Theoretical concepts. Intensity interferometry of identical particle pairs, such as $\pi\pi$, KK or pp pairs, can be used to extract information about the spacetime dynamics, freeze-out volume and reaction geometry of heavy-ion collisions. The method was originally devised by Hanbury-Brown and Twiss to measure the angular diameter of a star using the correlation of two photons [233]:

The probability of detecting two photons in coincidence in two different detectors is correlated to the relative separation between the two detectors. This correlation is connected to the angular diameter of the emitting source. This effect is commonly known as the *Hanbury-Brown–Twiss (HBT) effect*. It has been also observed in proton–antiproton annihilations [234].

By applying the HBT measurements to particles emitted in heavy-ion reactions, such as protons, pions or kaons, the two-particle correlation function yields the longitudinal and transverse radii as well as the lifetime and flow pattern of the emitting source at the moment of freeze-out [235–240]. The inverse widths R_{out} of the 'out' correlation function and R_{side} of the 'side' correlation function can be used to extract a measure for the duration of particle emission ($R_{out}^2 - R_{side}^2$) and the transverse size of the source (R_{side}) [238, 239].

The prolonged lifetime of the collision system in the mixed phase, which has already been discussed in section 3.3, can be observed through an enhancement of the ratio of inverse widths (R_{out}/R_{side}) of the two-particle correlation function in out- and side-direction [217, 238, 241, 242] For energy densities estimated to be reached in Pb + Pb collisions at the CERN/SPS one expects $R_{out}/R_{side} \sim 1.5$–2 [217]. Inclusion of the decays of long-lived resonances may however reduce the R_{out}/R_{side} ratio [243–247].

Final-state interactions between non-identical particles can provide information not only about the duration of the emission but also about its time-ordering. It has recently been shown that an anisotropy in the spacetime distribution of emitted particles reflects in the directional dependence of unlike-particle correlations (e.g. p–K) and can thus directly be used to measure the sequence of the emission of particles of different types [248]. Applying this technique to the correlation between a *strange* and an *anti-strange* particle (e.g. K^+K^- interferometry) [249] may result in the direct observation of the strangeness distillation process [250] (see section 3.6). That process—which is instrumental to the formation of so-called *strangelets*—predicts an enrichment of s quarks in the quark phase while the $\bar{s}$ quarks drift into the hadronic phase. The resulting time-ordering of the freeze-out for *strange* and *anti-strange* particles is to be compared with the (different) emission times due to the different mean free paths in a purely hadronic scenario [249].

A combined analysis of single- and two-particle spectra can yield a rather complex reconstruction of the geometry and dynamical state of the source at freeze-out [251]. This information can be used as a powerful test for dynamical simulations of the collision process.

3.4.2. Experimental status K^+K^+ and K^-K^- measurements at the SPS [253] show similar radii around 2.7 ($\pm$10%) fm for the system S + Pb. Since the K^-–nucleon interaction cross section is far larger than the K^+–nucleon cross section, this result indicates that the dominant interaction for kaons in the later reaction stages (close to freeze-out) at SPS energies are K–π interactions [255]. At AGS energies, the situation might be different: the baryon to meson multiplicity ratio is approximately one, there. A detailed analysis has yet to be performed. Radii extracted from $\pi\pi$ correlations are larger than those from KK, both at AGS and SPS energies [253, 256]. The differences are caused by different interaction cross sections and resonance decays [257,258], plus the effect of collective expansion [240,259]. More theoretical work is needed to separate these effects.

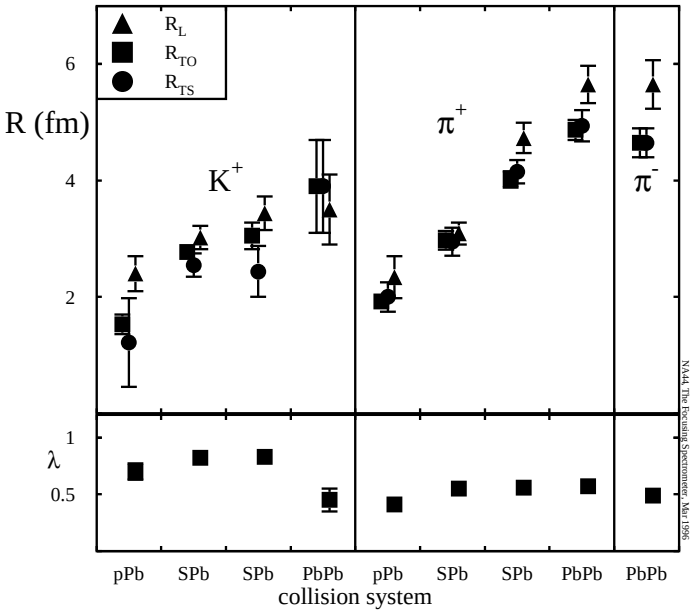

Figure 17. Systematics of HBT radius parameters, compiled from data by the NA44. The figure has been taken from [261].

For central collisions of heavy systems the extracted transverse radii are of the order of 5–7 fm for the $\pi\pi$ (both, AGS and SPS) and 3 fm (AGS) to 4 fm (SPS) for the KK system [260–264].

The longitudinal and transverse radii measured at the SPS are larger than the respective radii of both the projectile and the target, indicating an expansion of the system prior to freeze-out [251, 265]. Data with the sulfur beam at the SPS show that the longitudinal radii measured as a function of rapidity [266] could be fitted by a boost invariant longitudinal expansion [267]. Recent data taken with the lead beam by the NA49 collaboration confirm this finding for the Pb + Pb system [228, 262, 264, 268].

Transverse source radii for $\pi\pi$ show a decrease from 4 to 2.5 fm for S + S and from 6 to 4 fm for Pb + Pb, respectively, with increasing transverse momentum of the pions (see also figure 17) [262–264, 266]; this behaviour is to be expected in the presence of transverse flow [237–239]. Alternatively, it can also be explained by microscopic models which predict that high p_t particles are emitted in the early reaction stages (by heavy resonances or strings) and low p_t particles (which have rescattered more often) have late freeze-out times [137, 269]. Measurements of R_{out}/R_{side} indicate values on the order of 1 [265]. For the Pb + Pb system, a duration of emission of about 3–4 fm/c has been reported with the lifetime of the source being $\tau \approx 8$ fm/c [264].

Source radii cannot only be studied as a function of transverse momentum or beam energy, but also as a function of impact parameter related quantities, such as the number of participant nucleons. The latter analysis can be performed either by comparing central events of different systems or by comparing different centralities in very heavy systems.

Exciting preliminary results have been reported at QM '96 for the system Au + Au at 10.6 GeV/nucleon by the E866 collaboration [270], showing a dramatic increase of 40% in the source radius over the last 7% of highest centrality. More recent data sets of the same

collaboration suggest a more gradual increase with centrality [271]. The limited statistics, however, do not permit a final assessment, yet.

3.4.3. Discussion. At AGS energies hadronic transport models are well able to reproduce the measured source radii [256, 260]—at SPS energies a full analysis has not yet been performed, but early comparisons showed at least qualitative agreement [253, 256].

A strong first-order phase transition [238, 241] and even an infinite-order but rapid cross-over transition [217] should result in a lower pressure, slower expansion and perhaps a long-lived evaporating droplet of QGP. The rather short lifetime of $\tau \approx 8$ fm/c [264] for Pb + Pb at CERN/SPS suggests either the non-existence of such a low-pressure system or perhaps that the initial energy density that is needed to create a QGP is much higher [217, 238].

HBT interferometry so far shows no evidence for the characteristic time delay of QGP formation up to SPS energies. The main complication of HBT analysis in nuclear collisions is the existence of strong collective flow that (Doppler) distorts the interference pattern. The p_t dependence of the HBT radii has become a useful tool to probe this aspect of the reaction dynamics. It will be important to search for time signatures at RHIC and LHC.

3.5. Remnants of hadronization: strangeness enhancement

3.5.1. Theoretical concepts. In proton–proton collisions, the production of particles containing strange quarks is strongly suppressed as compared with the production of particles with u and d quarks [272, 273]. It has been argued that this suppression is due to the higher mass of the $s\bar{s}$ quark pair. The suppression increases with the strangeness content of the particles produced in proton proton collisions.

In the case of QGP formation, $s\bar{s}$ pairs can either be produced via the interactions of two gluons or of $q\bar{q}$ pairs. Leading order α_s pQCD calculations suggest that the second process dominates only for $\sqrt{s} \leqslant 0.6$ GeV [274]. The timescale of chemical equilibration of (anti-)strangeness due to gluon–gluon interaction is estimated—also based on first-order pQCD calculations—to be about 3–6 fm/c, depending on the temperature of the plasma [275].

Following this line of argument, the yield of strange and multi-strange mesons and (anti-) baryons has been predicted to be strongly enhanced in the presence of a QGP as compared to a purely hadronic scenario at the same temperature [276, 277]. However, the estimated equilibration times may not be sufficiently rapid to cause a saturation in the production of strange hadrons before QGP freeze-out.

In particular, assuming low chemical potentials, $\mu_d \approx \mu_u \approx 0 = \mu_s$ and a temperature T higher than the strange quark mass m_s, the densities of all quarks and antiquarks are nearly the same in the QGP. Hence, the probability of forming antihyperons by combining $\bar{u}$, $\bar{d}$ and $\bar{s}$ quarks is nearly the same as the probability of forming strange and non-strange baryons by combining u, d and s quarks if the freeze-out process is rapid and annihilation can be neglected.

In contrast, the production of an antihyperon–hyperon pair produced in nucleon–nucleon collisions is greatly suppressed by the Schwinger factor [278, 279] since it is necessary to tunnel the massive diquark and the strange quark through the potential wall in the chromo-electric field with the string tension $\kappa \approx 1$ GeV/fm [280]. The enhanced production of antihyperons ($\bar{\Lambda}$, $\bar{\Sigma}$, $\bar{\Xi}$ and $\bar{\Omega}$) can therefore be used as a QGP signal in the case of zero chemical potential [275].

If a QGP is created in heavy-ion collisions at AGS or SPS energies, it will most likely be characterized by nonzero chemical potentials μ_u and μ_d. This results in the densities of u and d quarks being larger than those of the s and $\bar{s}$ quarks, which in turn are larger than the $\bar{u}$ and $\bar{d}$ densities. Due to these different abundances the $\bar{s}$ quark is more likely to combine with a u or d quark to form a K^+ or K^0 (or with two non-strange quarks to form a Λ or Σ, respectively) than

it is for the s quark to recombine with a $\bar{u}$ or $\bar{d}$ quark thus forming a $\bar{K}^0$s or $\bar{K}^-$s. Therefore, in the QGP case the K^+/π^+ ratio in a relativistic heavy-ion collision is different from the K^-/π^- ratio [281].

The relative abundances of various strange particle species have been used for the determination of relative strangeness equilibration. To account for incomplete chemical equilibration, a strangeness fugacity γ_s is introduced in a thermochemical approach [49, 282–284]. One has also compared the measured ratios and the connected thermodynamic variables (such as T, μ_B and the entropy) with calculations, either assuming a hadron gas scenario or a QGP scenario including some hadronization scheme [155, 174, 285, 286].

There are certain drawbacks to the line of argument presented above: The strange particle abundances, after freeze out from a QGP, are very close to those of a fully equilibrated hadron gas at the same entropy content [287]. The reason is [281, 288, 289] that the volume of a hadron gas of the same total energy has to be larger due to the smaller number of available degrees of freedom. Consequently, one must expect that the abundance of strange quarks is diluted during the hadronization process. This dilution effect is clearly seen in hadronization models [277, 290], where gluons hadronize by conversion into quark–antiquark pairs, which predominantly feed the final pion channel. As a consequence, the K/π ratios are significantly reduced.

Furthermore, the computation of particle abundances in the QGP and the hadron gas scenario are mostly based on the assumption of chemical and thermal equilibrium (a non-equilibrium calculation has been published in [290]). For the hadronic case these assumptions cannot be justified. It has been shown via rate equations [277, 281] that the strangeness equilibration time exceeds the reaction time of a heavy-ion collision by at least one order of magnitude.

Strangeness production in the hadronic scenario is a non-equilibrium process. In the early (pre-equilibrium) reaction stages, typical longitudinal momenta are much higher than in the case of a thermal momentum distribution. This leads to enhanced strangeness production [232, 291]. The system then cools down in the course of the reaction. Its final 'equilibrium' temperature is therefore only partly connected to the measured strange particle yields and spectra.

3.5.2. Experimental status. An enhancement of the K/π ratio has been measured both at the AGS and at the SPS [292]. At the AGS, $K^+/\pi^+ \approx 0.2$ and $K^-/\pi^- \approx 0.04$. Furthermore K^+/K^-, $\bar{\Lambda}/\Lambda$ and $\bar{p}/p$ production ratios have been measured at the AGS [140]. At the SPS, enhanced production of (anti)hyperons, such as $\bar{\Lambda}$, $\bar{\Xi}$, Ω and $\bar{\Omega}$, has been observed and ratios of $\bar{\Lambda}/\Lambda$, $\bar{\Xi}/\Xi$, Ξ/Λ and $\bar{\Xi}/\bar{\Lambda}$ have been analysed by the NA36,WA85 and WA97 collaborations [293–300]. The WA94 collaboration has measured antihyperon ratios (i.e. the $\bar{\Xi}/\bar{\Lambda}$ ratio) in pp, pA and AA reactions. They find a smooth increase in the $\bar{\Xi}/\bar{\Lambda}$ value from pp over pA to AA [301].

Recently, very interesting values have been quoted for the $\bar{\Lambda}/\bar{p}$ ratio. It has been measured by the NA35, NA49, E866, E878 and E864 collaborations [153, 303–305]. Since it only contains newly produced antiquarks, it may therefore represent a rather clean measure for the $\bar{s}/\bar{u}$ quark ratio in the hot and dense matter. For pp and pA collisions this ratio is below 0.4, whereas in AA collisions preliminary analysis give values between 3 and 5 [144, 305]—these values are so high that they could not be obtained in either a hadron gas or QGP model with reasonable values for T, μ_B and μ_S.

The observed strong enhancement of multistrange (anti)hyperons (Ξ, Ω, $\bar{\Xi}$, and $\bar{\Omega}$) from light to heavy collision systems at the CERN/SPS [300–302] surely constitutes, on the experimental side, the most intriguing evidence for a possible non-hadronic enhancement of strangeness.

3.5.3. Discussion. Hadronic models for particle production [99, 287, 291, 306, 307] work quite well in the case of the observed K^+/π^+ enhancement [292] at the AGS (silicon beam). The reason for strangeness enhancement in a hadronic scenario is multistep excitation of heavy baryon and meson resonance states [291]. The AGS value of $K^+/\pi^+ \approx 0.2$ is compatible with a strangeness equilibrated hadron gas [174].

AGS data of K^+/K^-, $\bar{\Lambda}/\Lambda$ and $\bar{p}/p$ ratios can be fitted with an equilibrated hadronic fireball with $\mu_s/T = 0.54 \pm 0.11$ and $\mu_B/T = 3.9 \pm 0.3$ [155, 174, 308]. However, this does not mean that the system has always been in the hadronic phase, since an equilibrium state has no memory of how it has been produced. The system might as well have originated in the quark phase and then evolve along the phase boundary, thereby hadronizing with varying combinations of T, μ_B and μ_S. The point is that these ratios provide actually very little information about the properties of the early time dense system.

The ratios $\bar{\Lambda}/\Lambda$, $\bar{\Xi}/\Xi$, Ξ/Λ and $\bar{\Xi}/\bar{\Lambda}$ measured by the WA85 and WA97 collaborations [295–297] at the SPS can be fit in analogy to the ratios at the AGS by an equilibrium hadron gas model with $\gamma_s = 0.7$, $\mu_B = 0.24$ and $T = 180$ MeV [154]. Besides the three parameters T, μ_B and μ_S which are used in the grand-canonical formalism of statistical mechanics, the additional parameter γ_s accounts for incomplete saturation of strange particles in phase space. However, data can also be fitted with a hadron gas model and $\gamma_s \approx 1$ with $\mu_s/T = 0.24$–0.28 and $\mu_B/T = 1.05$ [156], respectively. The very same data can also be fit by an instantaneously hadronizing non-equilibrated QGP with strangeness neutrality and strangeness saturation $\gamma_s \geqslant 0.7$ [285, 309, 310].

Are the extracted temperatures and chemical potentials really reliable in view of the simple, static, thermal ansatz? Even hadron production in high energy pp and $p\bar{p}$ collisions has been calculated by assuming thermal and chemical equilibrium and fits the data well [311]. The fit temperature lies around 130–170 MeV, nearly independent of the centre of mass energy of the incident particles. A γ_s value of $\approx$0.5 is needed for the fit, indicating incomplete strangeness saturation already at the pp level. Does such a model make sense? The success of the fit can be interpreted as hadron production in elementary high energy collisions being dominated by phase space rather than by microscopic dynamics.

The extrapolation of this conclusion to heavy-ion collisions, however, may not be valid: even simple dynamical hadronization schemes [312], where thermodynamic equilibrium between a quark blob and the hadron layer is imposed, reveal a more complex picture (see figure 18). Particle ratios can be reproduced nicely with the same number of parameters as in the static ansatz of a hadron gas in equilibrium, while the spacetime evolution of the system shows strong changes of the strange and baryochemical potentials due to baryon- and strangeness-distillery [313, 314]. Taking (boost-invariant) longitudinal hydrodynamical expansion into account, the interplay of the evaporation process and the hydrodynamical expansion (and vice versa) leads to considerably shorter lifetimes of the mixed phase as compared with scenarios without hydrodynamical expansion [315]. It is very questionable whether final particle yields reflect the actual thermodynamic properties of the system at any one stage of the evolution.

Microscopic transport model calculations are in good agreement with the measured hadron ratios of the system S + Au at CERN/SPS [316, 317]. They show, however, that those ratios exhibit a strong rapidity dependence. Thus, thermal model fits to data may be distorted due to varying experimental acceptances for individual ratios. A thermal model fit to S + Au ratios calculated with the microscopic UrQMD transport model (and extracted within the same range of rapidity for all ratios) yields a temperature of $T = 145$ MeV and a chemical potential of $\mu_B = 165$ MeV [316]. Hadron ratios for the system Pb+Pb are predicted and can be fitted by a thermal model with $T = 140$ MeV and $\mu_B = 210$ MeV. Similar results have been obtained

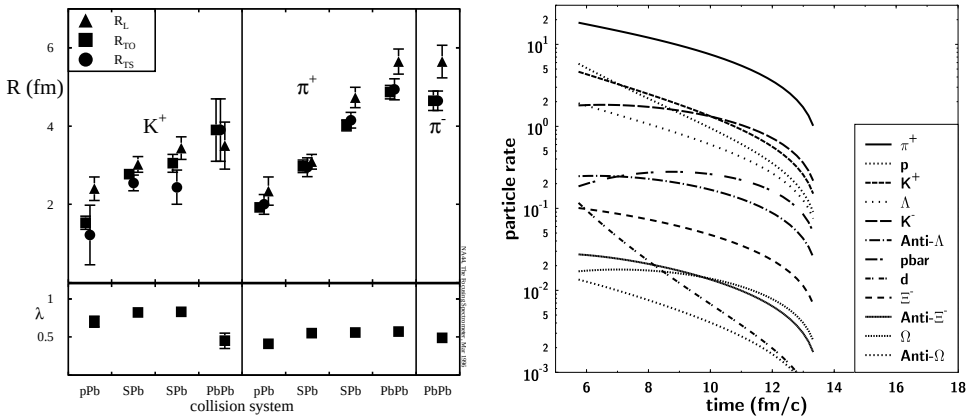

Figure 18. Left: final particle ratios computed in UrQMD (full circles) [316] and a non-equilibrium hadronization scenario (crosses) with initial conditions $A_{\rm B}^{\rm init} = 100$, $S/A^{\rm init} = 45$, $f_s^{\rm init} = 0$ and bag constant $B^{1/4} = 235$ MeV [314]. The data (open circles) are taken from various experiments as compiled in [156]. Right: corresponding particle production rates as a function of time. Strong differences in the time evolution of various particle ratios are observed.

with RQMD [317]. Analysing the results of a non-equilibrium transport model calculations in the framework of an equilibrium model may, however, not seem meaningful.

The smooth increase of the $\bar{\Xi}/\bar{\Lambda}$ ratio from pp via pA to AA reactions suggests that production volume and the degree of thermalization may not be relevant for the production of antihyperons. Already two overlapping strings (as typically produced in p + S reactions) are sufficient to yield strong deviations from the behaviour in pp [232, 318]. Clearly the detailed study of pA reactions yields important information on the production processes of antihyperons.

However, so far all models fail to describe the recently reported, unusually high $\bar{\Lambda}/\bar{p}$ ratio of $\approx$ 3–5 (proton–proton collisions yield a ratio of 0.2–0.3). One possible explanation could be that the $\bar{\Lambda}$ have a far lower annihilation cross section than the $\bar{\rm p}$. This difference in the annihilation cross section might account for the dramatic $\bar{\Lambda}$ enhancement. A straightforward way to test this hypothesis would be the measurement of $\bar{\rm p}$ and $\bar{\Lambda}$ (anti-)flow. For $\bar{\rm p}$, a strong anti-correlation with regard to the 'conventional' baryon flow is predicted [189]. This is due to their large annihilation cross section in dense matter. The same would only hold true for the $\bar{\Lambda}$, if its annihilation cross section is correspondingly large. If, however, $\bar{\Lambda}$ anti-flow is not observed, this would serve as clear indication for a low $\bar{\Lambda}$ annihilation cross section. Thus the above explanation for the $\bar{\Lambda}$ enhancement as being due to smaller σ_{ann} [319] would be supported by independent evidence.

Alternatively, the $\bar{\Lambda}/\bar{\rm p}$ enhancement could be explained by different medium modifications to the masses of non-strange and strange baryons which affect the production probabilities. If an attractive strange scalar condensate lowers the mass of the $\bar{\Lambda}$ in hot and dense hadronic matter, even below that of the $\bar{\rm p}$, this could account for the $\bar{\Lambda}/\bar{\rm p}$ enhancement [319, 320].

Thermal model analyses assume constant freeze-out temperatures and chemical potentials, but at least the more careful ones do not assume a static source; instead they allow for collective expansion flow. While the flow does not matter for an analysis of 4π yields, it becomes indeed important when comparing the model with data from limited windows in momentum space. Unfortunately, no conclusion is possible unless the freeze-out surface is known. Most people

use too simplistic isochronous (t = const.) freeze-out prescriptions which in fact correspond to a volume freeze-out. However, it has been shown in the framework of an expanding hadron gas that freeze-out is not a state but a reaction stage and that the various equilibria (i.e. chemical and thermal equilibrium) necessarily break down in the final stages [321]. Microscopic model calculations support this picture of a complicated sequential freeze-out depending on reaction rates and particle species [185, 187, 232]: Even if some particles are in thermal and chemical equilibrium during the final stages of the reaction, the problem of how to disentangle the thermal contribution from the early pre-equilibrium emission would remain. This problem has not been addressed satisfactorily so far (see section 3.2).

Hadronic transport models, which are based on a non-equilibrium scenario, however, are only able to describe the CERN/SPS (anti-)hyperon data by invoking non-hadronic scenarios such as colour ropes [116], breaking of multiple strings [117] or decay of multi-quark droplets [118]. Therefore, the (anti-) (strange-) baryon sector remains a topic of great interest. Specifically the strong enhancement of multi-strange (anti-)hyperons (Ξ, Ω, $\bar{\Xi}$, and $\bar{\Omega}$) heavy collision systems such as Pb + Pb at the CERN/SPS is of great importance [300] since it offers currently the best opportunity to discriminate hadronic from deconfinement scenarios in the sector of strangeness enhancement.

3.6. Ashes of the plasma: strangelets and hypermatter

3.6.1. Theoretical concepts. The observed abundant production of strange baryons at AGS and SPS energies led people to speculate about implications for hypermatter (multi-hyperon clusters or strange quark droplets) formation [322–326]. Speculations about the existence of such multi-strange objects, with baryon numbers $B > 100$, have been around for decades, in particular within astrophysics. Such states are allowed for by the standard model, although so far their existence has not been proven in nature, e.g. in the form of strange neutron stars.

Quark matter systems with $A > 1$ are unstable if they only consist of u and d quarks, due to the large Fermi energy of these non-strange quarks. The system's energy may be lowered by converting some of the u and d quarks into s quarks (i.e. introducing a new degree of freedom). The energy gain may over-compensate the high mass of the s quarks—thus such strange quark matter (SQM) may be absolutely stable [325].

Hadrons with $B > 1$ and $S < 0$ have been considered even before the advent of QCD [322,323]. However, the development of the MIT Bag model [327] allowed the modelling of such states. Long hypermatter lifetimes (for hundreds of quarks and a strangeness per baryon ratio of the order of one) have been predicted, up to 10^{-4} s [324]. Further detailed investigations of small pieces of SQM, so called *strangelets*, reveal possible (meta)stability for $B > 6$ [325, 326]. The simplest *strangelet* is the H-dibaryon with zero charge, $B = 2$ and $S = -2$, which consists of 2u, 2d and 2s quarks, followed by the *strange quark-α* with 6u, 6d and 6s quarks [325, 328].

For a QGP—hadron fluid first-order phase transition with nonzero baryo-chemical potential, a mechanism analogous to associated kaon production yields an enriched population of s quarks in the quark-gluon phase, while the $\bar{s}$ quarks drift into the hadron phase [250, 329]. This strangeness separation results in the distillation of metastable *strangelets* only if the Bag constants are very small, $B < 180$ MeV fm^{-3} [250].

Experimentally *strangelets* are distinguishable from normal nuclei due to their very small or even negative charge to mass ratio. The most interesting candidates for long-lived *strangelets* are lying in a valley of stability which starts at the *quark-α* and continues by adding one unit of negative charge, i.e. $(A, Z) = (8, -2), (9, -3) \ldots$ [330]. Recent calculations indicate that positively charged *strangelets* seem only to exist for $A > 12$ and very low bag parameters [330].

There exist, however, other forms of hypermatter with similar properties as *strangelets*: hyperclusters or MEMOs (metastable exotic multihyperon objects) consist of multiple Λ, Σ and Ξ hyperons [331], and—possibly—also nucleons. The double-Λ hypernucleus ${}^{6}_{\Lambda\Lambda}$He has been observed long ago [332]. Properties of MEMOs have been estimated using the relativistic mean field model. MEMOs can contain multiple negatively charged hyperons, therefore they may also have zero or negative charge-to-mass-ratios.

MEMOs or hyperclusters could form a doorway state to *strangelet* production, or vice versa: MEMOs may coalescence in the high-multiplicity region of the reaction. If strangelets are stronger bound than 'conventional' confined MEMOs, the latter may transform into *strangelets*. The cross sections for production of MEMOs in relativistic heavy-ion collisions rely heavily on model parameters (e.g. in the in the coalescence model p_0 and r_0). The predicted yields are typically $<10^{-8}$ per event [331, 333].

3.6.2. Experimental status. *Strangelet* searches are underway at the AGS [334–336] and SPS [337–341]. So far no long-lived ($\tau > 10^{-7}$ s) *strangelets* have been unambiguously identified—the upper limits for the production cross sections established by the experiment are still consistent with theoretical predictions for short-lived MEMOs since they cannot be tested in the present long-flightpath experiments. There has been a report of one candidate with $Z = -1$, $N/Z = 7.4$ GeV and $\tau > 85$ μs [339, 341, 342]. Therefore this exciting topic awaits more experimental effort.

Current experiments are designed to detect *strangelets* with a small charge-to-mass ratio and rather long lifetime ($\tau \geqslant 12$ μs in the case of [339, 340]). These experimental set-ups are hardly sensitive to the most promising long-lived and negatively charged *strangelet* candidates beyond the *strange quark-α*. Unfortunately, plans for extending experiment E864 at the AGS to look for highly charged strangelets with $B > 10$ [343] cannot be followed because the AGS fixed target heavy-ion programme has been put to rest.

Future experiments at collider energies (STAR at RHIC and ALICE at LHC) will be sensitive for short-lived metastable hypermatter, too [344, 345, 504].

3.6.3. Discussion. Due to the possibility of creating MEMOs in a hadronic scenario and their possible subsequent transformation into *strangelets*, the formation of a QGP is not a necessary prerequisite for the creation of *strangelets*. The discovery of *strangelets* would therefore be no hard proof for a deconfinement phase transition. So far there seems to be no clear way to distinguish *strangelets* from MEMOs. Both forms of hypermatter would be extremely interesting to study and the discovery of one or the other would be worth every effort. Therefore, experiments should be devoted to the search for short-lived (anti-)hyperclusters.

Large theoretical uncertainties remain, e.g. how the predicted yields depend on the model parameters. Both, theory and the current experimental results point towards a future search for *strangelets*/hyperclusters with rather short lifetimes. Experiments including a large TPC might be able to observe the decay short-lived hyperclusters. Indirect K^+K^- correlation measurements might offer another possibility of detecting *strangelets* or hyperclusters [249].

3.7. Radiation of the plasma: direct photons and thermal dileptons

3.7.1. Theoretical concepts. The most prominent process for the creation of direct (thermal) photons in a QGP are $q\bar{q} \rightarrow \gamma g$ (annihilation) and $gq \rightarrow \gamma q$ (Compton scattering). The production rate and the momentum distribution of the photons depend on the momentum distributions of quarks, antiquarks and gluons in the plasma. Infrared singularities occuring in perturbation theory are softened by screening effects [346–349]. If the plasma is in

thermodynamic equilibrium, the photons may carry information on this thermodynamic state at the moment of their production [346, 350–352].

The main hadronic background processes to compete against are pion annihilation $\pi\pi \rightarrow \gamma\rho$ and Compton scattering $\pi\rho \rightarrow \gamma\pi$ [346, 353]. The broad a_1 resonance may act as an intermediate state in $\pi\rho$ scattering and thus provide an important contribution [353, 354] via its decay into $\gamma\pi$. In the vicinity of the critical temperature T_C a hadron gas was shown to 'shine' as brightly (or even brighter than) a QGP [346].

A finite baryochemical potential yields at constant energy density a reduced multiplicity of direct photons from a QGP [355, 356].

Hydrodynamical calculations can be used to compare purely hadronic scenarios with scenarios involving a first/second-order phase transition to a QGP. They show a reduction in the temperature of the photon spectrum in the event of a first-order phase transition [357–359].

The rapidity distribution of direct hard photons reflects the initial rapidity distribution of the produced mesons or directly the QGP [360]. It may thus provide insight into the (longitudinal) expansion of the photon source: if the hot thermal source is initially at rest and is accelerated by two longitudinal rarefaction waves propagating inwards with the velocity of sound, the photon rapidity distribution is strongly peaked around mid-rapidity. In contrast, a Bjorken-like boost-invariant expansion results in a more or less flat photon rapidity spectrum.

If a very hot plasma is formed (e.g. at RHIC or LHC energies) a clear photon signal might be visible at transverse momenta in the range 2–5 GeV/c [361–363]. The lower p_t range (1–2 GeV/c) is dominated by the mixed phase; separated contributions of the different phases are difficult to see due to transverse flow effects [357]. These effects, however, can be important up to transverse momenta of 5 GeV. Transverse flow effects also destroy the correlation between the slope and the temperature of the photon spectrum [359].

Analogously to the formation of a real photon via a quark–antiquark annihilation, a virtual photon may be created in the same fashion which subsequently decays into a l^+l^- pair (a *dilepton*). Bremsstrahlung of quarks scattering off gluons can also convert into dileptons.

Dileptons can carry information on the thermodynamic state of the medium at the moment of production in the very same manner as the direct photons—since the dileptons interact only electromagnetically they can leave the hot and dense reaction zone basically undistorted, too.

The main background contributions stem from pion annihilation, resonance decays [364–368] (two pions can annihilate, forming either a virtual photon or a rho meson—both may then decay into a dilepton) and π–ρ interactions [369, 370] at low dilepton masses and Drell–Yan (DY) processes [371, 372] at high masses. Furthermore meson resonances such as the ρ-, ω- or ϕ-meson may be produced directly or in the decay of strings and heavier resonances. As all of those vector mesons carry the same quantum numbers as the photon, they may decay directly into a dilepton. Resonances can also emit dileptons via Dalitz decays. The DY process describes the annihilation of a quark of one hadron with an antiquark (in proton–proton collisions from the sea of $\bar{q}$) of the other hadron, again resulting in a virtual photon which decays into a dilepton. The open charm contribution to the dilepton mass spectrum has been estimated to be negligible for low dilepton masses [373] at the CERN/SPS. At RHIC and LHC energies, however, charm contributions dominate the dilepton mass spectrum above 2 GeV [374].

Most original calculations on dileptons as signals of a QGP at CERN/SPS energies focused on masses below the ρ-meson mass [365, 375–383]. The current understanding of hadronic background contributions [364, 366–368] shows that most probably dileptons originating from a QGP are over-shined by hadrons, with the possible exception of masses around 1–1.5 GeV [384, 385] where the rates from a plasma (at very high temperatures around

500 MeV) may suffice to be visible. At higher masses, the yield of DY processes from first nucleon–nucleon collisions most probably exceeds that of thermal dileptons from a QGP. Finite baryochemical potential will, at a given energy density, reduce the number of dileptons emitted from a QGP [386–388], due to the dropping temperature in that system.

The dependence of the yield of high-mass dileptons on the thermalization time is still a point of open debate [389, 390]. The parton cascade [391] and other models of the early equilibration phase [390, 392] predict an excess of dileptons originating from an equilibrating QGP over the DY background in the mass range 5–10 GeV. Then the early thermal evolution of the deconfined phase could be traced in an almost model-independent fashion [361].

The secondary dilepton production via quark–antiquark annihilation has also been studied on the basis of a hadronic transport code (UrQMD [110]). Here, one obtains a realistic collision spectrum of secondary hadrons for SPS energies. Using parton distribution functions and evaluating the contributions of all individual hadronic collisions one finds that meson–baryon interactions enhance the mass spectrum at mid-rapidity below masses of 3 GeV considerably [372]. Preresonance interactions are estimated to enhance this secondary yield by up to a factor of five.

3.7.2. Experimental status. Experiments to measure direct photons are carried out at the CERN/SPS by the WA80/WA98 and the CERES/NA45 collaborations. Whereas the final analysis of the WA80 collaboration for S + Au indicates a 5% photon signal over background (with a 0.8% statistical and a 5.8% systematical error) [393–395] the CERES/NA45 collaboration did not report any direct photons, but sets an upper limit of 7% for the integrated excess an unconventional photon source might have in central S+Au collisions [396–398]. The WA80 collaboration has reported upper limits for each measured k_t bin which yields important information for constraining the initial temperature of the reaction zone. Within the reported systematic errors the results of the WA80 and the CERES/NA45 collaborations are compatible with each other [399].

Dileptons can be measured at CERN in the form of dimuons by the HELIOS3, NA38 and NA50 [400–403] collaborations and in the form of electron pairs by the CERES collaboration [397]. Dimuons exhibit an excess in AA collisions in the mass range $0.2 < M < 2.5$ GeV/c^2 up to the J/Ψ, as compared to pp and pA collisions. For dielectrons an excess is observed in the low-mass region $0.2 < M < 1.5$ GeV/c^2, again relative to pp and pA collisions (cf figure 21).

3.7.3. Discussion. The Pb + Pb analysis on direct photons of the WA98 and NA45/CERES collaborations is in progress. Hydrodynamical calculations are only compatible with the S + Au data of WA80 if a phase transition with its cooling is taken into account [358, 359, 404–407] or if higher mass meson and baryon multiplets are included for the hadronic EoS.

Microscopic hadronic transport models, however, are not constrained by the assumption of thermal equilibrium, in particular in the initial stage, and yield results compatible with hydrodynamical calculations without invoking a phase transition scenario [408], as can be seen in figure 19. They shows that pre-equilibrium contributions dominate the photon spectrum at transverse momenta above $\approx$1.5 GeV. The hydrodynamics prediction of a strong correlation between the temperature and radial expansion velocities on the one hand and the slope of the transverse momentum distribution on the other hand thus is not recovered in a microscopic transport model [408].

Apart from these ambiguities in the interpretation of the data, the main problem with regard

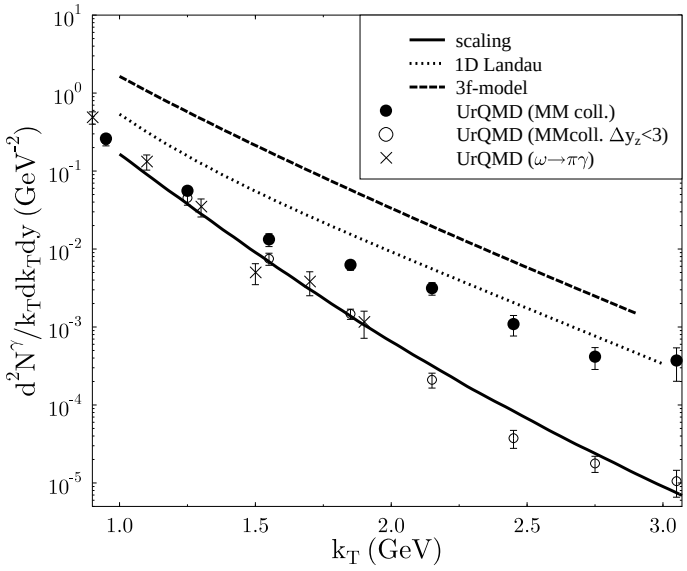

Figure 19. Transverse momentum spectrum of directly produced photons in Pb + Pb collisions at 160 GeV/nucleon calculated with the UrQMD model. The resulting spectrum is compared with different hydrodynamical calculations. In all models the processes $\pi\eta \mapsto \pi\gamma$, $\pi\rho \mapsto \pi\gamma$ and $\pi\pi \mapsto \rho\gamma$ are considered as photon sources. The figure has been taken from [408].

to the direct photon signal is the extremely small cross section in a difficult experimental situation, since photons from hadronic decays generate a huge hadronic background. The strong and dedicated effort to improve the measurements will be continued, also at the more promising collider energies.

Both the dielectron as well as the dimuon data seem to be compatible with a hydrodynamic approach assuming the creation of a thermalized QGP [409]. Hadronic transport calculations are not able to fully reproduce the observed excess [410–412]. However, at least part of the observed enhancement of lepton pairs at intermediate and low masses might be either caused by the previously neglected source of secondary DY processes [314] or by contributions of heavy mesons, such as the a_1 [413]. A detailed discussion of the dilepton data and its theoretical implications will follow in conjunction with the discussion on chiral symmetry restoration in section 3.8.

3.8. Restoration of chiral symmetry: vector mesons in dense matter

3.8.1. Theoretical concepts. The dilepton signal due to the decay of vector mesons, in particular from the ρ-meson, is of great interest: in conjunction with the chiral symmetry restoration [414–418] the ρ-, ω- and ϕ-mesons (and heavier meson resonances, e.g. the $a_1, a_2 \ldots$) are expected to change their spectral function in the hot, high baryon density medium: the breaking of the chiral $SU(3)_L \times SU(3)_R$ symmetry (an approximative symmetry of QCD) results in quark condensates $\langle q\bar{q}\rangle$ in the QCD vacuum and a 'Goldstone' boson, i.e. the pion. The dependence of $\langle q\bar{q}\rangle$ on the temperature T has been studied in the framework of lattice QCD [419] and chiral perturbation theory [420, 421]. Up to (0.7–0.8) T_C $\langle q\bar{q}\rangle$ remains nearly constant and then its absolute value decreases rapidly (see figure 20). The behaviour of the quark condensate at finite baryon densities is described in a model-independent fashion by the

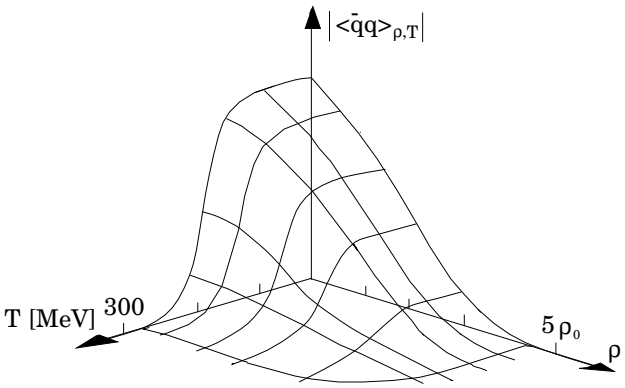

Figure 20. quark condensate $\langle q\bar{q}\rangle$ as a function of temperature T and baryon density ρ/ρ_0. The figure has been adapted from [414].

Feynman–Hellman theorem [422, 423]. A model calculation of the dependence of $\langle q\bar{q}\rangle$ on both the baryon density ρ/ρ_0 and temperature T can be seen in figure 20—the drop of $\langle q\bar{q}\rangle$ with ρ and T is quite analogous to the temperature and density dependence of the nucleon effective mass in the σ–ω model as noted in [424].

The reduction of the absolute value of the quark condensate $\langle q\bar{q}\rangle$ in a hot and dense hadronic environment might reflect itself in reduced masses of vector mesons [425–433]. However, a lowering of the mass of the ρ-meson—most commonly referred to as 'Brown–Rho scaling' [431]—is not synonymous with the restoration of chiral symmetry: It has been shown by employing current algebra as well as PCAC that to leading order in temperature, T^2, the mass of the ρ-meson remains nearly constant as a function of temperature [434], whereas the chiral condensate is reduced [420].

Restoration of chiral may manifest itself in different forms [417]: the masses of the ρ- and the a_1 meson may merge, their spectral functions could mix—resulting in peaks of similar strength at both masses (and causing a net reduction at the ρ-peak)—or both spectral functions could be smeared out over the entire mass range.

Dileptons from the in-medium decay of such vector mesons with modified masses and spectral functions would point towards the restoration of chiral symmetry at a phase transition.

3.8.2. Experimental status. At the BEVALAC the DLS collaboration has measured dielectron pairs in proton induced reactions as well as in d + Ca, He + Ca, C + C and Ca + Ca reactions [435–437]. Their latest results [437] for pair masses $M < 0.35$ GeV/c in the Ca + Ca system show a larger cross section than their previous measurements [436] and current model calculations [438, 439], suggesting large contributions from π^0 and η Dalitz decays. The cross section $\mathrm{d}\sigma/\mathrm{d}M$ scales with $A_P \cdot A_T$ up to pair masses of $M = 0.5$ GeV/c. For larger masses the Ca + Ca to C + C cross section ratio is significantly larger than the ratio of $A_P \cdot A_T$ values.

Unfortunately, there are no experiments capable of measuring dileptons in A + A collisions at ∼10 GeV/nucleon. However, in central sulfur–gold collisions at the CERN/SPS an enhancement has been measured in the invariant mass spectrum of muon pairs relative to the normalized proton–proton and proton–nucleus data at 200 GeV/nucleon taken by the HELIOS/3 and NA38 collaborations: while the pp and pA data seem well described by measured sources such as DY, open charm and hadronic decays, there is an excess in AA observed in the mass range $0.2 < M < 2.5$ GeV/c^2 (for the J/Ψ, a suppression of the peak

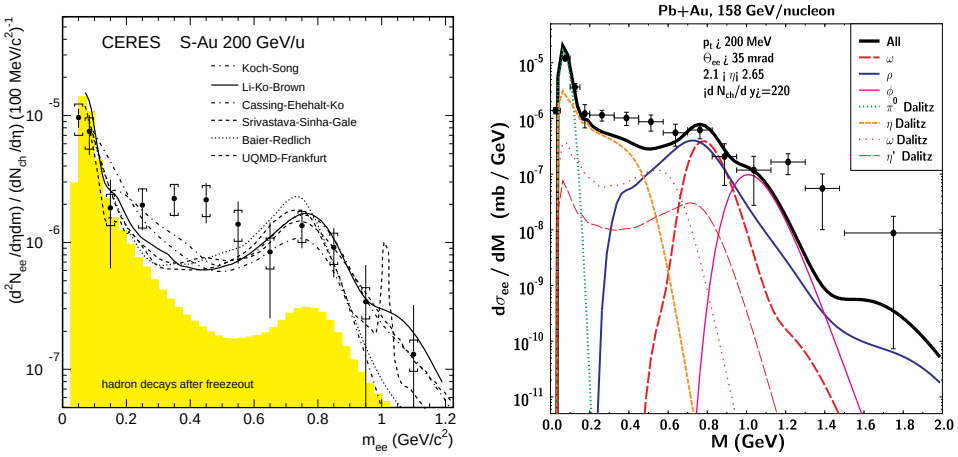

Figure 21. Left: inclusive e^+e^- mass spectra in 200 GeV/nucleon S + Au collisions as measured by the CERES collaboration [397]. The figures have been taken from [444]. The shaded area depicts hadronic contributions from resonance decays. The data are compared calculations based on a purely hadronic scenario [409, 410, 445, 447, 448]. Right: UrQMD prediction and data [441] for Pb + Au at 160 GeV/nucleon.

relative to this background is observed, cf section 3.9) [400–402]. Similarly, for dielectron pairs in S + Au an excess has been observed by the CERES collaboration [397] in the low-mass region $0.2 < M < 1.5$ GeV/c^2, again relative to pp and pA collisions (cf figure 21). As in the case of the dimuon excess, the pp and pA data can be well understood taking known hadronic sources into account. Data for Pb + Au confirm this low-mass dielectron excess [440–443].

3.8.3. Discussion. When searching for chiral symmetry restoration, thermal dileptons (see section 3.7) would serve as background. Due to the dominance of hadronic decays in the mass range up to 1.5 GeV, however, they do not pose a serious problem for the measurement of vector meson properties.

As already stated in section 3.7, both, the dielectron as well as the dimuon data at the SPS seem explainable in a hydrodynamic approach assuming the creation of a thermalized QGP [409].

On the other hand, the same data can be reproduced in the framework of microscopic hadronic transport models incorporating mass shifts of vector mesons [410, 411, 445–447].

However, even bare hadronic transport model calculations, without any mass shift included, miss only the data in the 400–600 MeV bins (by 2–3 standard deviations) [410, 411].

Calculations evaluating in-medium spectral functions, due to the coupling of the ρ with nucleon resonances and particle–hole excitations, also achieve a satisfactory reproduction of the CERES data [449], without requiring a dropping ρ-mass. Recent data on the p_t dependence of this phenomenon [450] indicate, however, that the enhancement is most pronounced at low p_t. This precludes the dominance of p-wave baryon resonance effects. Since the hadronic transport models did—up to now—neglect contributions, e.g. from current–current correlation functions [451] and from additional heavy meson resonances, it has yet to be determined whether partial restoration of chiral symmetry or Brown–Rho scaling is the only possible explanation of these interesting new data.

On the experimental side, the main problems lie with the low signal to background ratio of $\frac{1}{10}$ and limited statistics (<1000 lepton pairs in Pb + Au). In addition, the shape of the e^+e^-

excess at 0.25 GeV $< m_{ee} <$ 0.6 GeV coincides with that of the background. Currently a strong effort by the CERES collaboration is underway to upgrade the experiment with a TPC. The resulting increase in statistics and resolution should help to verify or falsify some of the conflicting hypotheses on the origin of the low-mass dilepton enhancement.

The latest DLS data gives rise to speculation that the observed enhancement in the mass range below the free ρ-meson mass may be due to enhanced ρ-meson production or a mass shift of the ρ in a dense hadronic medium—without the need for a deconfinement phase transition. However, all microscopic model calculations which have addressed this data so far [452, 453] have not been able to provide a reasonable explanation within the frameworks which work so well for dilepton production at CERN.

3.9. Quarkonia suppression: evidence for deconfinement or dynamical ionization

In 1986 Matsui and Satz proposed [454] that the suppression of heavy quarkonia-mesons could provide one of the signatures for deconfinement in QCD at high temperatures. The idea was based on an analogy with the well known Mott transition in condensed matter systems. At high densities, Debye screening in a QGP reduces the range of the attractive force between heavy quarks and antiquarks, and above some critical density screening prevents the formation of bound states. The larger bound states are expected to dissolve before the smaller ones as the temperature of the system increases. The ψ' and χ_c states are thus expected to become unbound just above T_c, while the smaller ψ state may only dissolve above $\approx 1.2T_c$. Heavier $\bar{\text{b}}\text{b}$ states offer the same features as $\bar{\text{c}}\text{c}$ states, but require much shorter screening lengths to dissolve [455]. The $\Upsilon(\text{b}\bar{\text{b}})$ state may dissolve only around $2.5T_c$, while the larger excited Υ' could also dissolve near T_c.

In order to determine the magnitude of suppression, it is obvious that the initial production mechanism must be well understood. Charm quark–antiquark pairs, $\text{c}\bar{\text{c}}$, are produced in rare pQCD gluon fusion processes [456], ($\text{gg} \rightarrow \text{c}\bar{\text{c}}$) with a cross section in pp reactions $\sigma_{c\bar{c}} \sim 10\mu$b at $\sqrt{s} = 20$ GeV. In the rare events when a pair is formed, both the charm and anti-charm quantum numbers remain approximately conserved, and either the $\text{c}\bar{\text{c}}$ emerge from the reaction in hidden charm quarkonium bound states, $J/\psi(1S_1 : 3097)$, $\psi'(2S_1 : 3686)$, $\chi_c(1P_{0,1,2} : 3500), \ldots$, or in continuum open charm states $D(1869)$, $D^*(2010), \ldots$. Even though only about 1% of the $\text{c}\bar{\text{c}}$ pairs emerge in pp collisions as J/ψ states, these vector hidden charm mesons are the easiest to measure because they are seen as sharp resonances on top of a broad continuum in the invariant mass spectrum of dileptons. In contrast, open charm production is much harder to measure. Semi-leptonic open charm decay contributes to the continuum yield of dileptons mainly below the M_ψ peak.

Above M_ψ, the DY process ($q\bar{q} \rightarrow \mu\bar{\mu}$) begins to dominate the continuum yield. The great importance of DY is that the absence of strong final-state interactions of the produced leptons makes it possible to compute the absolute DY cross section via pQCD. The nuclear number dependence of the cross section is then entirely determined by geometrical (Glauber) factors, $T_{AB}(\mathbf{b})$ (neglecting small nuclear dependence of the structure functions). Here, $T_{AB}(\mathbf{b})$ is the number of binary NN interactions per unit area as a function of the impact parameter. The measured DY yields thus provide an important constraint on the impact parameter range associated with specific centrality (E_T) triggers used in the experiment. The comparison of the centrality dependence of the J/ψ and DY cross section therefore provides a calibration tool to determine the magnitude of the suppression factor of charmonium in nuclear collisions.

Great interest in this proposed signature arose when NA38 found the first evidence of suppression in light-ion reactions. With the new preliminary Pb + Pb data of NA50 (see next section) which have been reported to show 'anomalous' suppression, it is especially

important to review critically some of the competing dynamical effects that could forge this QGP signature.

One of the main problems in the interpretation of the observed suppression as a signal for deconfinement is that non-equilibrium dynamical sources of charmonium suppression have also been clearly discovered in p + A reactions. The interaction of the pQCD produced $c\bar{c}$ pair with any QCD medium (confined or not) decreases significantly the probability of that pair to emerge in an asymptotic $J/\psi(1S)$ state. The observation of J/ψ suppression in p + A is direct proof of this fact since the formation of an equilibrated QGP in such reactions is not expected.

A phenomenological analysis of p + A data yields a dissociation cross section for both the J/ψ and the ψ' around 7.3 ± 0.6 mb [161, 457–459]. This finding is surprising since the transverse areas of those two mesons differ by more than a factor of two. This has led to the $c\bar{c}_8$ colour octet model interpretation of the (quantum) formation physics involved. In this model, it is assumed that the pair is formed in a small octet state accompanied by a soft gluon that can be easily stripped off as it propagates through a nucleus [462, 463]. This qualitatively accounts for the observed equal nuclear absorption cross sections since, as a result of time dilation, hadronization into the asymptotic J/ψ or ψ' states is delayed several fm/c at high energies [161, 463].

A recent development is the calculation of the hard contributions to the charmonium–nucleon and bottonium–nucleon cross sections based on the QCD factorization theorem and the non-relativistic quarkonium model [464]. The calculated p + A cross section agrees well with the data. The non-perturbative contribution to the charmonium cross section dominates at CERN/SPS energies and becomes a correction at LHC. The J/ψ production in nucleus–nucleus collisions at the CERN/SPS can then be reasonably well described by hard QCD, if the larger absorption cross section of the χ states that are predicted by QCD are taken into account.

While the octet model used in conjunction with the Glauber geometrical model can account for the pA observation, the corrections to this eikonal picture of nuclear absorption extrapolated to AA reactions are, however, not yet under theoretical control. For example, since the $c\bar{c}_8$ colour octet–soft gluon state is not an eigenstate of non-perturbative QCD, its effective hadronic absorption cross section may vary within the relaxation time. Also possible pile-up of matter and energy loss prior to the gluon fusion event are neglected. The importance of gaining better theoretical control of the nuclear absorption process is underscored by the fact that in central Pb–Pb reactions about one half of the NA50 observed factor of four suppression of J/ψ is estimated to arise from such non-equilibrium (quantum) formation physics.

The second major theoretical uncertainty in interpreting charmonium suppression is distinguishing dynamical 'background' dissociation processes such as $\psi + \rho \rightarrow D\bar{D}$ and $\psi + \Delta \rightarrow \Lambda_c\bar{D}$ from *transient* partonic dynamical processes (non-thermal colour field fluctuations) and from the sought-after screening mechanism in the plasma phase of QCD matter.

Purely hadronic dissociation scenarios have been suggested [465–470], which could, with suitable parameters, account for J/ψ and ψ' suppression without invoking the concept of deconfinement. These hadronic scenarios are referred to as *comover models*. Suppression in excess to that due to preformation nuclear absorption is ascribed in such models to interactions of the charmonium mesons with comoving mesons and baryons which are produced copiously in nuclear collisions. Unfortunately none of the required absorption cross sections are experimentally known and estimates are highly model-dependent. A general criticism of comover suppression estimates is the use of overly simplified Glauber geometry and idealized boost invariant expansion dynamics for the produced particles.

Studying the transverse momentum, p_t, dependence of J/ψ and ψ' production may yield additional information concerning the nature of the J/ψ-suppression mechanism [471, 472]. Two common scenarios have been considered: At sufficiently high p_t final-state interactions might disappear due to time dilation, while hadronic absorption effects should be similar for the J/ψ and ψ'. In a deconfinement scenario this idea suggests that J/ψ is suppressed only for low transverse momenta [473]. A second scenario assumes that J/ψ and ψ' acquire large transverse momenta through multiple elastic parton–parton collisions. Those multiple collisions, however, are most likely to occur in the high-density QGP region. The consequence would be that high p_t J/ψ and ψ' should be even more suppressed than those with low transverse momenta [474]. A purely hadronic scenario predicts an increase in the mean transverse momentum as a function of transverse energy for the heavy Pb + Pb system [475].

The above discussion emphasizes some of the uncertain theoretical elements in the interpretation of charmonium suppression as a signal for deconfinement. To isolate the final-state interaction effects from initial-state nuclear absorption, it has been proposed to combine all available data using a Glauber model geometric variable, 'L'. Since this is so popular we review below how this variable is defined.

The suppression of the J/ψ production cross section in A + B collisions can be expressed as

$$\sigma(AB \to J/\psi) = AB\sigma(pp \to J/\psi)\mathrm{e}^{-[\sigma^{abs}_{c\bar{c}N}\rho_0 L(A,B,E_T)]}S_{co}. \tag{3}$$

Here $\sigma^{abs}_{c\bar{c}N} \sim 5$–$7$ mb is an effective preformation nucleon absorption cross section, ρ_0 is the ground state nuclear density, and $L(A, B, E_T)$ is a measure of the mean nuclear thickness evaluated through the Glauber model

$$AB\mathrm{e}^{-[\sigma^{abs}_{c\bar{c}N}\rho_0 L(A,B,E_T)]}S_{co} = \int \mathrm{d}^2b\, P(E_T, b) \int \mathrm{d}z \int \mathrm{d}^2s\, \mathrm{d}z' \rho_A(\boldsymbol{s}, z)\rho_B(|\boldsymbol{b} - \boldsymbol{s}|, z')T_{co}(\boldsymbol{b}, \boldsymbol{s}) \times \mathrm{e}^{-\sigma^{abs}_{c\bar{c}N}\int \mathrm{d}z''\,(\theta(z''-z)\rho_A(b,z'')+\theta(z'-z'')\rho_B(\boldsymbol{b}-\boldsymbol{s},z''))}. \tag{4}$$

In the absence of preformation absorption ($\sigma^{abs}_{c\bar{c}N} = 0$) and the absence of comover absorption ($T_{co} = 0$), the above factor reduces to AB for untriggered data ($P = 1$). As shown in the next section this AB scaling (expected for any hard pQCD process without final state interactions) is observed to hold very well for DY pair production.

In addition to the uncertainties associated with (4), the assumed constancy of the density along the path in the nuclear overlap region (neglect of energy loss and density pile-up especially at moderate SPS energies) and the assumed spacetime independence of the effective cross sections of the pre-hadronic $c\bar{c}$ configuration, other sources of theoretical uncertainties are evident: a major source of model dependence of L enters for triggered data through the transverse energy impact parameter distribution, $P(E_T, b)$. The observed transverse energy, E_T, depends on the details of the experimental geometry and materials and is particularly difficult to simulate in the multi-target system of NA50. Often this distribution is simply parametrized such that its integral over impact parameters reproduces the the observed global $\mathrm{d}N/\mathrm{d}E_T$ distribution. The effective length $L(E_T)$ is computed with the above assumptions by setting $T_{co} = 0$.

The main advantage of defining L is that data from different AB systems and E_T triggers can be combined in one plot. However, we emphasize that unlike E_T, L is not a measured quantity and is model-dependent. Therefore, interpretations of data plotted as a function of L should be viewed with great caution. In contrast, it is theoretically much better to plot production cross sections as a function of AB to combine minimum bias data.

The comover absorption factor S_{co} depends sensitively on the magnitude and time dependence of the local comoving density of partons or hadrons as well as their absorption

cross section. In additional, feed-down processes associated with 'charmonium chemistry' must be taken into account in that calculation. The final J/ψ include contributions from radiative decay of higher mass charmonium states. In one estimate [476], it was assumed that $\mathrm{p}(\psi' \to \psi) \sim 12\%$ of the observed ψ arise from radiative ψ' decay, and $\mathrm{p}(\chi \to \psi) \sim 30\%$ from χ decay. Unlike the small ψ, the larger ψ' and χ states are expected to have significantly larger absorption cross sections $\sigma_{co}(nLJ)$. Evidence for comover absorption of ψ' has been claimed to be observed already in S + U. Neglecting, for illustration, nuclear absorption and the impact parameter variations , the comoving survival factor is thus of the generic form

$$S_{co} = \sum_{nLJ} p(nLJ)\mathrm{e}^{-\sigma_{co}(nLJ)\int_{\tau_0}^{\tau_f} \mathrm{d}\tau\, \rho_{co}(\tau)}. \tag{5}$$

Even if $\sigma_{co}(\psi(1S_1)) = 0$, $S_{co} \to 0.6$ if the higher mass charmonium states are absorbed.

Often simple scaling assumptions are assumed [476] for the evolution of the comoving density, $\rho_{co} \propto \mathrm{d}E_\perp/\mathrm{d}y(1/\tau R^2)$. With reasonable variations of the unknown parameters above, excellent fits to the NA38 S + U were obtained. However, even with these parameters fixed, comparisons for different AB systems require further dynamical assumptions. Especially important is the assumed A-dependence of the the comoving matter density. Linear Glauber models tend to fail to reproduce the larger suppression in Pb–Pb. However, nonlinear connections between $\rho_{co}(\tau_0)$ and E_T have been demonstrated to be also compatible with the data [160].

3.9.1. Experimental status. Systematic measurements of J/ψ, ψ' and 2–5 GeV continuum processes (DY processes, open charm decay, etc) have been performed by the NA38 collaboration using proton, oxygen and sulfur beams at CERN [477–480]. The first preliminary data on Pb + Pb $\to J/\psi$ was reported by the NA50 collaboration in 1996. The data analysis is still not complete but in a recent conference [481] all the data have been combined as a function of AB as shown in figure 22. The first striking result in the top left frame is that the DY yield of dileptons with mass >2.9 GeV scale within 20% as $\sigma_{DY}^{th} \propto$ AB over five orders of magnitude in that variable. The so called $K \sim 2$ factor depends on the choice of the proton structure functions. In the top right frame the deviation of the J/ψ production cross section from this simple scaling is obvious (data are depicted with open triangles). After rescaling data from different energies to 200 A GeV, all but the Pb–Pb data lie on what appears to be a universal curve, $(\mathrm{AB})^{0.92}$. The fact that the p + A data and S + U data lie on the same curve suggests the common preformation physics interpretation discussed before. The minimum bias Pb–Pb data point is about 25% below the curve extrapolated up to 208^2. This is the so-called anomalous suppression.

In the lower left and right frames the centrality E_T dependence of the J/ψ and DY yields are compared. (Note that recently the E_T scale has been recalibrated to be ∼10–20 smaller than shown here, but no final publication has appeared as of this writing). The low $E_T < 40$ GeV are more peripheral collisions with geometries comparable to central S + U. For $E_T > 50$ GeV corresponding to $b < 8$ fm central collisions, the shape of the DY and J/ψ distributions appear different. It should be noted that the J/Ψ and DY distributions are affected by systematical errors which do not affect the ratio between the two variables and therefore the direct comparison of theory to these distributions may be misleading. The ratio of J/ψ to DY yields for Pb + Pb as a function of E_t is displayed in figure 23 (full circles). Within the Pb + Pb sample a discontinuity has been hinted at around $E_t = 50$ GeV. New minimum bias data with highly improved statistics show a rather smooth increase with decreasing E_T. However, the data situation remains unclear for both the low and the high E_T limit. The $\langle p_t^2 \rangle$ does not increase anymore for $E_t \geqslant 100$ GeV in Pb + Pb collisions.

Finally in figure 24 the provocative 'L' plot [481] is shown that suggests that a sudden

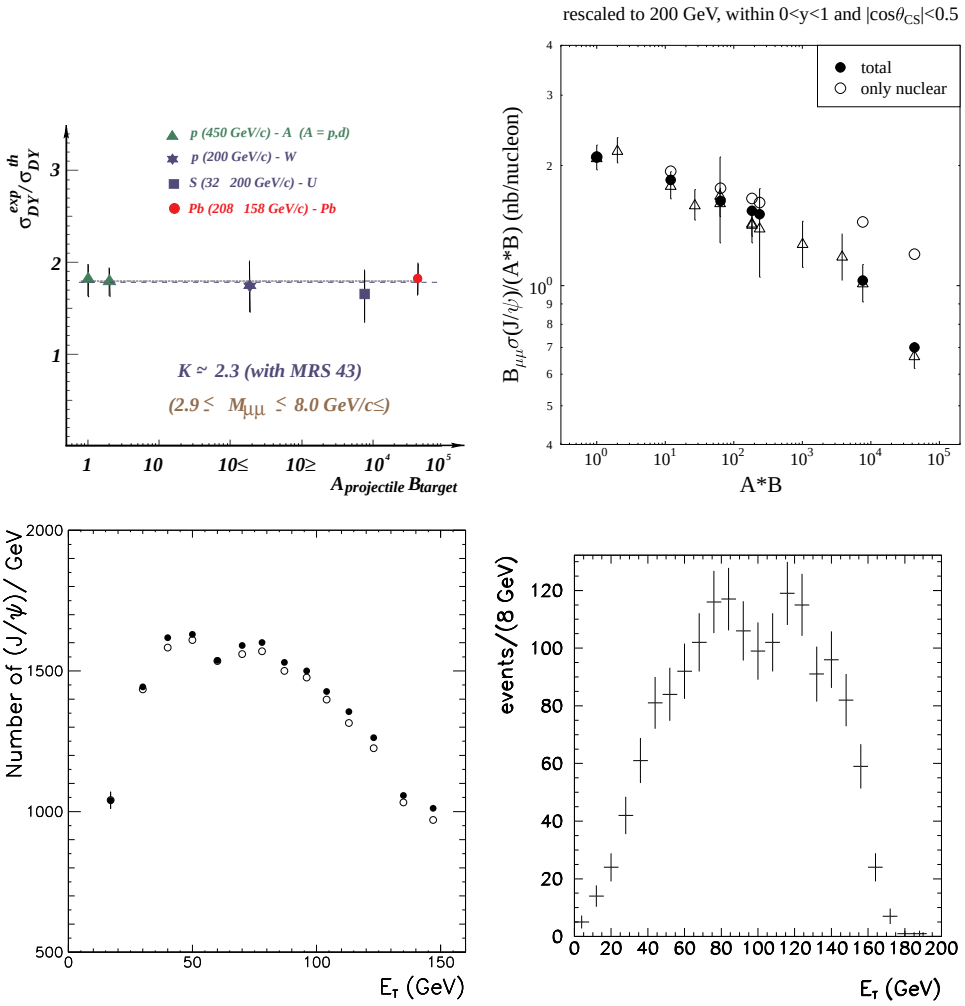

Figure 22. Preliminary J/ψ to DY data from NA50 [481, 482]. The top left frame shows that DY scale with A × B over five orders of magnitude. Note that the value of the K is actually 1.8 and not 2.3 which refers to GRV LV. The top right shows a suppression of J/ψ reaching almost a factor of 4 in Pb + Pb collisions (open triangles). The additional 25% suppression of J/ψ in Pb + Pb relative to extrapolation of p + A and S + U is referred to as anomalous. The full circles depict a UrQMD calculation [483] including comoving mesons whereas the open circles show the same calculation with only nuclear absorption. In the bottom left and right frames the number of ψ and DY pairs observed as a function of the uncorrected NA50 transverse energy are shown. The kink in the bottom left frame at $E_T \sim 40$–50 GeV shows the rapid onset of anomalous suppression in the impact parameter range estimated to be $b \sim 8$ fm.

increase in ψ absorption occurs for effective nuclear depths above ∼7–8 fm, while the larger ψ' state is similarly absorbed in S + U and Pb + Pb.

3.9.2. Discussion. The initial plasma interpretations of the J/ψ suppression in light nuclear beam data in 1987 have been reformulated as a result of extensive p + A data proving the importance of pre-formation absorption phenomena in confined QCD matter. In addition, the similar suppression of ψ and ψ' as a function of A have allowed the determination of

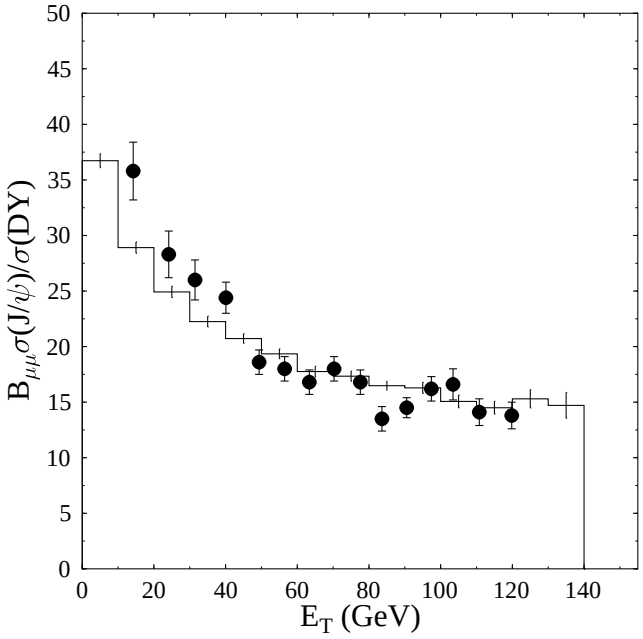

Figure 23. Ratio of J/ψ to DY as a function of the experimentally measured transverse energy for the system Pb + Pb at 160 GeV/nucleon. The data are taken from [481], the histogram is a UrQMD calculation [483]. Both data and calculation have been rescaled to 200 GeV/nucleon.

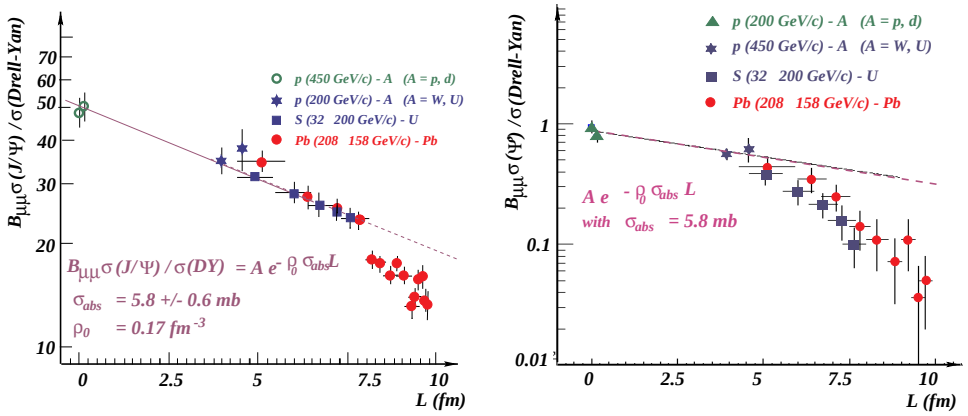

Figure 24. Preliminary data on J/ψ/DY and ψ'/DY plotted as a function of the Glauber model nuclear thickness parameter, L, discussed in text. This plot suggests a sudden extra suppression of J/ψ when the effective nuclear depth increases to about 8 fm.

the octet $c\bar{c}$ effective cross section. The light-ion suppression pattern and the p + A data are now commonly agreed to be consistent with hadronic (confined matter) dissociation scenarios [161, 457, 466, 467]. As pointed out , however, the pre-resonance $c\bar{c}_8$–g state is not an eigenstate of QCD and the use of an effective cross section for it in Glauber models is not without ambiguity.

The data by the NA50 collaboration with the Pb + Pb experiment has given rise to

renewed speculation on an additional suppression and on the possible creation of a deconfined phase [484–486]. Plotting the total J/ψ over DY cross section ratio as a function of collision system mass ($A_P \cdot A_T$) an additional suppression in the order of 20% is observed between S + U and Pb + Pb. However, when studying the cross section as a function of E_T, a discontinuity at $E_T > 50$ GeV may only be inferred when comparing the experimental J/ψ over DY ratio versus E_T with a Glauber-type calculation (without QGP formation) employing the same *comover* density as in the S + U case. The same Glauber-type hadronic absorption models [470] are also capable of reproducing the lead data of NA50 if a higher *comover* density is employed for Pb + Pb than for S + U [487]. For low transverse energies current hadronic *comover* models have difficulties in fitting the data. Therefore the issue whether simple *comover* models describe the lead data is not yet fully settled.

Hadronic transport model calculations incorporate the full collision dynamics and go far beyond the commonly used simplified version of the Glauber theory [483, 488–490]. These transport model calculations are very sensitive to certain input parameters such as the formation time of the J/ψ and the comovers. In a first round of early calculations the HSD transport model [488] was fully able reproduce the NA50 lead data while assuming a fixed formation time of 0.7–0.8 fm/c for both J/ψ and comovers. However, the hadron density which causes the suppression in the model may be unreasonably high. The UrQMD model [110], however, uses for the comovers a variable formation time emerging from the Lund string fragmentation formalism (here the formation time depends on the hadron mass) and zero formation time for the J/ψ. The assumption of zero formation time is valid if the J/ψ is considered as pre-resonance $c\bar{c}_8$–g state with a hadronic dissociation cross section of 7 mb. However, in this mode the UrQMD model did not reproduce the additional suppression of the Pb + Pb experiment [489]. The question of formation time might be a central issue since in the colour octet model the dissociation cross section is actually higher during the lifetime of the pre-resonance $c\bar{c}_8$–g state [484, 491] than after hadronization. Furthermore the amount of comover–charmonium interaction will crucially depend on the formation time (and thus the cross section) of the comovers and whether the comovers are allowed to interact within their formation time as 'pre-formed' states (analogously to the charmonium 'pre-resonance' states).

Recently, a new HSD calculation studied the influence of strings on the J/ψ suppression. The $c\bar{c}$ pairs were produced perturbatively and the influence of dissociation of those pairs by strings was taken into account by regarding strings as longitudinal geometrical objects with a specific transverse radius [490]. Good agreement with the data from NA38 and NA50 was found for a string radius of $R_s \approx 0.2$–0.3 fm. A new UrQMD calculation employs a microscopic Glauber simulation for J/ψ production and the full microscopic transport calculation for nuclear and comover dynamics as well as for rescattering [483]. The dissociation cross sections are calculated using the QCD factorization theorem [464], feeding from ψ' (5%) and χ states (40%) is taken into account and the $c\bar{c}$ dissociation cross sections increase linearly with time during the formation time of the charmonium state. Using only nuclear dissociation yields, a far smaller suppression than seen in the data is achieved. However, if comovers are taken into account ($\sigma_{meson} \approx 2/3\sigma_{nucleon}$), the agreement between theory and data is impressive (see figure 23). The strong dependence of these results on details, such as the treatment of the formation time or the time-dependent dissociation cross section, remain to be studied further.

Quantum effects such as energy-dependent formation and coherence lengths must be taken into account [492] before definite statements can be made with regard to the nature of the J/ψ suppression.

Whereas there exist techniques to calculate the J/ψ nucleon cross section without using the vector dominance model [493], the size of the $c\bar{c}$–comover interaction is still unclear.

TJNAF and HERMES experiments may be able to address the question of interaction of spatially small configurations with the nuclear medium. Such a research will help to understand the interaction of the $\overline{c}c$ wavepacket with comovers at comparatively low energies [494].

Interpretations of the data based on plasma scenarios are also increasingly evolving away from the original Mott transition analogue. For example, J/ψ suppression due to large coherent colour fields (strings/ropes) have been proposed [490]. Percolation of longitudinal strings of transverse radius $\sim$0.25 fm have been proposed to explain the possible sudden drop of the J/ψ yield at moderate impact parameters (low E_T) [495]. It is clear that much work needs to be done theoretically to sort through the many competing dynamical models of charmonium absorption. The observed effects are among the most striking results found in heavy-ion reactions and deserve the intense attention they now receive.

On the experimental side, it would be especially important to map out carefully the A-dependence in the intermediate mass range $30 < A < 200$ to confirm if there is a discontinuity or rapid change in the mechanism for moderate nuclear depths as was hinted at by the Pb data. In addition the functional dependence of the J/Ψ yield as a function of E_T needs to be clarified for the low ($E_T < 40$ GeV) and high E_T ($E_T > 100$ GeV) limit. The beam energy dependence would be valuable to know, given the very rapid variation in pp at present SPS energies and to study the suggested expansion of small wavepackets [464]. Finally, an independent experimental confirmation of the results is essential. Most likely only at RHIC will there be an independent experiment, PHENIX, capable of addressing this very important observable. While nominally running at $\sqrt{s} = 200$ A GeV, RHIC will be able to approach SPS conditions down to $\sim$30 A GeV.

Of course, one of the most important additional experimental checks would be the search for discontinuities in other observables such as the strangeness fraction and HBT radii for less central reactions with E_T in the region suggested by NA50 where new physics may arise. Thus far, the other experiments have concentrated on more central collisions and the observables have varied smoothly as a function of control parameters, A, E, ...

In summary, a striking pattern of charmonium suppression has been discovered by NA38/NA50 at the SPS. The theoretical debate on its interpretation is far from settled, but great strides have been made in the past decade to refine concepts and models. The rapid change in the suppression could be the smoking gun of deconfinement, but it is not likely to be due to simple Debye screening effect originally hoped for. Rather novel QCD dynamics in a non-equilibrium plasma (e.g. enhanced colour field fluctuations in moderate frequency $\omega \sim 0.5$–1.0 GeV) may emerge as the final culprit. A goal of further theoretical work will not be to continue to try to rule out more 'conventional' explanations, but to give positive proof of additional suppression by QCD-based calculations which actually *predict* the E_T-dependence of the conjectured signature. Consistency tests and a detailed simultaneous analysis of all the other measured observables are needed, if at least the same standards as for the present calculations involving other signatures are to be held up.

4. Summary and outlook

4.0.1. AGS and SPS milestones. In the last two years the heavy-ion research at Brookhaven and CERN have succeeded in achieving the measurement of a wide spectrum of observables with truly heavy-ion beams Au + Au and Pb + Pb. As these programmes continue to measure with greater precision the beam energy, nuclear size, and centrality dependence of those observables, it is important to recognize the major milestones past thus far in that work. Experiments have conclusively demonstrated the existence of strong nuclear A-dependence of

- *baryon stopping power* [134, 143]
- *hadronic resonance* production [149]
- *collective (transverse, directed, and elliptic) flow* of baryons and mesons both at AGS and SPS energies [223, 230, 231]
- *strangeness enhancement* [144, 293, 295, 303]
- *meson interferometric source radii* [253, 256, 260–264]
- *dilepton enhancement* below the ρ mass [397, 440]
- *anomalous J/ψ and ψ' suppression* [481, 482, 496].

These observables prove that high energy- and baryon density matter has been created in nuclear collisions. The global multiplicity and transverse energy measurements prove that substantially more entropy is produced in A + A than simple superposition of A $\times$ pp would imply. Multiple initial- and final-state interactions play a critical role in all observables. The high mid-rapidity baryon density and the observed collective radial and directed flow patterns constitute one of the strongest evidence for the existence of an extended period ($\Delta\tau \sim 10$ fm/c) of strong final state interactions. The enhanced ψ' suppression in S + U relative to p + A again attests to this fact. The anomalous low-mass dilepton enhancement shows that substantial in-medium modifications of multiple collision dynamics exists, possibly related to mass shifts or in-medium broadening of vector mesons. The systematics of the strangeness (and anti-strangeness) quantum number production shows that novel non-equilibrium production processes arise in these reactions. Finally, the centrality dependence of J/ψ absorption in Pb + Pb collisions hints towards the non-equilibrium nature of such reactions, but can also be seen—in the case of an anomalous centrality dependence—as indication that high-frequency gluon modes may be excited in such reactions. Is this the sought after QGP that thus far has only existed as a binary array of predictions inside teraflop computers? It is too early to tell. Theoretically there are still too many 'scenarios' and idealizations to provide a satisfactory answer. And there are experimental gaps such as lack of intermediate mass $A \sim 100$ data and the limited number of beam energies studied thusfar. The field is at the doorstep of the next milestone: A + A at $\sqrt{s} = 30$–200 A GeV due to begin at RHIC/BNL in 1999.

At the AGS, where particle spectra already have transverse slopes $T > T_C$, the highest chances for the discovery of partonic degrees of freedom lie in the measurement of the collective flow excitation function and the search for novel *strangelet* configurations. The investigation of the physics of high baryon density (i.e. partial restoration of chiral symmetry via properties of vector mesons), for which the gold beam at the AGS would be ideal, are unfortunately not accessible due to the lack of experimental setups capable of measuring electro-magnetic probes in AA collisions.

At the CERN/SPS new data on electro-magnetic probes, strange particle yields (most importantly multistrange (anti)hyperons) and heavy quarkonia will be interesting to follow closely. Energy densities estimated from rapidity distributions and temperatures extracted from particle spectra indicate that initial conditions should be near or just above the domain of deconfinement and chiral symmetry restoration. With respect to HBT (meson interferometry) source radii, the matter is not yet adequately resolved (extensive and precise comparisons with hadronic and deconfinement model calculations have yet to be performed). Directed flow has been observed—a flow excitation function, filling the gap between 10 A GeV (AGS) and 160 A GeV (SPS), would be extremely interesting to look for the softest point of the QCD EoS. An effort to perform experiments in this energy region at the SPS is underway. However, dedicated runs would be mandatory to really explore these intriguing effects in the excitation function. It is questionable whether this key programme will actually get support at the SPS. Also the excitation function of particle yield ratios (π/p, d/p, K/π ...) and, in particular,

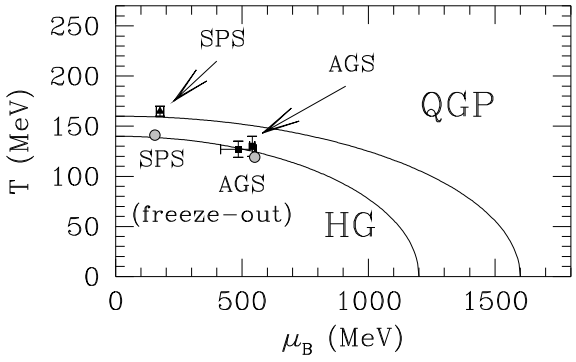

Figure 25. Phase diagram of nuclear matter, adapted from [49, 497]. The two curves mark the location of the expected phase boundary at its level of uncertainty. The data points mark thermal freeze-out parameters deduced from AGS and SPS data, taking flow into account. The arrows indicate how the freeze-out conditions may be reached during the expansion of the fireball. The two grey points show thermal model fits to UrQMD predictions for heavy collision systems.

multistrange (anti-)hyperon yields, may be a sensitive probe of changes in the physics of the EoS. Most intriguing, however, would be the search for novel, unexpected, forms of $SU(3)$ matter, e.g. MEMOS, *strangelets* or even *charmlets*. Such exotic QCD mesonic and nuclear configurations would extend the present periodic table of elements into hitherto unexplored flavour dimensions. A strong experimental effort should continue in that direction. The current status concerning the phase-diagram of nuclear matter is depicted in figure 25.

We note that exotic non-equilibrium phenomena such as disoriented chiral condensates (DCC) that could effect very small transverse momentum pion spectra and charge/neutral meson fluctuations should also be continued to look for. These are highly speculative and scenario-dependent phenomena, but worth searching for along with the above exotic mesonic and nuclear states.

Another intriguing possibility of observing the transition from nuclear matter to deconfined quark matter may lie in the timing structure of pulsar spin-downs [498]: pulsars contain a huge amount of angular momentum and rotational energy. The emission of electro-magnetic radiation and electron–positron pairs (over a timespan of millions of years) causes a reduction in the angular velocity and thus also a reduction in the centrifugal deformation of the pulsar. Consequently the interior density of the pulsar increases and may rise from below the critical density for a phase transition to above the critical value. In the resulting phase transition a conversion from rather incompressible nuclear matter to highly compressible quark matter will take place (starting at the centre of the pulsar) which reduces the radius of the pulsar and causes and anomalous decrease of the moment of inertia with decreasing angular velocity. This is superposed on the normal reduction of angular velocity due to radiation loss. In order to conserve angular momentum, the deceleration of the angular velocity may decrease or even change sign resulting in a pulsar spin-up. The timespan in which this effect may be observable is estimated to be in the order of 10^5 years. Since the mean life of pulsars is around 10^7 years, 1% of the 700 currently known pulsars may currently be undergoing this phase transition.

4.0.2. New facilities: RHIC and LHC. RHIC will begin operation in 1999 with four detectors: two medium-scale ones, BRAHMS and PHOBOS, as well as two large-scale detectors, PHENIX and STAR. BRAHMS (Broad RAnge Hadron Magnetic Spectrometer) is a conventional spectrometer (adapted from the AGS programme) with particle ID, covering

the cm rapidity range 0–4. PHOBOS is a two-arm magnetic spectrometer which will be able to measure low p_t charged hadrons *and* leptons at selected solid angles.

PHENIX is a large solenoid with a variety of multi-purpose detector arrays; its goal is the multiple detection of phase transition signatures via the measurement of hadrons, leptons and photons in the same central rapidity bin [499]. Apart from the QGP signatures which are already discussed, the PHENIX experiment will also search for a disoriented chiral condensate (DCC)† [77, 501, 502].

The main emphasis of the STAR (solenoidal tracker at Rhic) detector will be the correlation of many (predominantly hadronic) observables on an event-by-event basis‡ [504].

The great energy range and beam target range accessible with RHIC will allow a dedicated systematic search for the quark-gluon phase matter at energy density an order of magnitude above the transition domain. This occurs not only because the rapidity density of hadrons is expected to be 2–4 times larger than in central SPS collision, but also because pQCD dominated minijet initial conditions are finally reached at collider ($\sqrt{s} \sim 200$ A GeV) energy range. A whole class of new signatures involving hard pQCD probes (high p_T and jets) becomes available.

At yet higher energies at LHC, QGP research efforts and planning are centred around the ALICE detector. Its design is similar to that of STAR. However, dimuon arms (as in PHENIX) are also planned. ALICE will be the only large-scale heavy-ion detector set-up at LHC. At $\sqrt{s} \sim 5$ A TeV even bottom quarkonia are copiously produced and transverse momenta twice as high ($p_\perp \sim 60$ GeV/c) will be readily measurable to probe even deeper into the multiparticle dynamics in a QGP.

For applications to nuclear collision observables, an extension of the QGP concept to non-equilibrium conditions is required. The popular use of simple fireball models may provide convenient parametrizations of large bodies of data, but they will never provide a convincing proof of new physics. Microscopic transport models are required that can address simultaneously all the observables and account for experimental acceptance and trigger configurations. Present work in parton cascade dynamics is based largely on analogy of transport phenomena in known abelian QED plasmas. A significant new feature of QCD plasmas is its ultrarelativistic nature and the dominance of (gluon) radiative transport. These greatly complicate the equations. The role of quantum coherence phenomena beyond classical transport theories has only recently been established within idealized models. Much further work will be required in this connection. The outstanding theoretical task will be the development of practical (versus formal) tools to compute quantum non-equilibrium multiple collision dynamics in QCD. Recent work [505] along the lines of non-compact lattice formulations of gauge theories may provide one of the most promising avenues in that direction. As yet unrealized techniques utilizing supersymmetry and string theory should also be explored.

Experiments and data on ultra-relativistic collisions are essential in order to motivate, guide, and constrain such theoretical developments. They provide the only terrestrial probes of non-perturbative aspects of QCD and its dynamical vacuum. The understanding of confinement and chiral symmetry remains one of the key questions at the end of this millennium.

† A first preliminary result was published on the DCC search at CERN/SPS by the WA98 collaboration [500]: At a 90% confidence level they rule out a DCC admixture of greater than 20%.

‡ Recently, the NA49 collaboration presented first measurements of event-by-event fluctuations at the CERN/SPS, which may have significant implications for the issue of thermalization and critical fluctuations near a phase transition [503]. The measured disappearance of strong dynamical fluctuations in $\langle p_t \rangle$ suggest a high degree of equilibration or at least rescattering. The absence of non-Gaussian fluctuations furthermore may exclude the possibility that the system has been close to a phase transition.

Acknowledgments

We wish to express our thanks to our colleagues Adrian Dumitru, Jens Konopka, Christian Spieles, Markus Bleicher, Sven Soff and Lars Gerland for many fruitful discussions and suggestions. We are very grateful to Lonya Frankfurt, Carlos Lourenco and Dieter Röhrich for their comments and improvements to the manuscript. SAB, MG and HS thank the Institute for Nuclear Theory at the University of Washington for its hospitality and the Department of Energy for partial support during the completion of this work. Finally, SAB thanks Berndt Müller for many enlightening discussions.

This work was supported by DFG, GSI, BMBF and in part by DOE grant DE-FG02-96ER40945 and the A v Humboldt Foundation.

References

[1] Kerman A, Lederman L, Lee T D, Ruderman M and Weneser J (ed) 1974 BeV nucleon collisions of heavy ions—how and why *BNL-Report* 50445

[2] Schroeder L S (ed) 1974 Proceedings of the second high energy heavy ion study in Berkeley, USA *LBL-Preprint* 3675

[3] Bock R and Stock R (ed) 1978 *Symp. on relativisitic Heavy Ion Research at GSI (Darmstadt)* GSI-P-5-78

[4] Glendenning N K, Gyulassy M, Hendrie D, Schroeder L S and Poskanzer A M (ed) 1978 Proceedings of the fourth high energy heavy ion study in Berkeley, USA *LBL-Preprint* 7766

[5] Wilkinson D (ed) 1980 Heavy Ion Interactions at high energies *Prog. Part. Nucl. Phys.* **4**

[6] Gutbrod H H, Hendrie D, Pugh H G, Randrup J and Schroeder L S (ed) 1981 Proceedings of the fifth high energy heavy ion study in Berkeley, USA *LBL-Preprint* 12652

[7] Pugh H G (ed) Proceedings of the sixth high energy heavy ion study in Berkeley, USA *LBL-Preprint* 16281

[8] Bock R, Gutbrod H H and Stock R (ed) 1984 Proceedings of the seventh high energy heavy ion Study at GSI Darmstadt, Germany *GSI-Report* 85-10

[9] Schroeder L S *et al* (ed) 1987 Proceedings of the eighth high energy heavy ion study in Berkeley, USA *LBL-Preprint* 24580

[10] Chacon A D, Justice M and Ritter H G (ed) 1993 Proceedings of the ninth high energy heavy ion study in Berkeley, USA *LBL-Preprint* 35980

[11] Greiner W and Stöcker H (ed) 1990 *The Nuclear Equation of State (NATO ASI Series B 216)* (New York: Plenum)
Greiner W and Stöcker H (ed) 1989 *Proc. NATO Advanced Studies Institute (Peniscola, Spain, May)*

[12] Greiner W, Stöcker H and Gallmann A (ed) 1994 *Hot and Dense Nuclear Matter (NATO ASI Series B 335)* (New York: Plenum)
Greiner W, Stöcker H and Gallmann A (ed) 1993 *Proc. NATO Advanced Studies Institute (Bodrum, Turkey, October)*

[13] Stöcker H, Gallmann A and Hamilton J (ed) 1997 *Structure of Vacuum and Elementary Matter* (Singapore: World Scientific)
Stöcker H, Gallmann A and Hamilton J (ed) 1996 *Proc. Int. Conf. on Nuclear Physics at the Turn of the Millenium in Wilderness (South Africa, Marc)*

[14] Axelrod A, Bock R, Gutbrod H, Gyulassy M, Poskanzer A and Schroeder L S (ed) 1979 Proceedings of the first workshop in ultra-relativistic nuclear collisions in Berkeley, USA *LBL-Preprint* 8957

[15] Proceedings of the Workshop on Future Relativistic Heavy Ion Experiments, GSI, Darmstadt, Germany, 1980

[16] Satz H (ed) 1981 *Statistical Mechanics of Quarks and Gluons* (Amsterdam: North-Holland)

[17] Jacob M and Satz H (ed) 1982 *Quark Matter Formation and Heavy Ion Collisions* (Singapore: World Scientific)

[18] Ludlam T W and Wegener H E (ed) 1984 Quark Matter '83 *Proc. 3rd Int. Conf. on Ultra-Relativistic Nucleus–Nucleus Collisions (Brookhaven, NY) Nucl. Phys.* A **418**

[19] Kajantie K (ed) 1984 Quark Matter '84 *Proc. 4th Int. Conf. on Ultra-Relativistic Nucleus–Nucleus Collisions (Helsinki)* (Berlin: Springer)

[20] Schroeder L S and Gyulassy M (ed) 1987 Quark Matter '86 *Proc. 5th Int. Conf. on Ultra-Relativistic Nucleus–Nucleus Collisions (Asilomar, CA) Nucl. Phys.* A **461**

[21] Santo R, Satz H, Specht H and Stock R (ed) 1988 Quark Matter '87 *Proc. 6th Int. Conf. on Ultra-Relativistic Nucleus–Nucleus Collisions (Nordkirchen) Z. Phys.* C **38**

[22] Baym G, Braun-Munzinger P and Nagamiya S (ed) 1989 Quark Matter '88 *Proc. 7th Int. Conf. on Ultra-Relativistic Nucleus–Nucleus Collisions (Lenox, MA) Nucl. Phys.* A **498**
[23] Blaizot J P, Gerschel C, Pire B and Romana A (ed) 1991 Quark Matter '90 *Proc. 8th Int. Conf. on Ultra-Relativistic Nucleus–Nucleus Collisions (Menton, France) Nucl. Phys.* A **525**
[24] Awes T C, Obenshain F E, Plasil F, Strayer M R and Wong C Y (ed) 1992 Quark Matter '91 *Proc. 9th Int. Conf. on Ultra-Relativistic Nucleus–Nucleus Collisions (Gatlinburg, TN) Nucl. Phys.* A **544**
[25] Stenlund E, Gustafsson H A, Oskarsson A and Otterlund I (ed) 1994 Quark Matter '93 *Proc. 10th Int. Conf. on Ultra-Relativistic Nucleus–Nucleus Collisions (Borlänge, Sweden) Nucl. Phys.* A **566**
[26] Poskanzer A M, Harris J W and Schroeder L S (ed) 1995 Quark Matter '95 *Proc. 11th Int. Conf. on Ultra-Relativistic Nucleus–Nucleus Collisions (Monterey, CA) Nucl. Phys.* A **590**
[27] Braun-Munzinger P, Satz H, Specht H, Stock R and Stöcker H (ed) 1996 Quark Matter '96 *Proc. 12th Int. Conf. on Ultra-Relativistic Nucleus–Nucleus Collisions (Heidelberg, Germany) Nucl. Phys.* A **610**
[28] Hatsuda T, Miake Y, Yagi K and Nagamiya S (ed) 1998 Quark Matter '97 *Proc. 13th Int. Conf. on Ultra-Relativistic Nucleus–Nucleus Collisions (Tsukuba) Nucl. Phys.* A **638**
[29] Bertsch G F, Gelbke C K and Scott D K (ed) 1983 Nucleus–nucleus collisions *Nucl. Phys.* A **400**
[30] Gustaffson H A, Jakobsson B, Otterlund I and Aleklett K (ed) 1986 Nucleus–nucleus collisions II *Nucl. Phys.* A **447**
[31] Rafelski J (ed) 1995 Strangeness '95 *Proc. Conf. on Strangeness in Hadronic Matter (Tucson, AZ) (AIP Conf. Proc. 340)*
[32] Csoergoe T, Levai P and Zimanyi J (ed) 1996 Strangeness '96 *Proc. Conf. on Strangeness in Hadronic Matter (Budapest, Hungary)* (Budapest: Akademiai Kiado)
[33] 1997 SQM '97 *Proceedings of the Conference on Strangeness in Hadronic Matter (Santorini, Greece) J. Phys. G: Nucl. Part. Phys.* **23**
[34] Müller B 1985 *The Physics of the Quark Gluon Plasma* (Heidelberg: Springer)
[35] Hwa R 1990 *Quark-Gluon Plasma* vol 1 (Singapore: World Scientific)
[36] Hwa R 1995 *Quark-Gluon Plasma* vol 2 (Singapore: World Scientific)
[37] Csernai L P 1994 *Introduction to Relativistic Heavy Ion Collisions* (Chichester: Wiley)
[38] Wong C Y 1994 *Introduction to High Energy Heavy-Ion Physics* (Singapore: World Scientific)
[39] Shuryak E V 1980 *Phys. Rep.* **61** 71
[40] McLerran L 1986 *Rev. Mod. Phys.* **58** 1021
[41] Csernai L P and Kapusta J I 1986 *Phys. Rep.* **131** 225
[42] Stock R 1986 *Phys. Rep.* **135** 261
[43] Stöcker H and Greiner W 1986 *Phys. Rep.* **137** 277
[44] Clare R B and Strottman D 1986 *Phys. Rep.* **141** 179
[45] Schürmann B, Zwermann W and Malfliet R 1986 *Phys. Rep.* **147** 3
[46] Kajantie K and McLerran L 1987 *Ann. Rev. Mod. Nucl. Part. Sci.* **37** 293
[47] Singh C P 1993 *Phys. Rep.* **236** 147
[48] Müller B 1995 *Rep. Prog. Phys.* **58** 611
[49] Harris J and Müller B 1996 *Ann. Rev. Nucl. Part. Sci.* **46** 71
[50] Greiner W and Rischke D 1996 *Phys. Rep.* **264** 183
[51] Alam J, Raha S and Sinha B 1996 *Phys. Rep.* **273** 243
[52] Pochodzalla J *et al* 1995 *Phys. Rev. Lett.* **75** 1040
[53] Lee T D and Wick G C 1974 *Phys. Rev.* D **9** 2291
[54] Scheid W, Müller H and Greiner W 1974 *Phys. Rev. Lett.* **32** 741
[55] Collins J C and Perry M 1975 *Phys. Lett.* **34** 1353
[56] Polyakov A M 1977 *Phys. Lett.* B **72** 224
[57] Scheid W, Ligensa R and Greiner W 1968 *Phys. Rev. Lett.* **21** 1479
[58] Chapline G F, Johnson M H, Teller E and Weiss M S 1973 *Phys. Rev.* D **8** 4302
[59] Eskola K and Kajantie K 1997 *Z. Phys.* C **75** 515
[60] Bjorken J D 1983 *Phys. Rev.* D **27** 140
[61] Kapusta J I 1983 *Finite Temperature Field Theory* (Cambridge: Cambridge University Press)
[62] Braaten E and Pisarski R D 1990 *Nucl. Phys.* B **337** 569
[63] Thoma M 1995 *Quark Gluon Plasma* vol 2, ed R Hwa (Singapore: World Scientific)
[64] Baier R, Dokshitser Y L, Mueller A H, Peigne S and Schiff D 1996 *Nucl. Phys.* B **478** 577
[65] Kajantie K, Laine M, Rummukainen K and Shaposhnikov M 1997 *Nucl. Phys.* B **503** 357
[66] Vija H and Thoma M 1995 *Phys. Lett.* B **342** 212
[67] Braaten E and Nieto A 1996 *Phys. Rev. Lett.* **76** 1417
[68] Wilson K 1974 *Phys. Rev.* D **10** 2445

[69] See, for instance, Creutz M 1983 *Quarks, Gluons and Lattices* (Cambridge: Cambridge University Press)
[70] Laermann E 1996 *Nucl. Phys.* A **610** 1
[71] Blum T, Kärkkäinen L, Toussaint D and Gottlieb S 1995 *Phys. Rev.* D **51** 5153
[72] Bernard C *et al* 1998 *Phys. Rev. Lett.* **81** 3087
[73] Boyd G *et al* 1995 *Phys. Rev. Lett.* **75** 4169
[74] Boyd G *et al* 1995 *Phys. Lett.* B **349** 170
[75] Bernard C *et al* 1997 *Phys. Rev.* D **55** 6861
[76] Svetitsky B and Yaffe L G 1982 *Phys. Rev.* D **29** 963
[77] Pisarski R D and Wilczek F 1984 *Phys. Rev.* D **29** 338
[78] Rajagopal K and Wilczek F 1993 *Nucl. Phys.* B **399** 395
[79] Karsch F 1994 *Phys. Rev.* D **49** 3791
[80] Brown F R *et al* 1990 *Phys. Rev. Lett.* **65** 2491
[81] DeTar C 1988 *Phys. Rev.* D **37** 2328
[82] Rajagopal K 1998 *Nucl. Phys.* A **642** 26
[83] Shuryak E 1998 *Nucl. Phys.* A **642** 14
[84] Spieles C, Stöcker H and Greiner C 1998 *Phys. Rev.* C **57** 908
[85] Wang X N and Gyulassy M 1991 *Phys. Rev.* D **44** 3501
[86] Geiger K and Müller B 1992 *Nucl. Phys.* B **369** 600
[87] Wang X N and Gyulassy M 1992 *Phys. Rev.* D **45** 844
[88] Wang X N and Gyulassy M 1994 *Comput. Phys. Commun.* **83** 307
[89] Geiger K 1995 *Phys. Rep.* **258** 237
[90] Ellis J and Geiger K 1995 *Phys. Rev.* D **52** 1500
[91] Eskola K and Wang X N 1994 *Phys. Rev.* D **49** 1284
[92] Gyulassy M, Pang Y and Zhang B 1997 *Nucl. Phys.* A **629** 999
[93] Shuryak E V 1992 *Phys. Rev. Lett.* **68** 3270
[94] Biro T, van Doorn E, Müller B, Thoma M H and Wang X N 1993 *Phys. Rev.* C **48** 1275
[95] Geiger K and Kapusta J I 1993 *Phys. Rev.* D **47** 4905
[96] Xiong L and Shuryak E V 1994 *Phys. Rev.* C **49** 2207
[97] Yariv Y and Fraenkel Z 1979 *Phys. Rev.* C **20** 2227
[98] Cugnon J 1980 *Phys. Rev.* C **22** 1885
[99] Pang Y, Schlagel T J and Kahana S H 1992 *Phys. Rev. Lett.* **68** 2743
[100] Kruse H, Jacak B V and Stöcker H 1985 *Phys. Rev. Lett.* **54** 289
[101] Molitoris J J and Stöcker H 1985 *Phys. Rev.* C **32** R346
[102] Aichelin J and Bertsch G 1985 *Phys. Rev.* C **31** 1730
[103] Aichelin J, Rosenhauer A, Peilert G, Stöcker H and Greiner W 1987 *Phys. Rev. Lett.* **58** 1926
[104] Peilert G, Stöcker H, Rosenhauer A, Bohnet A, Aichelin J and Greiner W 1989 *Phys. Rev.* C **39** 1402
[105] Aichelin J 1991 *Phys. Rep.* **202** 233
[106] Sorge H, Stöcker H and Greiner W 1989 *Ann. Phys., NY* **192** 266
[107] Li B A and Ko C M 1995 *Phys. Rev.* C **52** 2037
[108] Weber K, Blattel B, Koch V, Lang A, Cassing W and Mosel U 1990 *Nucl. Phys.* A **515** 747
[109] Ehehalt W and Cassing W 1996 *Nucl. Phys.* A **602** 449
[110] Bass S A *et al* 1998 *Progr. Part. Nucl. Phys.* **41** 225
[111] Anderson B *et al* 1987 *Nucl. Phys.* B **281** 289
[112] Anderson B *et al* 1987 *Comput. Phys. Commun.* **43** 387
[113] Sjoestrand T 1994 *Comput. Phys. Commun.* **82** 74
[114] Werner K 1993 *Phys. Rep.* **232** 87
[115] Biro T and Knoll J 1984 *Nucl. Phys.* B **245** 449
[116] Sorge H, Berenguer M, Stöcker H and Greiner W 1992 *Phys. Lett.* B **289** 6
[117] Werner K and Aichelin J 1993 *Phys. Lett.* B **308** 372
[118] Aichelin J and Werner K 1993 *Phys. Lett.* B **300** 158
[119] Amelin N S, Csernai L P, Staubo E F and Strottman D 1992 *Nucl. Phys.* A **544** 463c
[120] Brachmann J, Dumitru A, Maruhn J A, Stöcker H, Greiner W and Rischke D H 1997 *Nucl. Phys.* A **619** 391
[121] van Hove L 1987 *Nucl. Phys.* A **461** 3
[122] Kajantie K 1989 *Nucl. Phys.* A **498** 355
[123] Busza W and Goldhaber A S 1984 *Phys. Lett.* B **139** 235
[124] Hartnack C, Zhuxia L, Neise L, Peilert G, Rosenhauer A, Sorge H, Aichelin J, Stöcker H and Greiner W 1989 *Nucl. Phys.* A **495** 303c
[125] Berenguer M, Hartnack C, Peilert G, Stöcker H, Greiner W, Aichelin J and Rosenhauer A 1992 *J. Phys. G:*

Nucl. Part. Phys. **18** 655
[126] Schmidt W, Katscher U, Waldhauser B, Maruhn J A, Stöcker H and Greiner W 1993 *Phys. Rev.* C **47** 2782
[127] Gyulassy M and Greiner W 1977 *Ann. Phys.* **109** 485
[128] Sorge H, Keitz A v, Mattiello R, Stöcker H and Greiner W 1990 *Phys. Lett.* B **243** 7
[129] Keitz A v, Winckelmann L, Jahns A, Sorge H, Stöcker H and Greiner W 1991 *Phys. Lett.* B **263** 353
[130] Schönfeld T, Stöcker H, Greiner W and Sorge H 1993 *Mod. Phys. Lett.* A **8** 2631
[131] Vance S E, Gyulassy M and Wang X N 1998 *Nucl. Phys.* A **638** 395
[132] Mattiello R 1995 *PhD Thesis* J W Goethe Universität, Frankfurt am Main
[133] Gonin M *et al* 1993 *Nucl. Phys.* A **566** 601c
[134] Videbaek F *et al* 1995 *Nucl. Phys.* A **590** 249c
[135] Boguta J 1981 *Phys. Lett.* B **109** 251
[136] Li Z, Mao G, Zhuo Y and Greiner W 1997 *Phys. Rev.* C **56** 1570
[137] Hofmann M, Mattiello R, Sorge H, Stöcker H and Greiner W 1995 *Phys. Rev.* C **51** 2095
[138] Roland G *et al* 1998 *Nucl. Phys.* A **638** 91
[139] Blobel V *et al* 1974 *Nucl. Phys.* B **69** 454
[140] Abbott T *et al* 1994 *Phys. Rev.* C **50** 1024
[141] Barrette J *et al* 1994 *Phys. Rev.* C **50** 3047
[142] Baechler J *et al* 1994 *Phys. Rev. Lett.* **72** 1419
[143] Wienold T *et al* 1996 *Nucl. Phys.* A **610** 76
[144] Bormann C *et al* 1997 *J. Phys. G: Nucl. Part. Phys.* **23** 1817
[145] The WA97 Collaboration *Proc. SQM'98* 1999 *J. Phys. G: Nucl. Part. Phys.* **25**
[146] Barrette J *et al* 1993 *Phys. Rev. Lett.* **70** 2996
[147] Barrette J *et al* 1994 *Nucl. Phys.* A **566** 411c
[148] Hemmick T *et al* 1994 *Nucl. Phys.* A **566** 435c
[149] Barrette J *et al* 1995 *Phys. Lett.* B **351** 93
[150] Baechler J *et al* 1991 *Z. Phys.* C **52** 239
[151] Alber T *et al* 1995 *Phys. Rev. Lett.* **74** 1303
[152] Alber T *et al* 1994 *Z. Phys.* C **64** 195
[153] Jones P G *et al* 1996 *Nucl. Phys.* A **610** 188
[154] Cleymans J and Satz H 1993 *Z. Phys.* C **57** 135
[155] Letessier J, Rafelski J and Tounsi A 1994 *Phys. Lett.* B **321** 394
[156] Braun-Munzinger P, Stachel J, Wessels J P and Xu N 1996 *Phys. Lett.* B **365** 1
[157] Jacobs P M *et al* (The NA49 collaboration) *Proc. Conf. on Heavy Ion Physics at the AGS (HIPAGS '96) (Wayne State University, Detroit)* and to be published
[158] Capella A and Kopeliovich B Z 1996 *Phys. Lett.* B **381** 325
[159] Geiger K and Srivastava D K 1997 *Phys. Rev.* C **56** 2718
[160] Geiger K and Müller B 1997 *Heavy Ion Phys.* **7** 207
[161] Kharzeev D, Lourenco C, Nardi M and Satz H 1997 *Z. Phys.* C **74** 307
[162] Gosset J, Gutbrod H H, Meyer W G, Poskanzer A M, Sandoval A, Stock R and Westfall G D 1977 *Phys. Rev.* C **16** 629
[163] Hagedorn R and Rafelski J 1980 *Phys. Lett.* B **97** 136
[164] Stöcker H, Ogloblin A A and Greiner W 1981 *Z. Phys.* A **303** 259
[165] van Hove L 1982 *Phys. Lett.* B **118** 138
[166] Kapusta J, Pratt S, Mc Lerran L and Gersdorff H v 1985 *Phys. Lett.* B **163** 253
[167] Gersdorff H v 1987 *Nucl. Phys.* A **461** 251c
[168] Sollfrank J, Koch P and Heinz U 1990 *Phys. Lett.* B **252** 256
[169] Lee K S, Heinz U and Schnedermann E 1990 *Z. Phys.* C **48** 525
[170] Schnedermann E, Sollfrank J and Heinz U 1993 *Phys. Rev.* C **48** 2462
[171] Schnedermann E and Heinz U 1994 *Phys. Rev.* C **50** 1675
[172] Mattiello R, Jahns A, Sorge H, Stöcker H and Greiner W 1995 *Phys. Rev. Lett.* **74** 2180
[173] Mattiello R, Sorge H, Stöcker H and Greiner W 1997 *Phys. Rev.* C **55** 1443
[174] Braun-Munzinger P, Stachel J, Wessels J P and Xu N 1995 *Phys. Lett.* B **344** 43
[175] Konopka J, Stöcker H and Greiner W 1995 *Nucl. Phys.* A **583** 357
[176] Konopka J 1996 *PhD Thesis* University of Frankfurt, Germany
[177] Sorge H 1996 *Phys. Lett.* B **373** 16
[178] Herrmann N *et al* 1996 *Nucl. Phys.* A **610** 49
[179] Xu N *et al* 1996 *Nucl. Phys.* A **610** 175
[180] Bleicher M, Spieles C, Ernst C, Gerland L, Soff S, Stöcker H, Greiner W and Bass S A 1998 *e-print* nucl-

th/9803346
Bleicher M, Spieles C, Ernst C, Gerland L, Soff S, Stöcker H, Greiner W and Bass S A *Phys. Lett.* B submitted
[181] Hagedorn R 1965 *Suppl. Nuovo Cimento* **III.2** 147
[182] Siemens P J and Rasmussen J O 1979 *Phys. Rev.* C **42** 880
[183] Hung C M and Shuryak E V 1995 *Phys. Rev. Lett.* **75** 4003
[184] Bleicher M *et al* 1997 *e-print* nucl-th/9704065
Bleicher M *et al* in preparation
[185] Weber H *Diploma Thesis* Frankfurt University, unpublished
Weber H in preparation
[186] Polleri A, Bondorf J P and Mishustin I N 1998 *Phys. Lett.* B **419** 19
[187] Sorge H 1995 *Phys. Lett.* B **373**16
[188] Bass S A, Mattiello R, Hartnack C, Stöcker H and Greiner W 1993 *Phys. Lett.* B **302** 381
[189] Jahns A, Spieles C, Mattiello R, Amelin N S, Stoecker H and Greiner W 1994 *Nucl. Phys.* A **566** 483c
[190] The WA98 Collaboration: Aggarwal M M *et al* 1998 *Phys. Rev. Lett.* **81** 4087
[191] Dumitru A and Rischke D H 1999 *Phys. Rev.* C **59** 354
Dumitru A and Rischke D H 1998 *eprint* nucl-th/9806003
[192] Wang X N 1998 *eprint* hep-ph/9804384
[193] Gyulassy M and Levai P *Phys. Lett.* B submitted
Gyulassy M and Levai P 1998 *eprint* hep-ph/9807247
[194] Hofmann J, Stöcker H, Heinz U, Scheid W and Greiner W 1976 *Phys. Rev. Lett.* **36** 88
[195] Hartnack C, Aichelin J, Stöcker H and Greiner W 1994 *Phys. Rev. Lett.* **72** 3767
[196] Stöcker H and Müller B *LBL-Preprint* 12471, unpublished
[197] Stöcker H, Maruhn J A and Greiner W 1980 *Phys. Rev. Lett.* **44** 725
[198] Stöcker H, Csernai L P, Graebner G, Buchwald G, Kruse H, Cusson R Y, Maruhn J A and Greiner W 1982 *Phys. Rev.* C **25** 1873
[199] Buchwald G, Graebner G, Theiß J, Maruhn J A, Greiner W, and Stöcker H 1984 *Phys. Rev. Lett.* **52** 1594
[200] Molitoris J J, Hoffer J B, Kruse H and Stöcker H 1984 *Phys. Rev. Lett.* **53** 899
[201] Molitoris J J and Stöcker H 1985 *Phys. Lett.* B **162** 47
[202] Hartnack Ch *et al* 1992 *Nucl. Phys.* A **538** 53c
[203] Gustafsson H-A *et al* 1984 *Phys. Rev. Lett.* **52** 1590
[204] Doss K G R *et al* 1986 *Phys. Rev. Lett.* **57** 302
[205] Gutbrod H H, Kampert K H, Kolb B W, Poskanzer A M, Ritter H G and Schmidt H R 1989 *Phys. Lett.* B **216** 267
[206] Renfordt R *et al* 1984 *Phys. Rev. Lett.* **53** 763
[207] Gosset J *et al* 1990 *Phys. Lett.* B **247** 233
[208] Ramillien V *et al* 1995 *Nucl. Phys.* A **587** 802
[209] Leifels Y *et al* 1993 *Phys. Rev. Lett.* **71** 963
[210] Kugler A *et al* 1994 *Phys. Lett.* B **335** 319
[211] Brill D *et al* 1997 *Z. Phys.* A **357** 207
[212] Hartnack Ch, Stöcker H and Greiner W 1990 *Proc. Nato Adv. Study Inst. on the Nucl. Equation of State (Pe niscola, Spain*) ed W Greiner and H Stöcker (New York: Plenum)
[213] Ollitrault J Y 1993 *Phys. Rev.* D **48** 1132
[214] Danielewicz P, Lacey R A, Gossiaux P B, Pinkenburg C, Chung P, Alexander J M and McGrath R L 1998 *e-Print Archive* nucl-th/980304
[215] Rischke D H, Bernard S and Maruhn J A 1995 *Nucl. Phys.* A **595** 346
[216] Rischke D H and Gyulassy M 1996 *Nucl. Phys.* A **597** 701
[217] Rischke D H and Gyulassy M 1996 *Nucl. Phys.* A **608** 479
[218] Bravina L V, Amelin N S, Csernai L P, Levai P and Strottman D 1994 *Nucl. Phys.* A **566** 461
[219] Rischke D H, Pürsün Y, Maruhn J A, Stöcker H and Greiner W 1995 *Heavy Ion Phys.* **1** 309
[220] Waldhauser B M, Theis J, Maruhn J A, Stöcker H and Greiner W 1987 *Phys. Rev.* C **36** 1019
[221] Chance J *et al* 1997 *Phys. Rev. Lett.* **78** 2535
[222] Barrette J *et al* 1994 *Phys. Rev. Lett.* **73** 2532
[223] Barrette J *et al* 1997 *Phys. Rev.* C **55** 1420
[224] Liu H *et al* for the E895 Collaboration 1998 *Nucl. Phys.* A **638** 451
[225] Ogilvie C *et al* 1998 *Nucl. Phys.* A **638** 57
[226] Pinkenburg C *et al Phys. Rev.* submitted
[227] Schnedermann E and Heinz U 1992 *Phys. Rev. Lett.* **69** 2908
[228] Appelshäuser H *et al* 1998 *Eur. Phys. J.* C **2** 661

[229] Peitzmann T *et al* 1997 QCD phase transitions *Proc. Int. Workshop on Gross Properties of Nuclei and Nuclear Excitation XXV Hirschegg, Kleinwalsertal (Austria)*
[230] Nishimura S *et al* 1998 *Nucl. Phys.* A **638** 549
[231] Appelshäuser H *et al* 1998 *Phys. Rev. Lett.* **60** 4136
[232] Sorge H 1997 *Talk given at 6th Int. Conf. on Nucleus–Nucleus Collisions (NN 97) (Gatlinburg, TN, 2–6 June)* submitted to *Nucl. Phys.* A
Sorge H 1997 *e-Print* nucl-th/970702
[233] Hanbury Brown R and Twiss R Q 1954 *Phil. Mag.* **45** 633
Hanbury Brown R and Twiss R Q 1956 *Phil. Mag. Nature* **177** 27
Hanbury Brown R and Twiss R Q 1956 *Phil. Mag. Nature* **178** 1046
[234] Goldhaber G, Goldhaber S, Lee W and Pais A 1960 *Phys. Rev.* **120** 300
[235] Koonin S E 1977 *Phys. Lett.* B **70** 43
[236] Yano F B and Koonin S E 1978 *Phys. Lett.* B **78** 556
[237] Pratt S 1984 *Phys. Rev. Lett.* **53** 1219
[238] Pratt S 1986 *Phys. Rev.* D **33** 1314
[239] Heinz U, Tomasik B, Wiedemann U A and Wu Y F 1996 *Phys. Lett.* B **382** 181
[240] Heinz U 1996 *Nucl. Phys.* A **610** 264c
[241] Bertsch G 1989 *Nucl. Phys.* A **498** 173c
[242] Pratt S 1994 *Phys. Rev.* C **49** 2772
[243] Schlei B R, Ornik U, Plümer M and Weiner R M 1992 *Phys. Lett.* B **293** 275
[244] Bolz J, Ornik U, Plümer M, Schlei B R and Weiner R M 1993 *Phys. Lett.* B **300** 404
[245] Bolz J, Ornik U, Plümer M, Schlei B R and Weiner R M 1993 *Phys. Rev.* D **47** 3860
[246] Schlei B R, Ornik U, Plümer M, Strottmann D and Weiner R M 1996 *Phys. Lett.* B **376** 212
[247] Wiedemann U A and Heinz U 1997 *Phys. Rev.* C **56** 3265
[248] Lednicky R, Lyuboshitz V L, Erazmus B, Nouais D 1996 *Phys. Lett.* B **373** 30
[249] Soff S *et al* 1997 *J. Phys. G: Nucl. Part. Phys.* **23** 2095
[250] Greiner C, Koch P and Stöcker H 1987 *Phys. Rev. Lett.* **58** 1825
Greiner *et al* demonstrated that during the phase transition there is a build-up of a large *anti*-strangeness content in the hadronic phase, while the QGP retains a large positive net strangeness, although the net strangeness of the combined system can be equal to zero. Previous model calculations (see e.g. the work of Lee K S, Rhoades-Brown M J and Heinz U 1986 *Phys. Lett.* B **174** 123) had assumed, however, that the net strangeness vanishes in each phase separately. This is thermodynamically not correct: the Gibbs conditions require that in phase equilibrium the *chemical potentials* are continuous across the phase boundary, whereas the corresponding *densities* are discontinuous. This had been discarded in the latter work. However, later calculations of that group (Heinz U, Lee K S and Rhoades-Brown M J 1987 *Mod. Phys. Lett.* A **2** 153) have confirmed the results of Greiner *et al*.
[251] Heinz U 1997 QCD phase transitions *Proc. Int. Workshop on Gross Properties of Nuclei and Nuclear Excitation XXV (Hirschegg, Kleinwalsertal, Austria)*
[252] Tserruya I 1995 *Preprint* CERN-PPE/95-185
Tserruya I *Invited Talk at the Int. Europhysics Conf. on High Energy Physics (Brussels, July 27–August 2)*
[253] Beker H *et al* 1994 *Z. Phys.* C **64** 209
[254] Beker H *et al* 1995 *Phys. Rev. Lett.* **74** 3340
[255] Murray M *et al* 1994 *Nucl. Phys.* A **566** 589c
[256] Sullivan J P *et al* 1993 *Phys. Rev. Lett.* **70** 3000
[257] Gyulassy M and Padula S 1988 *Phys. Lett.* B **217** 181
[258] Schlei B and Xu N 1996 *Phys. Rev.* C **54** 2155
[259] Heinz U, Tomasik B, Wiedemann U A and Wu Y F 1996 *Heavy Ion Phys.* **4** 249
[260] Miskowiec D *et al* 1996 *Nucl. Phys.* A **610** 227
[261] Franz A *et al* 1996 *Nucl. Phys.* A **610** 240
[262] Kadija K *et al* 1996 *Nucl. Phys.* A **610** 248
[263] Rosselet L *et al* 1996 *Nucl. Phys.* A **610** 256
[264] Roehrich D for the NA49 Collaboration 1997 QCD phase transitions *Proc. Int. Workshop on Gross Properties of Nuclei and Nuclear Excitation XXV (Hirschegg, Kleinwalsertal, Austria)*
[265] Jacak B *et al* 1995 *Nucl. Phys.* A **590** 215c
[266] Alber T *et al* 1995 *Z. Phys.* C **66** 77
[267] Makhlin A N and Sinyukov Y M 1988 *Z. Phys.* C **39** 69
[268] Appelshäuser H 1996 *PhD Thesis* Frankfurt University
[269] Bass S A, Hartnack C, Stöcker H and Greiner W 1994 *Phys. Rev.* C **50** 2167

[270] Baker M D *et al* 1996 *Nucl. Phys.* A **610** 213
[271] Ogilvie C *et al Proc. HIPAGS '96*
[272] Bailly J P *et al* 1987 *Phys. Lett.* B **195** 609
[273] Malhotra P K and Orava R 1983 *Z. Phys.* C **17** 85
[274] Glück M and Reya E 1978 *Phys. Lett.* B **79** 453
[275] Rafelski J and Müller B 1982 *Phys. Rev. Lett.* **48** 1066 (erratum: 1982 *Phys. Rev. Lett.* **56** 2334)
[276] Rafelski J 1982 *Phys. Rep.* **88** 331
[277] Koch P, Müller B and Rafelski J 1986 *Phys. Rep.* **142** 167
[278] Schwinger J 1962 *Phys. Rev.* **128** 2425
[279] Casher A, Kogut J and Susskind L 1974 *Phys. Rev.* D **10** 732
[280] For a review on the Schwinger Particle Production mechanism and its application to QGP physics, see e.g. Wong C Y 1994 *Introduction to High Energy Heavy Ion Collisions* (Singapore: World Scientific)
[281] Koch P 1990 *Quark Gluon Plasma* ed R Hwa (Singapore: World Scientific)
[282] Rafelski J 1991 *Phys. Lett.* B **262** 333
[283] Heinz U 1994 *Nucl. Phys.* A **566** 205c
[284] Sollfrank J and Heinz U *Quark Gluon Plasma* vol 2, ed R C Hwa (Singapore: World Scientific)
[285] Letessier J, Tounsi A and Rafelski J 1992 *Phys. Lett.* B **292** 417
[286] Letessier J, Tounsi A, Heinz U, Sollfrank J and Rafelski J 1995 *Phys. Rev.* D **51** 3408
[287] Lee K S, Rhoades-Brown M and Heinz U 1988 *Phys. Rev.* C **37** 1452
[288] Redlich K 1985 *Z. Phys.* C **27** 633
[289] McLerran L 1987 *Nucl. Phys.* A **461** 245c
[290] Barz H W, Friman B L, Knoll J and Schulz H 1988 *Nucl. Phys.* A **484** 661
[291] Mattiello R, Sorge H, Stöcker H and Greiner W 1989 *Phys. Rev. Lett.* **63** 1459
[292] E802 Collaboration, Miake Y *et al* 1988 *Z. Phys.* C **38** 135
Vincent P *et al* 1989 *Nucl. Phys.* A **498** 67
NA35 Collaboration, Vesztergomi G *et al* 1988 *Z. Phys.* C **38** 129
Bamberger A *et al* 1989 *Z. Phys.* C **43** 25
[293] Anderson E *et al* 1992 *Phys. Lett.* B **294** 127
[294] Anderson E *et al* 1994 *Phys. Lett.* B **327** 433
[295] Abatzis S *et al* 1994 *Nucl. Phys.* A **566** 499c
Abatzis S *et al* 1994 *Nucl. Phys.* A **566** 491c
Abatzis S *et al* 1994 *Nucl. Phys.* A **566** 225c
[296] Abatzis S *et al* 1993 *Phys. Lett.* B **316** 615
[297] DiBari D *et al* 1995 *Nucl. Phys.* A **590** 307c
[298] Kinson J B *et al* 1995 *Nucl. Phys.* A **590** 317c
[299] Helstrup H *et al* 1996 *Nucl. Phys.* A **610** 165c
[300] Kralik I *et al* 1998 *Nucl. Phys.* A **638** 115c
[301] Venables M *et al* 1997 *J. Phys. G: Nucl. Part. Phys.* **23** 1857
[302] Andersen E *et al* 1998 *Phys. Lett.* B **433** 209
[303] Alber T *et al* 1996 *Phys. Lett.* B **366** 56
[304] Akiba Y *et al* 1996 *Nucl. Phys.* A **610** 139c
[305] Armstrong T A *et al* 1997 *eprint* nucl-ex/9709005
[306] Matsui T, Svetisky B and McLerran L D 1986 *Phys. Rev.* D **34** 2047
[307] Brown G E, Ko C M, Wu Z G and Xia L H 1991 *Phys. Rev.* C **43** 1881
[308] Rafelski J and Danos M 1994 *Phys. Rev.* C **50** 1684
[309] Letessier J, Tounsi A, Heinz U, Sollfrank J and Rafelski J 1993 *Phys. Rev. Lett.* **70** 3530
[310] Sollfrank J, Gadzicki M, Heinz U and Rafelski J 1994 *Z. Phys.* C **61** 659
[311] Becattini F and Heinz U 1997 *Z. Phys.* C **76** 269
[312] Greiner C and Stöcker H 1992 *Phys. Rev.* D **44** 3517
[313] Spieles C, Bleicher M, Gerland L, Stöcker H and Greiner C 1997 *Structure of Vacuum and Elementary Matter* ed H Stöcker, A Gallmann and J Hamilton (Singapore: World Scientific)
[314] Spieles C, Stöcker H and Greiner C 1998 *Eur. Phys. J.* C **2** 351
[315] Dumitru A, Spieles C, Stöcker H and Greiner C 1997 *Phys. Rev.* C **56** 2202
[316] Bass S A, Belkacem M, Bleicher M, Konopka J, Spieles C, Stöcker H and Greiner W 1998 *Phys. Rev. Lett.* **81** 4092
[317] Sollfrank J, Heinz U, Sorge H and Xu N 1998 *e-print* nucl-th/9811011
Sollfrank J, Heinz U, Sorge H and Xu N *Phys. Rev.* C submitted
[318] Topor Pop V *et al* 1995 *Phys. Rev.* C **52** 1618

[319] Stöcker H 1997 *J. Phys. G: Nucl. Part. Phys.* **23** 2175
[320] Zschiesche D 1997 *Diploma-Thesis* Frankfurt University
Zschiesche D to be published
[321] Bebie H, Gerber P, Goity J L and Leutwyler H 1992 *Nucl. Phys.* B **378** 95
[322] Ivanenko D D and Kurdgelaidze D F 1965 *Astrophys.* **1** 251
[323] Bodmer A R 1971 *Phys. Rev.* D **4** 1601
[324] Chin S A and Kerman A K 1979 *Phys. Rev. Lett.* **43** 1292
[325] Farhi E and Jaffee R L 1984 *Phys. Rev.* D **30** 2379
[326] Witten E 1984 *Phys. Rev.* D **30** 272
[327] Chodos A *et al* 1974 *Phys. Rev.* D **9** 3471
[328] Michel F C 1988 *Phys. Rev. Lett.* **60** 677
[329] Lukacs B, Zimanyi J and Balazs N L 1987 *Phys. Lett.* B **183** 27
[330] Schaffner-Bielich J, Greiner C, Diener A and Stöcker H 1997 *Phys. Rev.* C **55** 3038
[331] Schaffner J, Greiner C and Stöcker H 1992 *Phys. Rev.* C **46** 322
[332] Prowse D J 1966 *Phys. Rev. Lett.* **17** 782
[333] Baltz A J *et al* 1994 *Phys. Lett.* B **325** 7
[334] Kumar S *et al* 1995 *Nucl. Phys.* A **590** 29c
[335] Rotondo F S *et al* 1996 *Nucl. Phys.* A **610** 297
[336] Barish K *et al* 1996 *Heavy Ion Phys.* **4** 423
[337] Borer K *et al* 1994 *Phys. Rev. Lett.* **72** 1415
[338] Dittus F *et al* 1995 *Nucl. Phys.* A **590** 347
[339] Klingenberg R *et al* 1996 *Nucl. Phys.* A **610** 306
[340] Appelquist G *et al* 1996 *Phys. Rev. Lett.* **76** 3907
[341] Pretzl K 1996 *Talk Given at the Int. Conf. on Nuclear Physics at the Turn of the Millenium: Structure of Vacuum and Elementary Matter (George, SA, March)*
[342] Kabana S *et al* 1998 *Nucl. Phys.* A **638** 411
[343] Sandweiss J Private communication
[344] Schukraft J 1997 *Structure of Vacuum and Elementary Matter* ed H Stöcker, A Gallmann and J Hamilton (Singapore: World Scientific)
[345] Spieles C, Gerland L, Stöcker H, Greiner C, Kuhn C and Coffin J P 1996 *Phys. Rev. Lett.* **76** 1776
[346] Kapusta J , Lichard P and Seibert D 1991 *Phys. Rev.* D **44** 2774 (erratum 1993 *Phys. Rev.* D **47** 4171)
[347] Baier R, Nakkagawa H, Niegawa A and Redlich K 1992 *Z. Phys.* C **53** 433
[348] Baier R, Nakkagawa H, Niegawa A and Redlich K 1992 *Phys. Rev.* D **45** 4323
[349] Thoma M H 1995 *Phys. Rev.* D **51** 51
[350] Shuryak E V 1978 *Sov. J. Nucl. Phys.* **28** 408
[351] Sinha B 1983 *Phys. Lett.* B **128** 91
[352] Hwa R C and Kajantie K 1985 *Phys. Rev.* D **28** 1109
[353] Song C 1993 *Phys. Rev.* C **47** 2861
[354] Xiong L, Shuryak E V and Brown G E 1992 *Phys. Rev.* D **46** 3798
[355] Dumitru A, Rischke D H, Stöcker H and Greiner W 1993 *Mod. Phys. Lett.* A **8** 1291
[356] Traxler C T, Vija H and Thoma M H 1995 *Phys. Lett.* B **346** 329
[357] Alam J, Srivastava D K, Sinha B and Basu D N 1993 *Phys. Rev.* D **48** 1117
[358] Dumitru A, Katscher U, Maruhn J A, Stöcker H, Greiner W and Rischke D H 1995 *Phys. Rev.* C **51** 2166
[359] Neumann J J, Seibert D and Fai G 1995 *Phys. Rev.* C **51** 1460
[360] Dumitru A, Katscher U, Maruhn J A, Stöcker H, Greiner W and Rischke D H 1995 *Z. Phys.* A **353** 187
[361] Strickland M T 1994 *Phys. Lett.* B **331** 245
[362] Srivastava D K, Sinha B, Gyulassy M and Wang X N 1992 *Phys. Lett.* B **276** 285
[363] Chakrabarty S, Alam J, Raha S , Sinha B and Srivastava D K 1992 *Phys. Rev.* D **46** 3802
[364] Cleymans J, Redlich K and Satz H 1991 *Z. Phys.* C **52** 517
[365] Koch P 1993 *Z. Phys.* C **57** 283
[366] Gale C and Lichard P 1994 *Phys. Rev.* D **49** 3338
[367] Song C, Ko C M and Gale C 1994 *Phys. Rev.* D **50** R1872
[368] Winckelmann L A, Sorge H, Stöcker H and Greiner W 1995 *Phys. Rev.* C **51** R9
[369] Baier R, Dirks M and Redlich K 1997 *Phys. Rev.* D **55** 4344
[370] Murray J, Bauer W and Haglin K 1996 *e-Print Archive* hep-ph/9611328
Murray J, Bauer W and Haglin K *Phys. Rev.* D submitted
[371] Drell S D and Yan T M 1970 *Phys. Rev. Lett.* **25** 316
[372] Spieles C, Gerland L, Hammon N, Bleicher M, Bass S A, Stoecker H, Greiner W, Lourenco C and Vogt R 1998

Eur. Phys. J. C **5** 349
[373] Braun-Munzinger P, Miskowiec D, Drees A and Lourenco C 1998 *Eur. Phys. J.* C **1** 123
[374] Gavin S, McGaughey P L, Ruuskanen P V and Vogt R 1996 *Phys. Rev.* C **54** 2606
[375] Shuryak E V 1978 *Phys. Lett.* B **78** 150
[376] Domokos G and Goldman J I 1981 *Phys. Rev.* D **23** 203
[377] Kajantie K and Miettinen H I 1981 *Z. Phys.* C **9** 341
[378] Kajantie K and Miettinen H I 1982 *Z. Phys.* C **14** 357
[379] Chin S A 1982 *Phys. Lett.* B **119** 51
[380] Cleymans J and Fingberg J 1986 *Phys. Lett.* B **168** 405
[381] Cleymans J, Fingberg J and Redlich K 1987 *Phys. Rev.* D **35** 2153
[382] Siemens P J and Chin S A 1985 *Phys. Rev. Lett.* **55** 1266
[383] Seibert D 1992 *Phys. Rev. Lett.* **68** 1476
[384] Ruuskanen P V 1991 *Nucl. Phys.* A **525** 255c
[385] Ruuskanen P V 1992 *Nucl. Phys.* A **544** 169c
[386] Ko C M and Xia L H 1989 *Phys. Rev. Lett.* **62** 1595
[387] Dumitru A, Rischke D H, Schönfeld T, Winckelmann L A, Stöcker H and Greiner W 1993 *Phys. Rev. Lett.* **70** 2860
[388] He Z and Zhang J 1995 *J. Phys. G: Nucl. Part. Phys.* **21** L49
[389] Kapusta J, McLerran L and Srivastava D K 1992 *Phys. Lett.* B **283** 145
[390] Kämpfer B and Pavlenko O P 1992 *Phys. Lett.* B **289** 127
[391] Geiger K and Kapusta J 1993 *Phys. Rev. Lett.* **70** 1920
[392] Shuryak E V and Xiong L 1993 *Phys. Rev. Lett.* **70** 2241
[393] Kampert K H *et al* 1993 *Nucl. Phys.* A **544** 183
[394] Santo R *et al* 1994 *Nucl. Phys.* A **566** 61c
[395] Albrecht R *et al* 1996 *Phys. Rev. Lett.* **76** 3506
[396] Irmscher D *et al* 1994 *Nucl. Phys.* A **566** 347c
[397] Agakichiev G *et al* 1995 *Phys. Rev. Lett.* **75** 1272
[398] Baur R *et al* 1996 *Z. Phys.* C **71** 571
[399] Awes T C *et al* 1995 *Nucl. Phys.* A **590** 81c
[400] Mazzoni M A *et al* 1994 *Nucl. Phys.* A **566** 95
[401] Masera M *et al* 1995 *Nucl. Phys.* A **590** 93
[402] Abreu M C *et al* 1994 *Nucl. Phys.* A **566** 77
[403] Abreu M C *et al* 1996 *Nucl. Phys.* A **610** 1
[404] Srivastava D K and Sinha B 1994 *Phys. Rev. Lett.* **73** 2421
[405] Arbex N, Ornik U, Plumer M, Timmermann A and Weiner R M 1995 *Phys. Lett.* B **354** 307
[406] Huovinen P, Ruuskanen P V and Sollfrank J 1998 *Nucl. Phys.* A **638** 503
[407] Huovinen P, Ruuskanen P V and Sollfrank J 1998 *e-print* nucl-th/980707
[408] Dumitru A, Bleicher M, Bass S A, Spieles C, Neise L, Stöcker H and Greiner W 1998 *Phys. Rev.* C **57** 3271
Dumitru A, Bleicher M, Bass S A, Spieles C, Stöcker H and Greiner W 1997 *e-print* hep-ph/9709487
[409] Srivastava D K, Sinha B, Gale C, Pal D and Haglin K 1996 *Nucl. Phys.* A **610** 350c
[410] Winckelmann L A *et al* 1996 *Nucl. Phys.* A **610** 116c
[411] Ko C M, Li G Q and Brown G E 1996 *Nucl. Phys.* A **610** 342
[412] Bratkovskaya E and Cassing W 1997 *Nucl. Phys.* A **619** 413
[413] Li G Q, Brown G E, Gale C and Ko C M 1997 *e-print* nucl-th/9712048
[414] Weise W 1993 *Nucl. Phys.* A **553** 59c
[415] Birse M C 1994 *J. Phys. G: Nucl. Part. Phys.* **20** 1537
[416] Brown G E and Rho M 1996 *Phys. Rep.* **269** 333
[417] Ko C M, Li G Q and Koch V 1997 *Ann. Rev. Nucl. Part. Sci.* **47** 505
[418] Koch V 1997 *Int. J. Mod. Phys.* E **6** 203
[419] Bernard C, Ogilvie M C, DeGrand T A, Detar C, Gottlieb S, Krasnitz A, Sugar R L, and Toussaunt D 1992 *Phys. Rev.* D **45** 3854
[420] Gerber P and Leutwyler H 1989 *Nucl. Phys.* B **321** 387
[421] Gasser J and Leutwyler H 1989 *Phys. Lett.* B **184** 83
[422] Drukarev E G and Levin E M 1990 *Nucl. Phys.* A **511** 679
[423] Cohen T D and Furnstahl R J and Griegel K 1992 *Phys. Rev.* C **45** 1881
[424] Theis J, Graebner G, Buchwald G, Maruhn J, Stöcker H, Greiner W and Polonyi J 1983 *Phys. Rev.* D **28** 2286
[425] Pisarski R D 1982 *Phys. Lett.* B **110** 155
[426] Bochkarev A I and Shaposhnikov M E 1984 *Phys. Lett.* B **145** 276

[427] Gale C and Kapusta J 1987 *Phys. Rev.* C **35** 2107
[428] Dosch H G and Narison S 1988 *Phys. Lett.* B **203** 155
[429] Furnstahl R J, Hatsuda T and Lee S H 1990 *Phys. Rev.* D **42** 1744
[430] Gale C and Kapusta J 1991 *Nucl. Phys.* B **357** 65
[431] Brown G E and Rho M 1991 *Phys. Rev. Lett.* **66** 2720
[432] Seibert D, Mishra V K and Fai G 1992 *Phys. Rev.* C **46** 330
[433] Karsch F, Redlich K and Turko L 1995 *Z. Phys.* C **60** 519
[434] Dey M, Eletzky V L and Ioffe B L 1990 *Phys. Lett.* B **252** 620
[435] Roche G *et al* 1989 *Phys. Rev. Lett.* **62** 2652
[436] Matis H *et al* 1995 *Nucl. Phys.* A **583** 617c
[437] Porter R J *et al* 1997 *Phys. Rev. Lett.* **79** 1229
[438] Wolf G, Cassing W and Mosel U 1993 *Nucl. Phys.* A **552** 549
[439] Bratkovskaya E, Cassing W and Mosel U 1996 *Phys. Lett.* B **376** 12
[440] Ullrich T *et al* 1996 *Nucl. Phys.* A **610** 317
[441] Agakichiev G *et al* 1998 *Phys. Lett.* B **402** 405
[442] Jouan D *et al* 1998 *Nucl. Phys.* A **638** 438
[443] Braun-Munzinger P and Stachel J 1998 *Nucl. Phys.* A **638** 3c
[444] Drees A 1996 *Nucl. Phys.* A **610** 536
[445] Cassing W, Ehehalt W and Ko C M 1995 *Phys. Lett.* B **363** 35
[446] Cassing W, Ehehalt W and Kralik I 1996 *Phys. Lett.* B **377** 5
[447] Li G Q, Ko C M and Brown G E 1995 *Phys. Rev.* Lett **75** 4007
[448] Koch V and Song C 1996 *Phys. Rev.* C **54** 1903
[449] Rapp R, Chanfray G and Wambach J 1997 *Nucl. Phys.* A **617** 472
[450] The CERES/NA45 collaboration, Agakishiev G *et al* 1998 *Phys. Lett.* B **422** 405
[451] Weise W 1996 *Nucl. Phys.* A **610** 35
[452] Ernst C, Bass S A, Belkacem M, Stöcker H and Greiner W 1998 *Phys. Rev.* C **58** 447
[453] Bratkovskaya E, Cassing W, Rapp R and Wambach J 1998 *Nucl. Phys.* A **634** 168
[454] Matsui T and Satz H 1986 *Phys. Lett.* B **178** 416
[455] Karsch F and Satz H 1991 *Z. Phys.* C **51** 209
[456] Baier R and Rückl R 1993 *Z. Phys.* C **19** 251
[457] Gerschel C and Hüfner J 1988 *Phys. Lett.* B **207** 253
[458] Gerschel C and Hüfner J 1992 *Nucl. Phys.* A **544** 513c
[459] Lourenco C 1996 *Nucl. Phys.* A **610** 552
[460] Frankfurt L and Strikman M 1988 *Phys. Rep.* **160** 235
[461] Frankfurt L and Strikman M 1991 *Prog. Part. Nucl. Phys.* **27** 135
[462] Wittmann R and Heinz U 1993 *Z. Phys.* C **59** 77
[463] Kharzeev D and Satz H 1996 *Phys. Lett.* B **366** 316
[464] Gerland L, Frankfurt L, Strikman M, Stöcker H and Greiner W 1998 *Phys. Rev. Lett.* **81** 762
[465] Neubauer D, Sailer K, Müller B, Stöcker H and Greiner W 1989 *Mod. Phys. Lett.* A **4** 1627
[466] Gavin S, Gyulassy M and Jackson A 1988 *Phys. Lett.* B **207** 257
[467] Vogt R, Prakash M, Koch P and Hanson T H 1988 *Phys. Lett.* B **207** 263
[468] Gavin S and Vogt R 1990 *Nucl. Phys.* B **345** 104
[469] Gavin S and Vogt R 1996 *Nucl. Phys.* A **610** 442
[470] Gavin S and Vogt R 1997 *Phys. Rev. Lett.* **78** 1006
[471] Blaizot J P and Ollitrault J Y 1987 *Phys. Lett.* B 499
[472] Karsch F and Petronzio R 1988 *Phys. Lett.* B **212** 255
[473] see e.g. Satz H 1990 *Quark-Gluon Plasma* ed C Hwa (Singapore: World Scientific) and references therein
[474] Kharzeev D, Nardi M and Satz H 1997 *Phys. Lett.* B **405** 14
[475] Gavin S and Vogt R 1996 *Preprint* hep-ph/961043
[476] Vogt R 1997 *Preprint* hep-ph/970829
[477] Baglin C *et al* 1989 *Phys. Lett.* B **220** 471
[478] Baglin C *et al* 1990 *Phys. Lett.* B **51** 465
[479] Baglin C *et al* 1991 *Phys. Lett.* B **270** 105
[480] Drapier O *et al* 1994 *Nucl. Phys.* A **544** 209c
[481] Romana A for the NA50 Collaboration 1998 *Proc. XXXIIIrd Rencontres de Moriond (21-028 March, Les Arcs, France)* to be published
[482] Ramello L *et al* 1998 *Nucl. Phys.* A **638** 261
[483] Spieles C, Vogt R, Gerland L, Bass S A, Bleicher M, Stöcker H, Greiner W, Frankfurt L and Strikman M 1998

e-print hep-ph/9810486
Spieles C, Vogt R, Gerland L, Bass S A, Bleicher M, Stöcker H, Greiner W, Frankfurt L and Strikman M to be published
[484] Kharzeev D 1996 *Nucl. Phys.* A **610** 418
[485] Wong C Y 1996 *Nucl. Phys.* A **610** 434
[486] Blaizot J P and Ollitrault J Y 1996 *Phys. Rev. Lett.* **77** 1703
[487] Gavin S Private communication
[488] Cassing W and Ko C M 1997 *Phys. Lett.* B **396** 39
[489] Gerland L *Diploma Thesis* University of Frankfurt
Gerland L to be published
[490] Geiss J, Greiner C, Bratkovskaya E L, Cassing W and Mosel U 1998 *e-print* nucl-th/9803008
Geiss J, Greiner C, Bratkovskaya E L, Cassing W and Mosel U to be published
[491] Braaten E 1996 *Nucl. Phys.* A **610** 386
[492] Hüfner J and Kopeliovich B 1996 *Proceedings of PANIC '96 and e-print* nucl-th/9606010
[493] Brodsky S J, Frankfurt L, Gunion J F, Mueller A H and Strikman M 1994 *Phys. Rev.* D **50** 3134
[494] Frankfurt L, Miller G A and Strikman M 1994 *Ann. Rev. Nucl. Part. Sci.* **44** 501
[495] Nardi M and Satz H 1998 *Phys. Lett.* B **442** 14
[496] Gonin M *et al* 1996 *Nucl. Phys.* A **610** 404
[497] With permission from the Annual Review of Nuclear and Particle Science, Volume 46, copyright 1996, by Annual Reviews Inc
[498] Glendenning N, Pei S and Weber F 1997 *Phys. Rev. Lett.* **79** 1603
[499] Gregory J C *et al* 1994 *Nucl. Phys.* A **566** 287
[500] Wyslouch B for the WA98 Collaboration 1996 *Paper Presented at ICHEP-96 (Warsaw, Poland)*
[501] Bjorken J D 1992 *Int. J. Mod. Phys.* A **7** 4189
[502] Rajagopa K 1995, *Quark Gluon Plasma* vol 2, ed R Hwa (Singapore: World Scientific)
[503] Stock R Private communication
[504] Harris J *et al* 1994 *Nucl. Phys.* A **566** 277c
[505] Friedberg R, Lee T D, Pang Y and Ren H C 1995 *Phys. Rev.* D **52** 4053
Friedberg R, Lee T D, Pang Y and Ren H C 1996 *Ann. Phys.* **246** 381